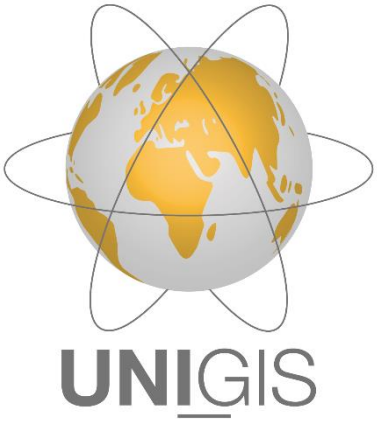

Master's Thesis

submitted within the UNIGIS MSc programme
Interfaculty Department of Geoinformatics - Z_GIS
University of Salzburg

Using GIS for identifying water abstraction locations from rivers

by

Simon de Waal
566519

A thesis submitted in partial fulfilment of the requirements of
the degree of
Master of Science (Geographical Information Science & Systems) – MSc (GISc)

Advisor:

Anna Karnassioti

Bloemfontein, 01/06/2018

This page was intentionally left blank

Science Pledge

By my signature below, I certify that my thesis is entirely the result of my own work. I have cited all sources I have used in my thesis and I have always indicated their origin.

Bloemfontein, 1 June 2018 
(Place, Date) (Signature)

Acknowledgements

I would like to thank Anna Karnassioti and Christian Neuwirth for continouis communication and commitment regarding my study.

Special thanks to my sister Dr. Caroli de Waal (Diener) for the valuable time and effort she took in reviewing and guiding me through my study.

I would like to thank De Waal & Nortje Land surveyors for allowing me to use data collected by them and the valuable information and discussions regarding survey results.

Last but not least I would like to thank all my family for the support and assistance during my studies. It would not have been possible without you.

Abstract

Water abstraction locations in rivers are crucial for many urban and agricultural water supply systems around the world. However, abstraction locations are often poorly situated in view of factors such as sediment build-up, erosion due to stream power or high flow velocities, which can adversely affect their function. This study aims to use GIS to analyse, river topography and morphology to identify optimal water abstraction locations, using a section of the Vaal River, Northern Cape, South Africa as case study. The following models were constructed: (i) an accurate DEM created from topographic and bathymetric survey data for use in hydraulic modelling and GIS analysis; (ii) a 1D and 2D hydraulic model of the river section based on a hydrograph created from measures of daily average flow rates observed during 2014-2017; and (iii) spatial analysis surfaces created, based on the hydraulic model results. Due to anisotropy occurring within the river, a TIN model was used for creating an accurate DEM. The 1D hydraulic model supplied accurate results whereas the 2D lacked effective modelling next to embankments due to finite mesh cell size limitations. A homogeneous increase in hydraulic properties for the hydrograph range was found for the study area. The spatial analysis was based on extreme high and low flow rates and consisted of relationships between velocity, depth and distance between stages, resulting in a single surface indicating desirable abstraction locations. Four desirable abstraction locations were identified and were compared to existing and proposed abstraction locations for the study area. An alternating pattern of weir effects was identified within the river and is highly related to optimal abstraction locations. In contrast to the conventional method of identifying abstraction locations, this study shows that the concave bank of a river bend is often not the best location for abstraction locations. Rather, optimal abstraction points are situated after weir effects in deep sections where less sediment build-up and lower, surface velocities and stream power may cause less damage to equipment and incur lower maintenance costs.

Contents

List of tables

List of figures

Special terms and Acronyms

1D- one dimensional

2D- two dimensional

ArcGIS- Product Developed by Esri.

Bathymetry – The below water ground surface, usually measured as a depth value from the reference water surface.

DEM- Digital Elevation Model

ESRI -Environmental Systems Research Institute

Extension – Additional software sold by Esri for use with the ArcGIS platform, includes many additional tools and functionality not included in the standalone ArcGIS software.

GIS -Geographic Information System

GPS- Global Positioning System

HEC-GeoRAS Hydrologic Engineering Center GIS Tools for Support of HEC-RAS using ArcGIS

HEC-RAS Hydrologic Engineering Center River Analysis System

Hydrology- Scientific study of the movement, distribution, and quality of water on earth.

Hydraulic- Flow of liquid in pipes, rivers and channels.

Interpolation – Estimation of surface values at unsampled locations based on known values of neighbouring points.

LIDAR Light Detection and Ranging

TIN-Triangulated irregular network

Raster – A cell-based data model used to store information for faster processing and analysis within a computerized environment. Sometimes referred to as a grid.

River Morphology- Changes in a river.

Spatial Analyst – An Extension to ArcGIS software with additional functionality for analysis of spatial features, one such spatial feature is the interpolation from points to a raster surface.

Sonar-Sound Navigation and Ranging

Topography – The ground surface in an arrangement of the natural and artificial physical features of an area, usually represented in a raster surface.

Stage- Water surface elevation and extent

Chapter 1 Introduction

Water shortage is a global problem. According to the World Health Organisation, 3 in 10 people worldwide lack access to safe, readily available water at home (World Health Organisation 2017). This is particularly relevant in South Africa a semi-arid country, with an average rainfall of about 450mm, which is well below the world average of about 860mm per year (SA Water board 2005). Water sources in South Africa are highly under stress and polluted (SA Water board 2005). It is estimated that, based on current usage trends, water demand will exceed availability by 2025 (SA Water board 2005). The main resources of water supply in South Africa is surface water (SA Water board 2005), including reservoirs, dams, lakes and rivers. The destination of the water could be a municipal water supply or an irrigation system (KSB Pumps 2013).

The availability of water is influenced by factors such as climate change and pollution, which affect both the quantity and quality of surface water and groundwater. There is evidence that global temperatures are rising, with some climatic models suggesting that this could cause a decrease in runoff in South Africa, spreading progressively from west to east during the next few decades (National Water Resource Strategy 2004). Physical water scarcity occurs as a result of pressure on the supply and demand (SA Water board 2005). Economic water scarcity, in contrast, occurs as a result of the "lack of capital investment or appropriate institutions to support the use of that capital" (Jansen 2008) . This causes many poor households to remain without access to water and basic sanitation, even in areas where water is available. Attempts to deal with water scarcity have focused primarily on addressing supply shortages, including options such as building or enlarging dams, drilling wells and building pump stations and pipelines.

Many communities abstract water directly from rivers, usually by means of a pump. Water abstraction refers to the process of drawing water from a natural or man-made source (KSB Pumps 2013). Usually this is the first step before water directed to a treatment plant or a distribution system (KSB Pumps 2013). The two main factors influencing abstraction locations in South Africa are sediment and sufficient water for abstraction. Due to the highly variable flow conditions and high sediment loads in our rivers, sediment deposition often occurs at the abstraction locations (Bosman et al. 2002). Slow approach flow velocities at

the abstraction location usually create an area of sediment build-up, which is damaging to the operation and sustainability of pumps and results in high pump maintenance and replacement costs. This in turn produces unreliable and ineffective operation of the abstraction equipment.

According to Basson (2006), 60 to 80% of the transported sediment in South African rivers is not sand but silt and clay. These fine granules have almost uniform distribution in all directions and therefore it is difficult to apply the sediment rejection principle when considering the total flow rate, using secondary currents at a bend. Fine sediment that is diverted could lead to sediment build-up in the diversion structure but is often not harmful to pumps and pipelines. Bedload sediment rejection is an important consideration in most South African river abstraction designs, because pumps and pipelines are generally prone to damage from sand transportation (Basson 2006). Generally, the intake of an abstraction location should be located on a stable reach to ensure that the intake is directed to the main current and that the flow path does not deviate (Basson 2006).

To avoid the build-up of sediment, many features were designed around abstraction points to allow bulk extraction. Designs of this scale include barrages, weirs, sluice gates, gravel traps, dividing walls and channels to wash sediment away and prevent build-up. However, these designs involve large construction projects and are very expensive.

Conventionally, abstraction points in rivers are determined from hydraulic flow tendencies from obstructions, river morphology and ideal open channel flow models. Historically, aerial photography and satellite images were used to evaluate the morphology and stability of a river reach (Coordinates : River Cross-Section Surveying Using RTK Technology 2006). Usually the optimal location of an intake is just below the vertex of a concave bank (Tan 1996). For example, river bends prove to be ideal for abstraction works and a diversion structure should be on the outside of the bend to take advantage of secondary (spiral or curvilinear) flow which creates a deep pool on the outside, which is very important when abstracting water during droughts (Basson 2006). However, current survey and software technology allow for better modelling of river beds and may increase the efficiency of extraction points and the accuracy of their placement.

The geology of abstraction locations is an important parameter to take into account. Factors such as the stability of the riverbanks and erosion possibilities need to be taken into account (Basson 2006). Special attention should be given to bends of meandering rivers since they generally erode rapidly, and secondary channels can form that may lead to the river bypassing the intake. Several rules were developed in the past to determine the best location of the intakes on the outside of a bend in the river, based on observation and experience. The predicted positions of the scour holes on the many different channels call for a look at the accuracy of certain models claiming to predict the scour position (Basson 2006). The study area and many other rivers in South Africa are meandering rivers where abstraction locations are determined by the empirical rules for identifying scour hole locations.

Many surface water extraction sites in South Africa require lower volumes to be extracted in order to serve smaller communities and agricultural operations. However, the funding for these supply systems is significantly lower than for large scale extraction projects. Therefore, it is necessary to find ways to optimise water extraction without large financial implications. Specifically, it is important to take into account environmental conditions such as natural river features, river morphology, flow and depth to identify optimal abstraction locations.

Cross-section surveys of water bodies are a key part of hydrographic engineering surveys. Traditional methods of cross-section surveys of a river include theodolite intersection, theodolite stadia, electronic distance measurement, depth-surveying bar, lead line and echo sounder (Coordinates : River Cross-Section Surveying Using RTK Technology 2006). The application of real-time kinematic (RTK) GPS positioning techniques have opened a new avenue for the cross-section survey of rivers(Coordinates : River Cross-Section Surveying Using RTK Technology 2006). The simultaneous usage of the GPS and single beam depth sounder supply greatly improved accuracy of these techniques. This is due to the depth being stored at each GPS measured location. Multi-beam sounders are available that produce scanned values of the river bed. This method produces highly detailed models of the river bed. Green waveform Lidar is one of the latest technologies in bathymetry mapping. This technology provides accurate and detailed data, with a variety of advantages.

However, limitations to bathymetry lidar surveying includes depth, coverage over vegetation or structures and cost.

With more accurate and complete data available for river beds it is possible to better model the flow in rivers. Subsurface structures and profiles can be identified and taken into account to predict flow directions across the river bed. These models can then be used to assist in identifying optimal water abstraction locations from the river.

Specifically, river flow is estimated using hydrological modelling, while hydraulic modelling is required to compute water depths and velocities in order to assess the actual tendency and consequences of a certain river flow (Betsholtz, Alexander 2017). GIS offer an extensive set of tools for spatial analysis and data management that can be integrated with a hydraulic model. One of the most widely known hydraulic modelling software is HEC-RAS along with the HEC-GeoRAS extension for ArcGIS.

Although several studies have investigated flood management and topographic and bathymetric data interpolation (Merwade 2009; Legleiter 2014; Legleiter and Kyriakidis 2008a), many of these did not account for surface interpolation and the effect of the surface on hydrological modelling along embankments. This study aims to model the optimal placement of water extraction locations within a river by incorporating hydrological modelling based on an accurately interpolated surface, because abstraction points are normally located on or close to embankments.

Aim

The aim of this study is to use GIS to identify optimal water extraction locations within a river. The study is constructed as a case study on a 12 km section of the Vaal River near Riverton, Northern Cape province, South Africa. The Vaal River is of great importance to the water supply for agricultural and rural use in large semi-arid parts of South Africa. This study further aims to effectively model flow within the river and to investigate the suitability of 1D and 2D flow models and the respective model parameters.

Specifically, this study aims to:

1) Create an accurate DEM from topographic and bathymetric survey data for use in abstraction location identification.

2) Determine hydrograph limits for identifying abstraction location flow models and water surface stage effects.
3) Determine if 1D and 2D models are sufficient for identifying abstraction locations due to transverse flow and complex hydraulics that might occur next to embankments.
4) Determine abstraction locations through spatial analysis based on results from hydraulic models.
5) Determine if the conventional theory of abstraction location placement differ from optimal identified locations obtained through spatial analysis.

These objectives will be addressed by using lidar and hydrological survey data to create an accurate DEM of the terrain and river and to create 1D and 2D models of the flow of the river. Spatial analysis and GIS will we applied to predict optimal abstraction locations and to compare the placement of existing abstraction locations to the optimal locations identified.

Chapter 2 Theoretical Background

Geographic Information Systems (GIS) are widely used in most studies on water resources, especially when the topography and geomorphology of study area are considered (Aksoy et al. 2016). Flow within a river can be studied through the analysis of hydrological, hydraulic and topographical inputs. Hydraulic analysis is used to determine hydraulic characteristics of water flow such as depth, stream power, water elevation surfaces and flow velocities. The modelling and interpretation of flow within a river can be considered as a three-step process, which will be discussed below. The first step comprises the creation of an accurate and reliable topographic surface or DEM of the study area from survey data. The second step involves the setup of model parameters related to the geometry, hydraulic properties and channel morphology. Hydraulic models are greatly dependent on the quality of input data for reliable results. The third step is where results are further processed, interpreted and analysed through the GIS environment.

2.1 Elevation measurement and surveying

The conventional way of measuring river bathymetry is through cross-sectional surveys where bathymetric profiles are collected at certain locations across the river, depending on the available resources, river morphology and intentional use of the data (Merwade 2009). The technology for measuring elevation has improved with the utilization of Global Positioning Systems (GPS). GPS and computerized mathematics have simplified the process of obtaining point measurements of greater accuracy than conventional methods. Sub centimetre accuracy and the ability to validate the measurements using real-time base stations allow for overall confidence in the DEM creation from remote sensors (Rodriguez 2015). GPS coupled with sonar and Lidar technology allow for relatively fast and effective hydrographic surveying.

2.1.1 Sonar

Sound Navigation and Ranging (Sonar) technology uses sound waves and transmits a sound pulse return once it reaches a feature below the water. One of the main concerns in hydrographic surveys is to achieve a good resolution together with high accuracy in using Sonar Systems (Gámez 2014). Two main sonar surveying systems exist, namely single beam and multibeam surveying systems (Figures2-1,2-2). Single-beam bathymetric survey

systems are configured with a transducer mounted on a transom to the boat. These systems measure the water depth directly beneath the research vessel. The sonar produces a sound pulse as a thin beam below the boat. The sound wave is reflected off the bottom or subsurface feature beneath the boat and received at the transducer. The returned pulse time is received by the transducer and calculated. The fast-continuous recording of water depth below the boat result in high-resolution measurements during the survey. The multibeam system operates similar to the single beam sonar in recording the depth except that this sonar has several transducers that allow a large swath of area to be surveyed. This enables much faster and more complete data for surveys. The swath width is determined by the depth of the river bed being surveyed. The echo is produced over a much wider span from the transducer. The farther away the object, the more area there is for the sound to echo off due to the angle of the transducer. These sonars are synced with GPS systems to record depth at a specific location and elevation.

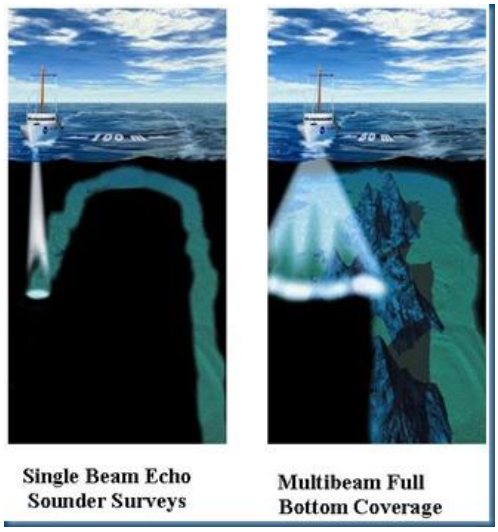

Figure 2-1 Example of the difference between single beam and multibeam sonar surveying.(Alvarado n.d.)

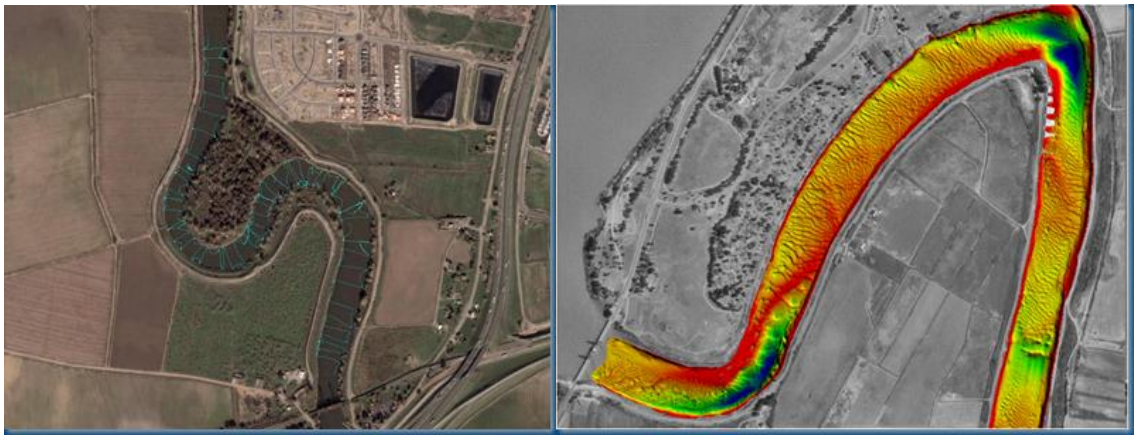

Figure 2-2 Example of data acquired with single beam (Left) and multibeam (right) sonar surveying (Alvarado n.d.).

2.1.2 LiDAR

Lidar, which stands for Light Detection and Ranging, is a method used in remote sensing and uses light in the form of a laser to measure distances to the earth. The light pulses, combined with other data recorded, generate accurate, three-dimensional information about the surface of the earth (US Department of Commerce 2017). Topographic lidar usually emits a red laser pulse to map land, while bathymetric lidar incorporates green light for penetrating water, resulting in the measurement of bathymetric elevations. The use of airborne lidar bathymetry is efficient with compared to vessels in shallow waters, where both the difficulty of surveying and the low coverage of vessels makes it a less suitable alternative. Another advantage of the lidar technology is its ability to acquire data both from the river bed and the adjacent banks, making it a perfect tool to produce a seamless product suitable for many applications (Gámez 2014). Lidar produces a dense cloud dataset of the terrain. The capturing method of lidar systems is not selective. Many surfaces of different materials reflect enough intensity of radiation to be captured by the lidar sensor. The interest is normally in the ground points since true topographic data is of interest. The filtering of data can be done through various methods such as the physical characteristics of the signal, statistical characteristics or morphometric characteristics. These filters can be applied before- or during the interpolation of the DEM (digital elevation model).

2.2 Surface interpolation

Rivers are shaped by a combination of the bed topography, the flow field, and the movement of sediment (Legleiter 2014). River bathymetry has a great influence on modelling of flow hydrodynamics, sediment transport, ecological and geomorphologic assessments (Merwade 2009). Topographic information is fundamental to geomorphic inquiry, and spatial interpolation of bathymetric elevations from irregular survey data is an important component of many reach-scale studies (Legleiter and Kyriakidis 2008a). The conventional way of measuring river bathymetry is through cross-sectional surveys where ground profiles are collected along the river depending on available resources, river morphology and end use of the data(Merwade 2009). The traditional approach to studying flow, sediment, and other hydraulic properties in river channels is through one-dimensional models that incorporate bathymetric information in the form of cross-sections (Merwade 2009). Bathymetric data are incorporated into 2D models from an interpolated surface where elevations are extracted or interpolation between cross-sections. Therefore, the accuracy of bathymetric surfaces used in 2D models is dependent upon the ability of interpolation methods in making accurate predictions at unmeasured locations using discrete data (Chen and Liu 2017). Recent studies have shown that available interpolation algorithms such as natural neighbour, inverse distance weighted, splines or kriging that assume isotropy in data create inaccurate river bathymetric surfaces (Merwade 2009; Amante and Eakins 2016; Huang et al. 2014; Legleiter and Kyriakidis 2008b; Zhang et al. 2016). Most interpolation methods assume the distribution to isotropic and ignore trends within river bathymetry that is parallel to the flow direction and perpendicular to cross-sections. It is recommended to use methods that account for river flow direction and topographic trend for interpolating discrete bathymetry data (Merwade 2009). The choice of interpolation methods are limited to specialised or customised methods such as shortest temporal distance and anisotropic kriging (Zhang et al. 2016; Legleiter and Kyriakidis 2008b). This particular study focusses on flow anomalies close to river banks. Therefore, the integration of topographic and bathymetric data integration and resulting interpolation will have great influence on the hydraulic models flow variation results. When comparing interpolated surfaces from various interpolation algorithms, the accuracy and suitability of methods vary. This estimation of surface values between sampled points based on known surface values of surrounding points is necessary due to the lack of measurements within an

area. There is a great variety of interpolation methods and the correct method needs to be chosen from a variety of factors. The choice of interpolation method to be used will be greatly affected by the knowledge of the surface to be modelled and the available data, as well as the distribution of sample points over the surface. This includes density and distribution over abrupt changes and trends within the environment. The two main groups of interpolation techniques are deterministic and geostatistical methods. Deterministic interpolation techniques create surfaces from measured points based on the extent of similarity and rely on the first law of geography (Deterministic Methods for Spatial Interpolation 2018). Measured values that are the closest to the interpolated location will have greater influence on that location. Geostatistical interpolation techniques use statistical properties of the measured points. For this study a deterministic method specifically, a TIN (Triangulated Irregular Network) method will be used. This method uses the sample data points and triangulates them using the Delaunay triangulation method. This method creates triangles by drawing lines between data points. The original points are connected in such a way that no triangle edges are intersected by other triangles (Yang et al. 2004). This interpolation technique widely used in geographic models. One of the most widely used advantages of TIN models is the ability to edit and manipulate triangulated surfaces. This allows for customised connections between sample points where necessary. It is especially useful for the integration of topographic and bathymetric data due to the ability to modify triangles along the banks. This is done by assuming that the river morphology along embankments is parallel to the direction of flow. A major disadvantage of creating a DEM using TIN is that the editing of the triangles is time consuming but usually with accurate results, due to the fact that a multi-directional trend can be accounted for and corrected within a meandering river.

2.3 Hydraulic modelling

Hydrological modelling has become an indispensable tool for studying flood-related processes and water management in catchments (Nicandrou 2010). Hydraulic models have been used for decades to assess and represent flow and flooding for hydrographic features. Several processes are observable in a hydrologic system. It is impossible to account and simulate all these processes due to the complexity of the influences on the system. Therefore, simplified hydraulic models are created to try and represent the ‘real world’

phenomena. With these models we try to incorporate the most influential factors regarding the phenomenon we want to study (Haile 2005). There are a variety of hydraulic models available both in research and in commercial applications. The types of models vary in the way that the governing equations are formulated, in the numerical solution of the governing equations, as well as in the way that the geometric properties of the system is described (Betsholtz, Alexander 2017). The fluvial hydraulic models concern the study of stream flow in natural open channels. Hydraulic modelling is fundamental for the design, planning and flow propagation in rivers (Gharbi et al. n.d.). Hydraulic modelling can solve hydraulic tendencies in order to limit harmful environmental effects of flooding or to investigate fluvial flow effects. The three main types of hydraulic models typically used is, one-dimensional, two-dimensional, and three-dimensional. One dimensional models will consider flow in one dimension along cross-sections. Two and three dimensional modelling allows the numerical simulation to take into account the expansion of the river in two or three dimensions, respectively (Gharbi et al. n.d.). A 1D-2D model combination can be conducted to benefit from the advantages each model has to offer.

2.3.1 1D flow models

1D river models are used to model fluvial flow and flooding events. These models are made up of a series of cross sections describing the topography of the river and water levels are calculated using the 1-dimensional form of the governing equations (Betsholtz and Nordlöf 2017). The key characteristic of a 1D model is that the flow paths can be determined and specified in advance by defining cross sections, floodplain storage areas, spills and other constraints. The 1D model is good at representing weirs, sluices and other structures within a channel and at representing conveyance in channels with complex cross sections (Brunner et al. 2015). In addition, 1D models often require less data than 2D models due to the cross-sections used for defining roughness, obstructions, ineffective flow and topography. While 1D models perform well when flow is restricted between channel banks, 2D modelling has shown to better estimate flows in topographically complex floodplains, where the flow is considered largely 2-dimensional (Betsholtz and Nordlöf 2017). Within a 1D model velocities are only shown as an average over the cross section and only velocities are calculated that are normal to the cross-section. A requirement for one-dimensional modelling is that the velocity and depth change extensively in one direction along the channel. The computational direction of a one-dimensional model is along the channel centreline since a

natural channel often meander. Features such as the river bed, embankments, blocked obstructions ineffective flow areas and flood plain are represented by cross sections perpendicular to the centre line. The 1D model is ideal for flow restrictions in one direction.

2.3.2 2D flow models

2D models can determine flow paths automatically without the need of defining paths prior to the analysis. This is advantageous where complex flow paths exist. The 2D model is defined by a 2D computational finite mesh representing the underlying topography by connected cells. 2D models may lack the ability to represent detailed topography such as channels due to the grid cell size, depending on computational capabilities of hardware and software. 2D models need continuous topographical data, covering the whole area that is to be modelled in 2D (Betsholtz and Nordlöf 2017). No flow paths and other components need to be defined for 2D models and therefore usually have a quicker setup. 2D models generate velocity estimates averaged over a model grid rather than averaged over a cross section. This results in 2D models being better at mapping velocity than 1D models. The output of a 2D is in raster format and easily interpreted and visualised within the GIS environment.

2.3.3 1D/2D Flow models

1D- 2D models aim to make the best of both worlds by representing channels and floodplains with the most appropriate model type. 1D models are good at modelling channels and 2D models tend to be better at modelling complex flow routes often obtained on floodplains. This is accomplished by taking the 1D model of a reach of river and connect it dynamically to one or more detailed 2D models to provide a more detailed description of the flows in specific areas of interest. A second method is where one or more 1D model reaches may be connected within a 2D model to provide a better description of in-bank channel flows, and flows through hydraulic structures such as culverts, weirs and bridges (Ball et al. n.d.).

2.4 Open channel hydraulics

The modelling of a river can be treated as an open channel flow. Open channel flow is defined as fluid flow with a free surface open to the atmosphere. Examples of open channels include streams and rivers. When investigating open channel flow the assumption is made that the pressure at the surface is constant and the hydraulic grade line is at the surface of the fluid (Open Channel Flow 2018). Due to its free surface the analysis of open

channel flow is generally more complex than that of closed conduit flow. The free surface is likely to vary in space and time. If the free surface varies in space the flow is referred to as varied. When it varies in time it is referred to as unsteady.

All hydraulic flows are three dimensional in nature and involve complex turbulent flow motion in vertical and horizontal directions (ARR: A Guide to Flood Estimation n.d.). The type of hydraulic computations to be done will depend on the problem and available data. Therefore, the appropriate analysis techniques need to be determined. Free surface flows are due to gravity and resisted by shear forces and friction on the channel bed and drag forces on objects such as vegetation and obstructions (ARR: A Guide to Flood Estimation n.d.). Channels can be prismatic or nonprismatic. Prismatic channels are usually man made where nonprismatic channels usually represent natural channels such as rivers. Within a nonprismati channel the shape and size of the cross section varies along the channel (Ponce 2014). The cross-sections of natural channels are irregular, usually broader than they are deep and often consisting of a deeper in-bank channel (ARR: A Guide to Flood Estimation n.d.). Meanders in rivers have been extensively investigated through various studies (Camporeale et al. 2005; Harrison et al. 2011; Mosaddad, Bidokhti, and Ezam 2009). The geomorphology caused by meanders are currently extensively used for identification of water abstraction locations. Within bends in rivers natural cross-sections are asymmetrical and they tend to be deeper on the outside of the bend due to the effect of helicoidal secondary currents. These currents tend to erode the outside of the bend and deposit sediment at the inside of the bend (Figure 2-3).

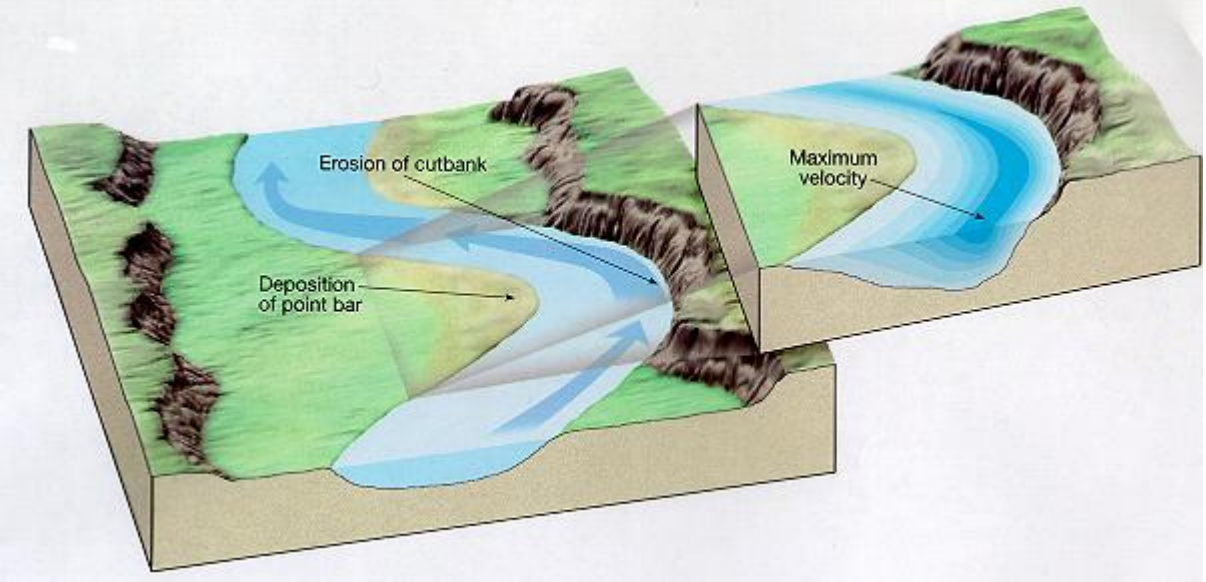

Figure 2-3 River bend showing areas of deposition and erosion and characteristic cross-section. (Rivers | World Machine Development Diary n.d.)

Open channel flows are three dimensional in nature but are often treated as one dimensional. This is due to the advanced computation required for the approximation of turbulence and are not feasible to use in large scale modelling (ARR: A Guide to Flood Estimation n.d.). New methods and advancements in computational technology have allowed common usage of unsteady 2D depth averaged models in flood hydraulics simulation.

2.4.1 Classification of open channel flow

Open channel flow can be classified according to the flow characteristics. The flow characteristics is concerned with flow characteristics and hydraulic behaviour of the fluid in an open channel. This needs to be considered when planning and conducting hydraulic modelling for the purpose of identifying abstraction locations. Flow properties and conditions may vary due to the influence of different flow rates, complex topography and connecting reaches.

2.4.1.1 Steady and unsteady flow

Flow with in an open channel is steady when the hydraulic variables such as discharge, flow area, mean velocity and flow depth does not change with time. If the variables change with time and space, the flow is unsteady.

2.4.1.2 Uniform and equilibrium

Flow is uniform when the channel is prismatic and dimensional variables are constant. If the channel is non-prismatic and the hydraulic variables are approximately constant, the flow is in equilibrium.

2.4.1.3 Gradually varied, rapidly varied and spatially varied

Gradually varied flow is when the flow rate is constant but the hydraulic dimensional variables vary gradually. Under gradually varied flow the pressure distribution in the vertical direction, normal to the flow is very close to hydrostatic (Ponce 2014). Rapidly varying flow is when the flow rate is constant but the hydraulic variables vary rapidly in space in such a way that a hydrostatic pressure distribution *cannot* be assumed in the vertical direction normal to the flow (Ponce 2014). Flow can also be spatially varied and occur when the flow rate varies in space.

2.5 Roughness coefficients

The channel roughness affects the flow within the channel. It is important to be able to quantify the roughness. The roughness in channels is determined by the materials from which the channel is made. This includes any vegetation in the channel. In channels where the morphology changes the roughness will change. This is particularly the case in natural channels especially where high sediment transport and seasonal vegetation growth occur. The challenge of determining the appropriate roughness to use in hydraulic modelling computations should not be under-estimated and is often based on experience and should be validated or calibrated where possible(ARR: A Guide to Flood Estimation n.d.). There are mainly three uniform flow resistance equations commonly used for quantifying the effects of boundary resistance in turbulent flows. These are the Manning equation, Chezy equation and Darcy-Weisbach equation. The Chezy and Manning equations are more often used for open channel flow and the Darcy-Weisbach used for pipeline frictional losses. The Chezy and Manning formulas relate the cross-sectional averaged velocity to the channel slope, the hydraulic radius and an empirical parameter which is used to encapsulate the effects of the resistance to flow(ARR: A Guide to Flood Estimation n.d.).

2.5.1. Manning Formula

The manning equation is an empirical equation that applies to uniform flow in open channels and is a function of the channel velocity, flow area and channel slope. The equation is as follows:

$$V = \frac{k}{n} R_h^{2/3} \cdot S^{1/2}$$

V = cross-sectional average velocity.

k = conversion factor.

n = Manning coefficient and is unitless.

R_h = hydraulic radius.

S = slope of the water surface or the linear hydraulic head loss.

The hydraulic radius is a measure of a channel flow efficiency. Flow speed along the channel depends on its cross-sectional shape and the hydraulic radius is a characterisation of the channel efficiency. The hydraulic radius is defined as the ratio of the channel cross-sectional area of the flow to its wetted perimeter. Frictional losses typically increase with an increasing wetted perimeter. The hydraulic radius formula is:

$$R_h = \frac{A}{P}$$

R_h = hydraulic radius

A = cross-sectional area of flow

P = wetted perimeter

The Manning roughness coefficient *n* is an experimentally determined constant. Manning roughness coefficient tables exist that indicate estimated values for the constant for channel scenarios. Its value depends upon the nature of the channel and its surface. Factors influencing the manning constant is as follows.

- Surface Roughness

  The roughness of the material on the wetted perimeter influence the manning n. Fine material has a lower n value and courser material a higher n value. The manning coefficient is highly related to the shape and size of the grains over the wetted perimeter.
- Vegetation

  Vegetation influence the surface roughness and is often dependent on seasonal change. The manning n coefficient will vary according to season, type, density and

height. Vegetation is often related to certain depth and may vary greatly over the channel.

- Channel Irregularity

  Irregular channel dimensions are caused by the change in shape and size of the channel and influence the wetted perimeter over cross-sections.

- Channel Alignment

  A relatively straight channel will have a low manning n coefficient where as a meandering channel with sharp turns will have a higher manning n coefficient.

- Silting and Scouring

  The silting up of a channel may produce a more even slope and reduce the manning n coefficient whereas scouring will create prominent variations in slope and increase the manning n coefficients.

- Obstruction

  When obstructions are present within the channel the manning n coefficient will increase. These obstructions consist of weirs, bridge columns, rock formations, boulders, trees, logs etc.

- Water level and flow rate

  The n value in most streams decreases when the water level and flow rate increase.

An example of a table of Manning n is given in Table 2-1.

Table 2-1 Values of Roughness Coefficient n for different channel conditions(ARR: A Guide to Flood Estimation n.d.)

Description of channel	Minimum	Normal	Maximum
Glass, plastic, machined metal	0.009	0.01	0.013
Fabricated steel channels	0.011	0.012	0.017
Planed timber, joints flush	0.01	0.012	0.014
Sawn timber, joints uneven	0.011	0.013	0.015
Concrete, trowel finished	0.011	0.013	0.015
Concrete, shuttering	0.012	0.014	0.017
Brickwork	0.012	0.015	0.018
***Excavated channels:**			
earth, clean	0.016	0.022	0.03
gravel	0.022	0.025	0.03
rock cut, smooth	0.025	0.035	0.04
rock cut, jagged	0.035	0.04	0.06
***Natural channels:**			
clean, regular section	0.025	0.03	0.04
some stones and weeds	0.03	0.035	0.045
some rocks and/or brushwood	0.05	0.07	0.08
very rocky or with standing timber	0.075	0.1	0.15
Flood plains:			
short grass pasture	0.025	0.03	0.035
mature crops	0.025	0.035	0.045
brushwood	0.035	0.05	0.07
heavy timber or other obstacles	0.05	0.1	0.16

In 1D models the roughness is assigned according to the cross-sections. For 2D models the roughness is generally specified as a spatially varying grid/mesh over the 2D model domain (ARR: A Guide to Flood Estimation n.d.). For adequate hydraulic modelling not only, the geometry but also the roughness of the Earth's surface is required. This include the roughness of the objects thereon. The floodplain roughness is usually based on land cover maps derived from orthophotos (Dorn, Vetter, and Höfle 2014). The effects of bend losses as a result of change in directional momentum are modelled in a full 2D hydraulic model depending on the grid resolution that is feasible (ARR: A Guide to Flood Estimation n.d.). The grid structure of 2D models allow for the inclusion of physical obstructions and do not have the need for compensating for these features within the roughness coefficient. A variety of areas can be identified and digitised into land-use polygons representing zones of similar loss characteristics and applied within 2D hydraulic models. The Manning *n* coefficient

varies slightly in 2D models from 1D models due to the non-boundary energy losses that are taken into account. Table 2-2 indicates surface roughness according to land use.

Table 2-2 Valid Manning 'n' Ranges for Different Land Use Types(ARR: A Guide to Flood Estimation n.d.)

Land Use Type	Manning 'n'
Residential areas – high density	0.2 – 0.5
Residential areas – low density	0.1 – 0.2
Industrial/commercial	0.2 – 0.5
Open pervious areas, minimal vegetation (grassed)	0.03 – 0.05
Open pervious areas, moderate vegetation (shrubs)	0.05 – 0.07
Open pervious areas, thick vegetation (trees)	0.07 – 0.12
Waterways/channels – minimal vegetation	0.02 - 0.04
Waterways/channels – vegetated	0.04 – 0.1
Concrete lined channels	0.015 – 0.02
Paved roads/car park/driveways	0.02 – 0.03
Lakes (no emergent vegetation)	0.015 – 0.35
Wetlands (emergent vegetation)	0.05 – 0.08
Estuaries/Oceans	0.02 – 0.04

2.6 Open channel flow equations

Flow characteristics within rivers can vary greatly depending on the dimensional and hydraulic variables. The study of abstraction locations in rivers not only depends on the morphology and flow tendencies. Therefore, not only the dynamic equilibrium but also the inundation of flow in rivers need to be analysed. There are three main types of flow conditions used to calculate flow in rivers namely steady flow unsteady flow and moveable boundary flow. The fundamental hydraulic equations that define 1D steady flow and gradually-varied flow include the continuity equation, energy equation, and flow resistance equation (Kristen, Christopher, and Thornton 2005). The equations related to important hydraulic concepts are indicated in the following section. The Saint Venant equations provide a model of free surface water flow in a channel and is a common hydraulic model used to study flow depths and total energy loss along a reach of a river system. Water surface profiles are computed between cross-sections by solving the energy equation with an iterative procedure called the standard step method (Brunner 2016). The basic equations for 1-D hydrodynamic modelling are derived considering conservation of mass and momentum (Ahmad and Simonovic 1999). These equations are based on the following assumptions.

• Flow is one-dimensional or two-dimensional. Vertical variations in velocity and flow can be neglected.

• Hydrostatic pressure prevails and vertical accelerations are negligible

• Streamline curvature is small.

• Bottom slope of the channel is small.

• Manning's and Chezy's equation are used to describe resistance effects

• The fluid is incompressible

• Channel boundaries are considered fixed and therefore not susceptible to

erosion or deposition.

2.6.1 1D Steady Flow

2.6.1.1 Continuity Equation

The continuity equation assumes the flow rate as constant and continuous over time. The following equation indicate the average velocity in terms of flow rate.

$$v = \frac{Q}{A}$$

where:

A = cross-sectional area normal to the direction of flow

Q = Flow rate m^3/s

v = average velocity m/s

2.6.1.2 Energy equation

Total energy at any point along an open-channel system can be defined as the total head of water. This is done by calculating the total head at each cross section from the velocity, flow depth and channel depth. The following equation indicates the steady flow energy equation:

$$h = z + y + \frac{\alpha v^2}{2g}$$

where:

α = kinetic energy correction coefficient

g = acceleration of gravity in m/s^2

h = total head of water in meters

v = average velocity at a cross section in m/s

y = flow depth at a cross section in meters

z = bed elevation at a cross section in meters

2.6.1.3 Froude Number

It is important to consider the effect of gravity on the state of the flow. Within a steady flow model flow can be subcritical, critical or supercritical. The flow regime is determined by the Froude Number and is a dimensionless parameter measuring the ratio of the inertial force divided by gravitational force and is given by the following formula:

$$Fr = \frac{V}{\sqrt{g h_m}}$$

Fr= Froude number

V = Water velocity

h_m = Hydraulic depth (cross sectional area of flow)

g = Gravity

When:

Fr = 1 - The flow is critical

Fr > 1 - The flow is supercritical and therefore flows fast and rapidly

Fr < 1 - The flow is subcritical and therefore flows slowly

The Froude number is applicable in fluid where the gravitational force of the fluid is of relevance.

2.6.1.4 Conservation of energy

From Bernoulli's theorem based on the conservation of energy equation, water surface profiles and grade lines can be calculated. The Bernoulli equation is useful when solving problems involving fluids. For a non-viscous, incompressible fluid in a steady flow, the sum of pressure, potential and kinetic energies per unit volume is constant at any point

(Bernoulli Equation n.d.). The following conservation of energy equation is applied to an open channel.

$$y_2 + z_2 + \frac{\alpha_2 v_2^2}{2g} = y_1 + z_1 + \frac{\alpha_1 v_1^2}{2g} + h_t$$

where:

α_1 = downstream cross section kinetic energy coefficient

α_2 = upstream cross section kinetic energy coefficient

g = gravitational acceleration

h_t = total energy loss between adjacent cross sections

v_1 = downstream cross section average velocity

v_2 = upstream cross section average velocity

y_1 = downstream cross section flow depth

y_2 = upstream cross section flow depth

z_1 = channel bed elevation at the downstream cross section

z_2 = channel bed elevation at the upstream cross section

Total energy loss between adjacent cross sections in terms of head loss (meters) are shown in this equation:

$h_t = h_f + h_e + h_c$

where:

h_c = head loss due to channel contraction

h_e = head loss due to channel expansion

h_f = head loss due to friction

h_t = total energy loss between adjacent cross sections

2.6.2 1D unsteady flow

With unsteady flow the principle of conservation of mass and conservation of momentum apply. The 1D unsteady flow continuity and momentum equations are also derived from the shallow water St Venants Equations.

2.6.2.1 Continuity equation

The conservation of mass for a control volume states that the net rate of flow into the volume be equal to the rate of change of storage inside the volume (Brunner 2016). The following equation indicates the 1D continuity equation:

$$\frac{\partial(Q)}{\partial x} + \frac{\partial A}{\partial t} - q = 0$$

Where:

Q = flow rate

A = cross sectional area

q =lateral inflow per unit length.

2.7.2.2 Momentum equation

The conservation of momentum for a control volume states that the net rate of momentum entering the volume plus the sum of all external forces acting on the volume be equal to the rate of accumulation of momentum (Brunner 2016). The formulation of the momentum equation will be different depending on the forces that are considered such as pressure, gravity and frictional resistance (Betsholtz and Nordlöf 2017). The 1D momentum equation is as follows.

$$\frac{\partial V}{\partial t} + g\frac{\partial}{\partial x}\left(\frac{V^2}{2g} + h\right) = g(S_o - S_f)$$

Where:

V = flow velocity

g = gravitational acceleration

h = water depth

S_o = channel slope

S_f = friction slope

2.6.3 2D unsteady flow

The 2D hydrodynamic model is based on the numerical solution of depth-averaged equations describing the conservation of mass and momentum in horizontal dimensions x and y (ARR: A Guide to Flood Estimation n.d.). The Navier-Stokes equations describe the motion of fluids in three dimensions. These equations are simplified by the assumptions made. Especially for 2D modelling, the momentum equation is adapted to certain flow characteristics. This is done to reduce computational time. The continuity equation for 2D unsteady flow is as follows.

$$\frac{\partial H}{\partial t} + \frac{\partial (hu)}{\partial x} + \frac{\partial (hv)}{\partial y} + q = 0$$

Where:

x = distance along the channel

t = time

Q = flow rate

A = cross-sectional area

S = storage from non-conveying portions of cross section

q_l = lateral inflow per unit distance

The Navier-Stokes vertical momentum equation can be used to justify that pressure is nearly hydrostatic. When the horizontal length is much larger than the vertical length the volume conservation implies that the vertical velocity is small. Therefore, the vertical velocity and components is neglectable for open channel flow. The momentum equation for 2D unsteady flow is as follows:

Momentum equation in x direction of velocity

$$\frac{\partial u}{\partial t} + u\frac{\partial u}{\partial x} + v\frac{\partial u}{\partial y} = -g\frac{\partial H}{\partial x} + v_t\left(\frac{\partial^2 u}{\partial x^2} + \frac{\partial^2 u}{\partial y^2}\right) - c_f u + fv$$

Momentum equation in y direction of velocity

$$\frac{\partial v}{\partial t} + u\frac{\partial v}{\partial x} + v\frac{\partial v}{\partial y} = -g\frac{\partial H}{\partial x} + v_t\left(\frac{\partial^2 v}{\partial x^2} + \frac{\partial^2 v}{\partial y^2}\right) - c_f v + fu$$

Where:

u = velocity in x direction

v = velocity in y direction

g = gravitational acceleration

v_t = horizontal eddy viscosity coefficient

c_f = friction coefficient

R = hydraulic radius

f = Coriolis parameter.

2.6.4 Momentum Simplification

The importance of properties accounted for in the momentum equation can vary significantly depending on relevance for certain flow conditions. In some conditions it may be possible for simplifying assumptions to be made either to the equations themselves or to the way in which individual terms are treated numerically (ARR: A Guide to Flood Estimation n.d.). The most commonly used simplifications are the diffusive wave approximation and the kinematic wave approximation. With the diffusive wave approximation, the unsteady, advection, turbulence and Coriolis terms of the momentum equation can be disregarded to obtain a simpler equation (Brunner 2016). This approximation can be used to describe gradually varied flows in areas with moderate to steep slopes. Backwater effects are included but has the limitation that it cannot be used to simulate flow separations, eddies or main channel and overbank momentum transfers. With the kinematic wave approximation, the surface slope of the water is assumed to be the same as the bed slope. Backwater effects are not included and the water can only flow downstream. The kinematic wave approximation can only be used to describe gradually varied flows in reaches with moderate to steep slopes where backwater effects can be neglected (ARR: A Guide to Flood Estimation n.d.).

Chapter 3 Methodology

This study aims to accurately model hydrological flow tendencies along a river section for the purpose of identifying optimal and sustainable water abstraction locations. GIS analysis were used for identifying optimal abstraction locations.

This study involved three major processes :1) the creation of an accurate DEM; 2) the creation of 1D and 2D hydraulic models for the section of river; 3) the analysis, interpretation and visualisation of results within the GIS environment. Figure 3-1 represents an overview of the study processes along with the required input data.

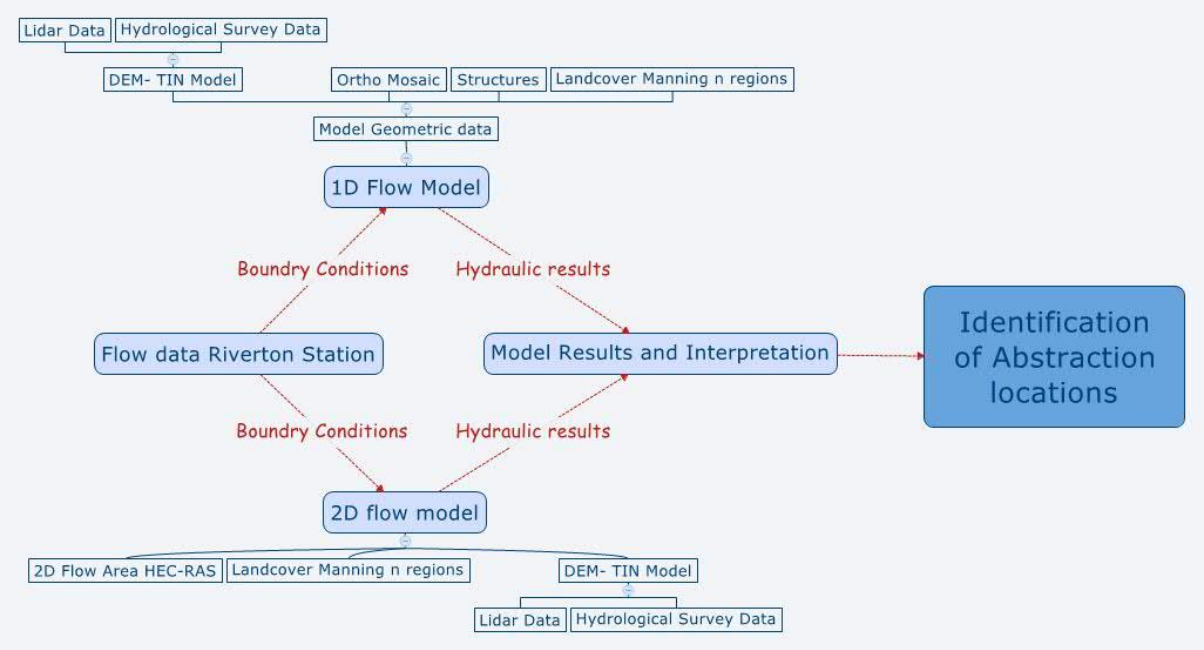

Figure 3-1 Flowchart illustrating the input data for the study models.

3.1 Study area

The study area is located on a section of the Vaal River in the Northern Cape, South Africa (Figure 3-2). The Vaal river originates in the Mpumalanga Province and is the largest tributary of the Orange River. A large section of the Vaal River runs through arid parts of the country where many agricultural and urban communities rely on the Vaal River as their main water source. The section of the river used in the study is about 12km long and is meandering from the settlement of Riverton to the north. The flow within the river is greatly affected by manmade structures. In particular, the river flow is regulated through reservoirs such as the Vaal Dam, Bloemhof Dam and Vaalharts Dam. The Vaalharts Dam is the first upstream reservoir from the study area. The study area was selected in accordance with a project by Tokologo Local Municipality for water supply to the towns of Boshof and Dealesville in the Free State province, South Africa. The project started in 2015 with the purpose

of identifying an abstraction location in the Vaal River and the planning and building of a 110km long pipeline to the identified towns.

Figure 3-2 Map of the Vaal River study area location with the river section indicated.

3.2 Data collection

The survey was conducted in March 2015 by De Waal & Nortje Land surveyors. Most of the surveys were conducted with RTK GPS technology connected to a base station for corrections. A geoid model (South Africa Geoid 2010) was applied to all measurements for accurate elevation determination. Benchmarks were established with calibration to local trigometrical beacons. A total of 5 GCP's (ground control points) were placed. All data acquired were based on connected reference marks and site calibrations conducted. This ensured that data were on the same system with minimal error in the x, y and z directions. The projected coordinate system used for the survey and in effect for the study is WG25. The projection parameters can be seen in Figure 3-3.

The topographic survey was conducted using airborne LiDAR technology accompanied by aerial imaging and was also connected to the base station. The aerial survey was conducted by AAM Group and they were responsible for processing, classification, filtering,

orthorectification and accuracy of the Lidar points and ortho mosaic images. The resulting elevation data is a filtered dense cloud of ground points of over 1.35 million points and exclude features such as buildings and vegetation.

The bathymetric survey was conducted by De Waal & Nortje Land surveyors. This was done with a Sonarmite single beam survey grade echo sounder. The transducer was connected to an RTK GPS, aligned and instrument elevation differences applied for accurate results. A Trimble R10 rover with xFill technology was used to ensure seamless connectivity. This was done to minimise the effect of radio signal loss and enable surveying under trees bridges and close to embankments for optimal coverage. Due to limitations of single beam sonar technology the survey was conducted as a continued topographic survey with measurements every 5 meters. At each measurement the depth was stored and applied in post processing. Cross sections of the river were taken 40-50 meters apart and where possible along embankments. This resulted in 13824 effective measurements within the river. The collected survey data can be seen in the Figure 3-3.

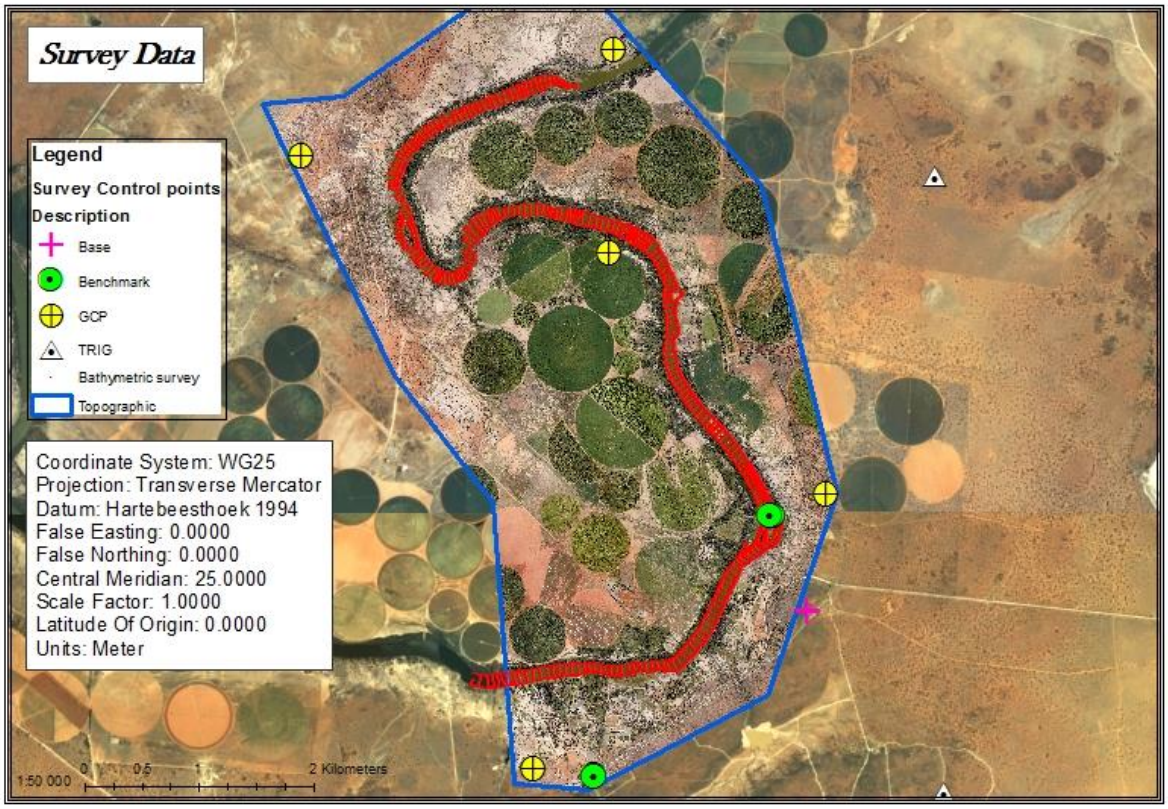

Figure 3-3 Map of survey data of the study area in the Vaal River. Base - GPS base station used for corrections during an RTK survey; Benchmarks - permanent control stations for the survey area; GCP – Ground control points used for referencing aerial imagery and lidar data; TRIG - trigometrical beacons built by government and used as local reference points; Bathymetric survey- indicate the points measured along with the depth within the river using a boat and are indicated as red points; Topographic – indicate the extent of the lidar and orthorectified imagery obtained through the aerial survey.

Flow data were recorded daily at the Riverton station (Station C9H003, Figure 3-4) by the Department of Water and Sanitation of The Republic of South Africa. The station has a catchment area of 121070km^2 and is located at Latitude -28.51344 and Longitude 24.69708. Flow data at this location is available from 1909 and can be queried through the Department of Water Affairs Hydrological Services website (http://www.dwa.gov.za/Hydrology/). The daily flow averages for the past four years (2014-2017) have been extracted. The flow data are displayed in Figure 3-5. It can be seen that the flow within the river is greatly regulated. The norm of the flow rate is around 20 m^3/s. Higher flow rates do occur but decrease in frequency as the flow rate increase. It can be seen that occasional low-level flooding took place in in March-April for 2014 and February - March for 2017. This moderate fluvial flooding may be advantageous in flushing away

sediment build-up at abstraction locations but is not the norm. The disastrous floods that were recorded from 1910 were not included and consisted of flow rates of 1000 m3/s up to 4000 m3/s. However, these events are extreme cases and not included for the purpose of the study. The study will make use of a hydrograph for modelling different conditions between $0m^3/s$ and $500m^3/s$. Extreme low flow rates have great influence on the effective and consistent water abstraction whereas flooding is considered a disaster. For the purpose of hydraulic modelling, verified measurements of flow and gauge plate readings were extracted in order to create a hydrograph for computations.

Figure 3-4 Riverton waterworks station(Department of Water Affairs n.d.).

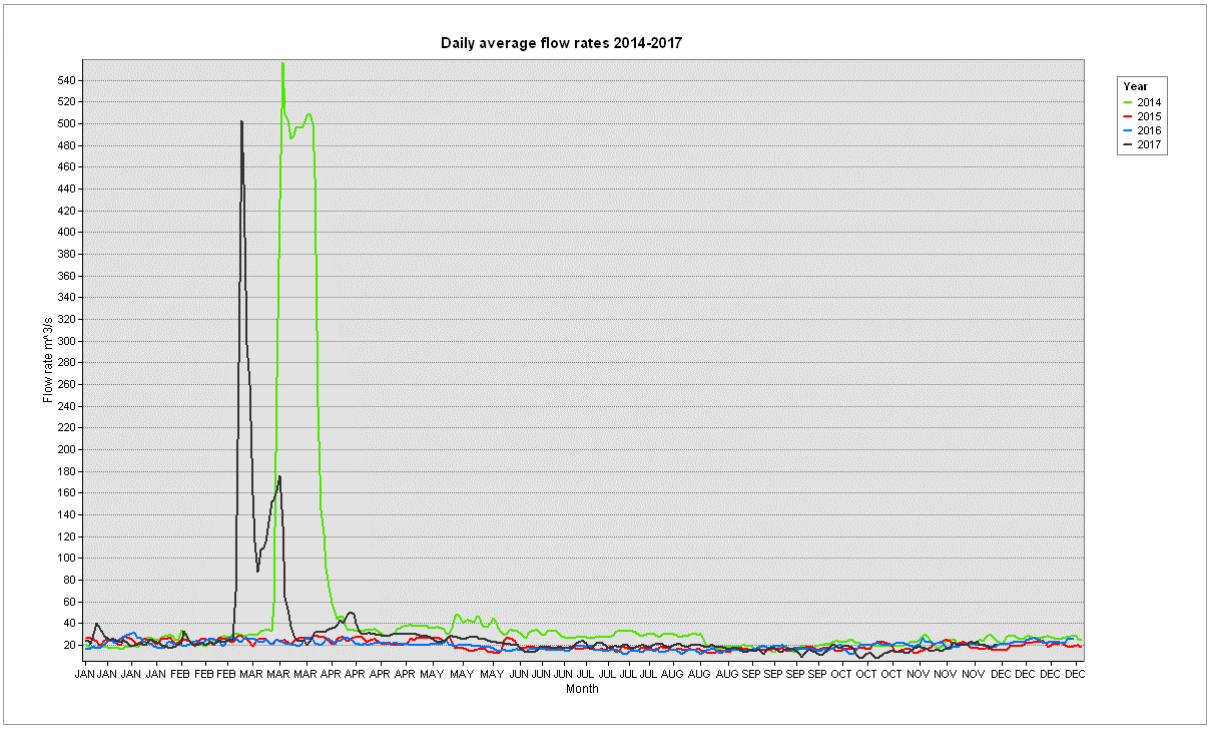

Figure 3-5 Four year daily average flow rates at Riverton station (C9H003) in the Vaal River, South Africa. Green-2014, Red-2015, Blue-2016, Black-2017.

3.3 Software

The main software used for conducting the analysis were ArcGIS and HEC-RAS. ArcGIS was mainly used for creating surface models from the elevation data. HEC-RAS and its accompanying ArcGIS extension HEC-GeoRAS were used for the flow modelling.

ArcGIS for Desktop is a suite of integrated applications, including ArcMap, Arc Catalog, Arc Scene and Arc globe. This is an extensive software used by GIS professionals for a comprehensive range of GIS activities including data compilation, mapping, modelling, spatial analysis, sharing, visualization, data management and geoprocessing. One main analysis that was conducted for the study is surface interpolation for the effective integration of the topographic and bathymetric data. This software was also used to interpret and create the results through spatial analysis of the hydraulic results.

Within the software, elevation data can be represented in various ways. The measured elevation data were represented by points with X, Y and Z values at the measured location. Due to the highly anisotropic spatial distribution of measured points, standard interpolation methods and algorithms could not be used for predictions. This resulted in the elevation

data being converted to a more flexible TIN (Triangulated irregular network) model and further converted to raster data.

The method used to create a DEM from the topographic and bathymetric data was the TIN surface, through the Triangulated Surface tools located under 3D Analysis tools within the Arc Toolbox. The TIN model was used due to the ability to create a high precision surface. This was enabled by the TIN Editing toolbar available in ArcGIS for adding, editing and modification of nodes, edges and break lines.

HEC-GeoRAS is designed for ArcGIS and is a set of tools to process geospatial data for use with the Hydrologic Engineering Center's River Analysis System (HEC-RAS) (Cameron and Ackerman 2012). This extension allows the creation of an HEC-RAS import file containing geometric data from the digital terrain model (DTM), the defined geometry along with the related datasets. The import file, referred to as the RAS GIS Import File, containing river, reach and station identifiers; cross-sectional cut lines; cross-sectional surface lines; cross-sectional bank stations; downstream reach lengths for the left overbank, main channel, and right overbank; and cross-sectional roughness coefficients was created using HEC-GeoRAS (Cameron and Ackerman 2012). Additional geometric data defining levee alignments, ineffective flow areas, blocked obstructions, and storage areas may be written to the RAS GIS Import File (Cameron and Ackerman 2012). HEC- GeoRAS are essentially used within the study to create and setup geometric data for hydraulic computations.

HEC-RAS is an integrated system of software, designed for interactive use in a multi-tasking environment(Brunner 2016). The system is comprised of a graphical user interface, separate analysis components, data storage and management capabilities, graphics and reporting facilities (Brunner 2016). HEC-RAS is designed to perform one-dimensional and two-dimensional hydraulic calculations for a network of natural or constructed channels. This software is used for performing 1D and 2D computations, model setups and modelling of the study area. The model created in HEC-RAS may include various types of analyses included in the HEC-RAS package (Brunner 2016). The data files for a project are categorized as follows: plan data, geometric data, steady flow data, unsteady flow data, quasi-steady flow data, sediment data, water quality data, and hydraulic design data (Brunner 2016). This Software was used for creating hydraulic models of the study area.

3.4 Digital Elevation Model

The digital elevation model was created using data from the Lidar and hydrographic survey points. The classified Lidar points were obtained from an aerial survey conducted by AAM Group. The aerial survey was transformed to the ground control points to ensure that it is on the same datum as ground and hydrographic survey points, based on the established benchmarks. Automatic and semi-automatic algorithms were used for classification of the lidar point cloud. This enabled the removal of dense vegetation and buildings from the surface and prevent an elevated surface where flow will occur. First return ground points were used for the DEM used in the study. An average thinned point spacing of 4m were obtained from the lidar survey along with aerial imagery with a resolution of 0.1m X 0.1m.

The laser pulses of the lidar cannot penetrate the water surface and therefore a hydrographic survey of the river bed was conducted. A site calibration was applied with respect to the benchmarks to ensure measurements being on the same system. Cross sections were measured at an average of 40-50 meters apart with a 5m point spacing. More detail was measured at features such as bridges and where significant changes occur.

The combination of the topographic and hydrographic survey data produced irregular spaced survey points between the topographic and hydrographic survey data (Figure 3-6).

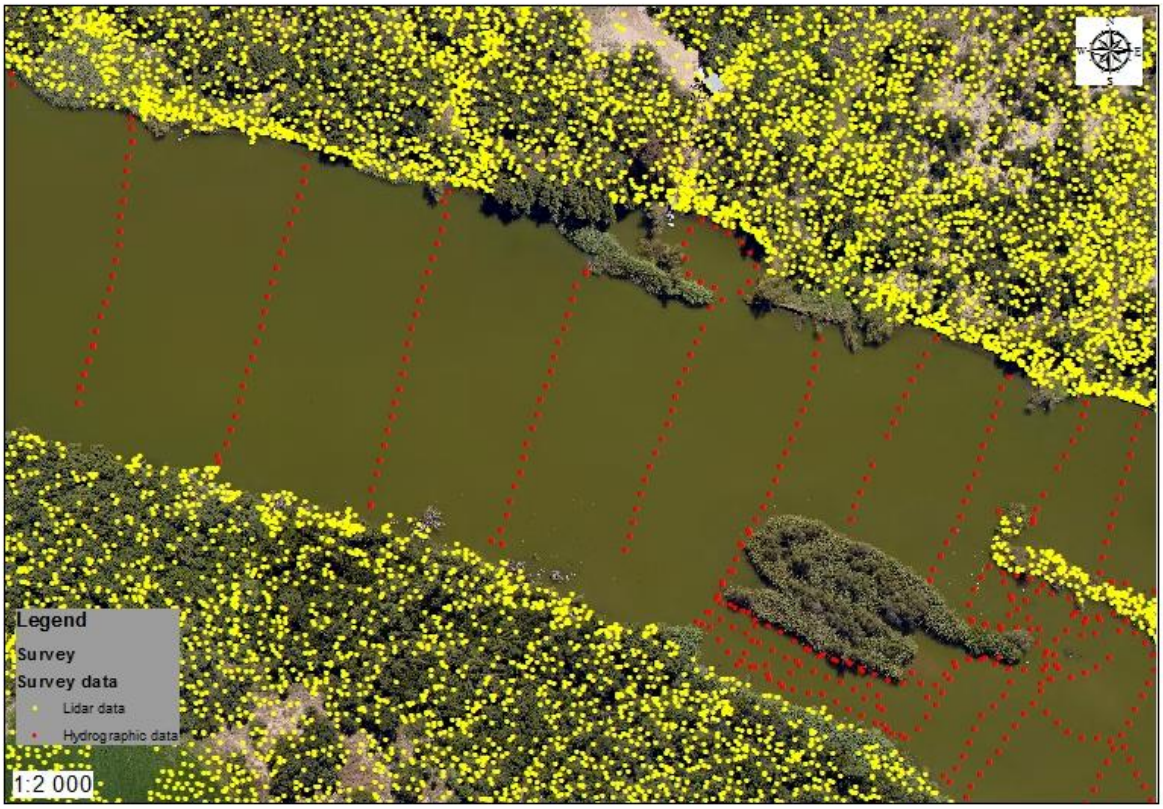

Figure 3-6. Survey point distribution sample in the study section of the Vaal River near Riverton, South Africa. Yellow indicates the lidar survey points. Red indicates hydrographic survey points.

Due to the distribution and directional varying trend that occurred, a TIN model was used for creating an elevation surface for the anisotropic data. The TIN model was created from the elevation points (Figure 3-7). The ellipse indicates errors occurring within the triangulation at the embankments due the varying spatial distribution between cross sections and lidar data.

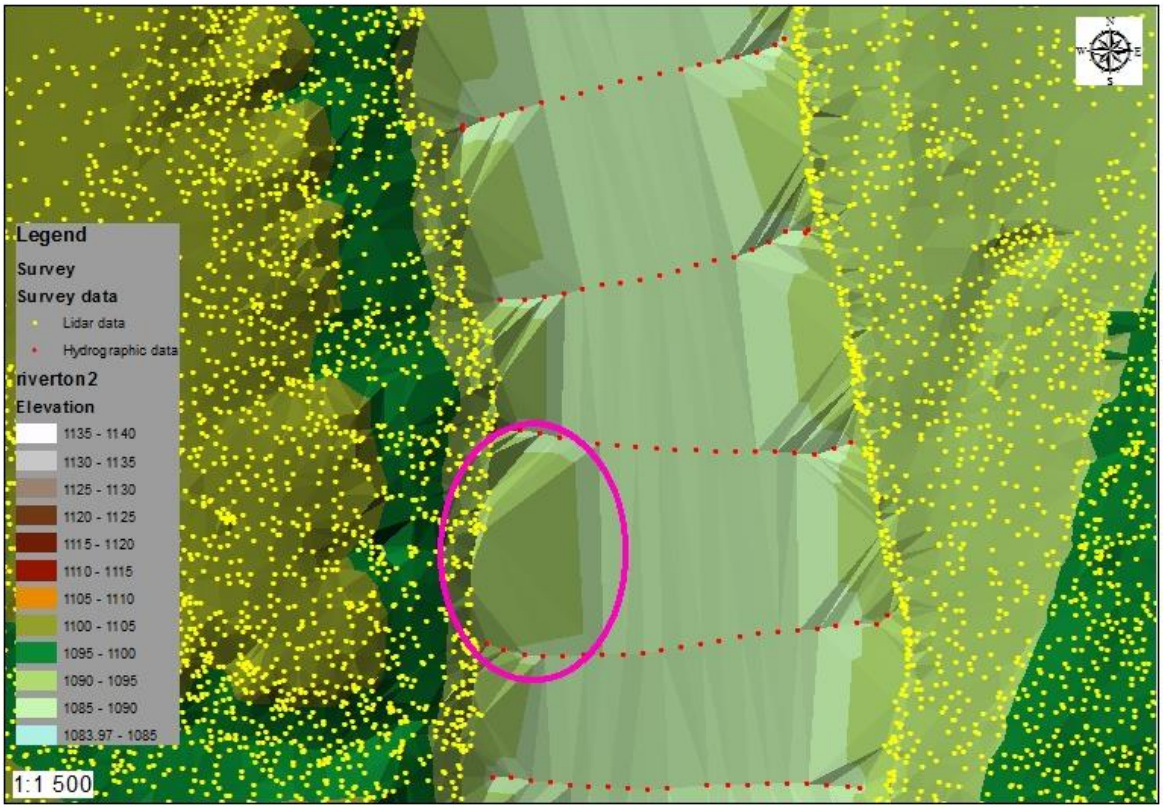

Figure 3-7. TIN model with triangulated errors. Pink ellipse indicates wrongly interpolated area between cross-sections.

Due to these errors, break lines and manual editing of triangle edges were used for correcting and optimising the interpolated triangulated surface. This was done based on the assumption that the embankments are parallel with the flow direction. A break line between the hydrographic survey points and lidar points were incorporated. This resulted in triangles not crossing the break line and producing a more consistent embankment profile. Even with break lines incorporated, not all the triangle faces were correct throughout the meandering river as the morphology changed. By using the TIN editing toolbar within ArcGIS, the triangle edges were modified to best represent the respective surfaces. Figure 3-8 represent the same extent as figure 3-7, but with the corrected triangulation.

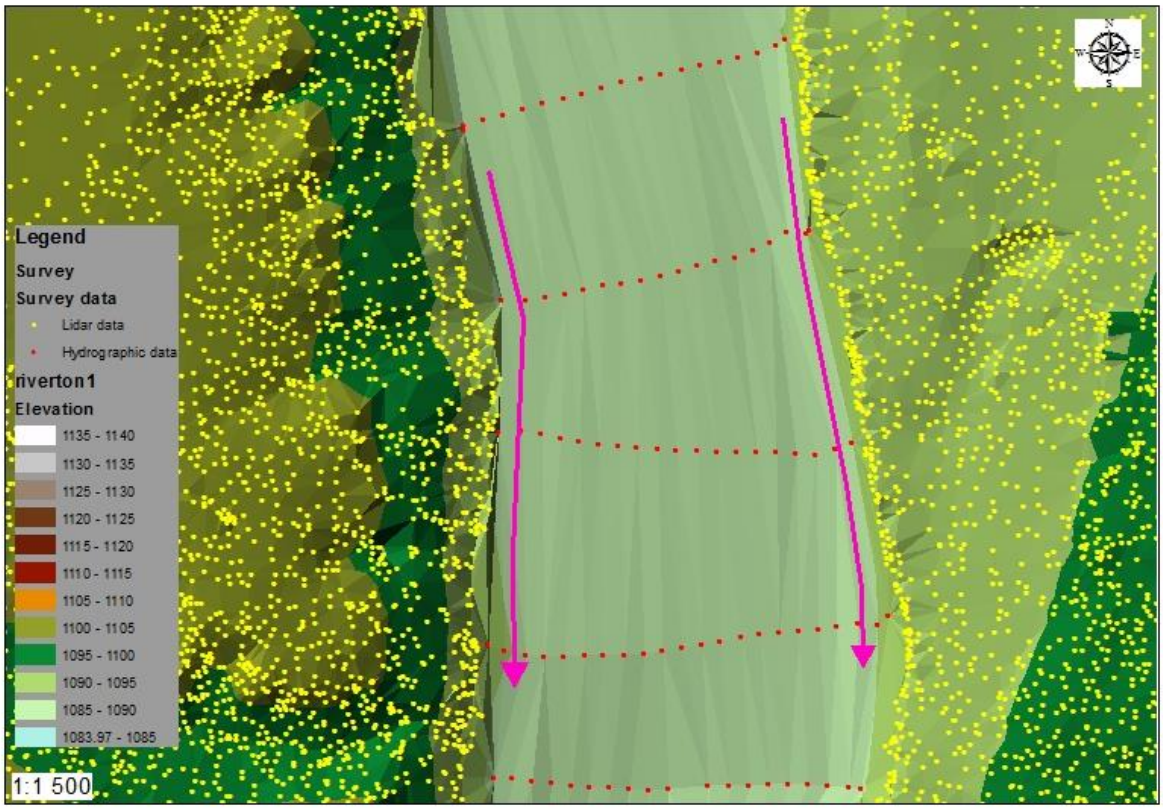

Figure 3-8 Final TIN model with corrected triangles. Pink arrows indicate assumed flow directions along embankments.

HEC-RAS uses a gridded format for importing the surface elevation. Therefore, the 3D Analyst Tools were used to convert the TIN model to raster format. The TIN to Raster conversion tool was used to create a 1m X 1m resolution raster of the terrain using a linear interpolation. This raster was then converted to a file of binary floating-point values representing the raster data using the Raster to Float tool.

3.5 Manning n values

The study area is affected by agricultural land, natural vegetation, rock formations and previously mined areas. Since this is not a study for overbank flood modelling, the main influencing coverage is the channel, rock formations within and close to the river and natural vegetation along the banks. A shapefile representing the respective Manning n values for each type of land cover was created, where high values denote more resistance to flow and low values less resistance to flow. This is done from the aerial imagery along with the DEM. The respective land cover was classified within 8 classes namely:

Main channel- The main channel with mainly bare soil and sediment at bottom

Channel side- The channel side with more prominent aquatic vegetation

Low vegetation- Grass with scattered bushes and shrubs

Open field- Mainly grass with no trees

Reeds- Reed bushes

Rock- Prominent rock formations

Scattered trees- Low vegetation with scattered trees

Thick trees- Thick and high trees and bushes

The respective Manning n values were then assigned to each cover type using table 2-1. The digitised polygons along with the respective assigned Manning n values can be seen in Figure 3-9.

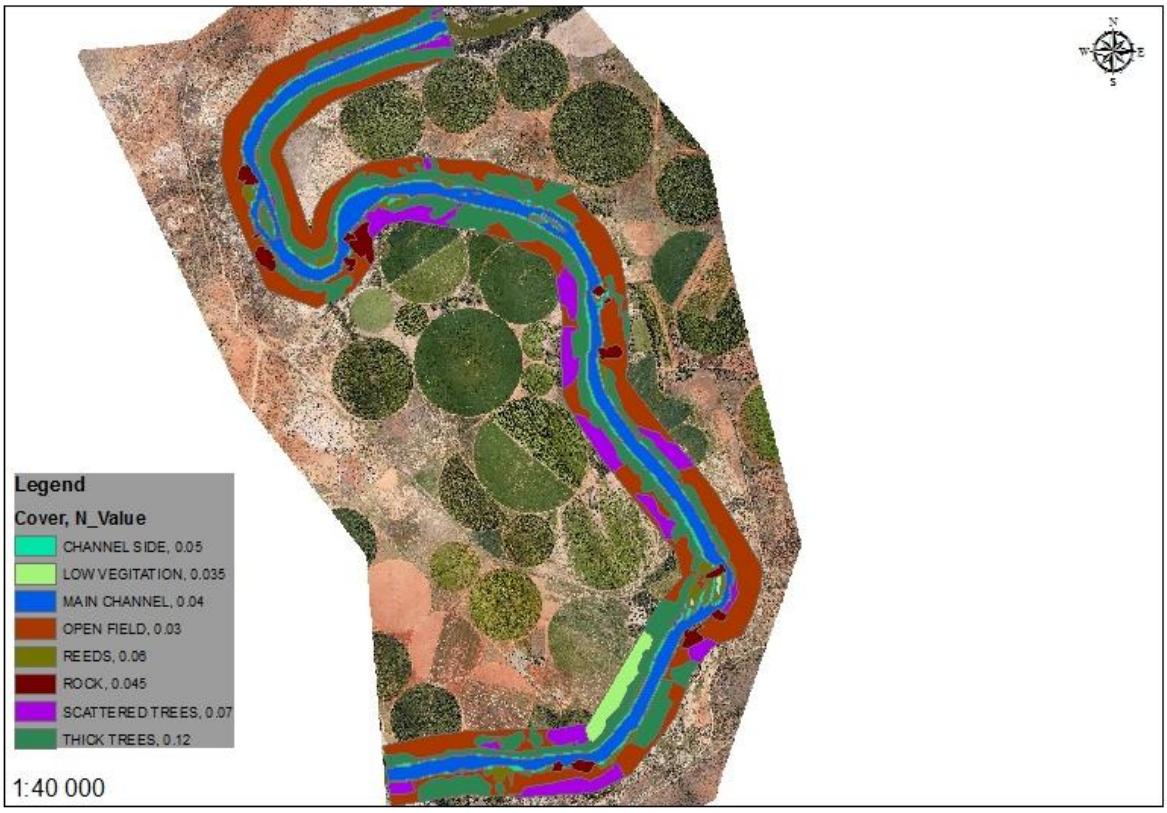

Figure 3-9 Land cover with respective Manning n values.

3.6 Flow data

Flow data were used as a boundary condition for the hydraulic model. Since the extent of the study area is in a section of the Vaal River with no inflow of tributaries, lateral inflow was ignored. The flow through the study area is greatly regulated by reservoirs and therefore sub catchments were ignored. The hydraulic properties of flow at specific instances for identifying abstraction locations are not time related as with flood modelling.

Flow measurements are only available at the Riverton station, which is located at the 930m cross section from the downstream boundary. The data can therefore be used as an observed rating curve for the gauge location.

Flow data at the Riverton station is based on stage measurements. The measurements are taken from a gauge plate with a calculated flow rate from a stage hydrograph at the station. The stage measurements represent the elevation with respect to the stage where the flow rate is 0m^3/s.

Water level measurements were obtained during the survey at different times. Since the gauge plate readings are taken every 12 minutes, the stage at the relative flow rates can be calibrated to the survey datum. This was done by matching GPS survey times to the station stage measurements. The stage elevation was subtracted from the GPS elevation to obtain a value for the gauge plate datum. The average of all the water level measurements (1091.341m± 0.023 SD) was used for the calculations. This may be due to GPS elevations being accurate to 15mm when surveying a topographic point survey style within RTK or rod placement during observations. Table 3-1 indicates the GPS, station measurements and calculated data for datum correction.

Table 3-1. Gauge plate datum correction data and calculations. Name- Name of the GPS field observation point; Z- GPS observation elevation; Code- Reference to water level observation; GPS Date- Date of observation; GPS Time- Time of observation; Q- Flow rate measured at gauge plate; Q Time- Time of flow rate measurement; Stage- Measured stage above gauge plate. Calibrated- Stage of water as meters above sea level based on the survey reference elevations.

Name	Z (m)	CODE	GPS DATE	GPS TIME	Q m^3/s	Q time	Stage (m)	Calibrated (m)
WL1	1091.511	WL	25-Mar-15	07:31:14	27.784	07:25:00	0.159	1091.352
WL2	1091.500	WL	25-Mar-15	10:31:32	29.204	10:25:00	0.167	1091.333
WL4	1091.490	WL	25-Mar-15	11:00:07	29.026	11:01:00	0.166	1091.324

WL5	1091.500	WL	25-Mar-15	11:04:36	29.026	11:01:00	0.166	1091.334
WL6	1091.474	WL	25-Mar-15	11:09:27	29.026	11:01:00	0.166	1091.308
WL7	1091.487	WL	25-Mar-15	11:14:09	29.026	11:13:00	0.166	1091.321
WL8	1091.520	WL	25-Mar-15	11:17:46	29.026	11:13:00	0.166	1091.354
WL9	1091.511	WL	25-Mar-15	11:18:00	29.026	11:13:00	0.166	1091.345
WL10	1091.562	WL	25-Mar-15	11:22:34	30.093	11:25:00	0.172	1091.390
WL11	1091.521	WL	25-Mar-15	11:26:05	30.093	11:25:00	0.172	1091.349
							Average	1091.341
							St Dev	0.023

Since this study is related to hydraulic occurrences at specific flow conditions and not to time dependent modelling, a theoretical hydrograph was created from the Riverton station measurements at specified flow rates. A range of flow rates between $0m^3/s$ and $500m^3/s$ was created. The corresponding stage measurements from the Riverton station were identified from the 2016 and 2017 measurements. Recent data were used to minimise the effect of river morphology. The respective stage measurements were converted to the study datum. The flow hydrograph created can be seen in Table 3-2.

Table 3-2. Flow Hydrograph at station 930 (Riverton station). Q- Flow rate; Gauge Z- Stage with reference to gauge plate; Calibrated Stage- Stage referenced to survey elevation.

Q m/s	Gauge Z	Calibrated Stage
0	0.000	1091.341
5	0.036	1091.377
10	0.058	1091.399
20	0.115	1091.456
30	0.172	1091.513
40	0.227	1091.568
50	0.283	1091.624
60	0.338	1091.679
70	0.392	1091.733
80	0.446	1091.787
90	0.499	1091.840
100	0.552	1091.893
150	0.809	1092.150
200	1.056	1092.397
250	1.292	1092.633
300	1.520	1092.861
350	1.741	1093.082
400	1.955	1093.296
450	2.168	1093.509
500	2.366	1093.707

3.7 1D Geometry setup

In order to conduct 1D hydraulic modelling, the geometry of the river had to be defined. The geometry set up was done though HEC-GeoRAS within ArcGIS. The RAS GIS import file consisted of geometric data necessary to perform hydraulic computations in HEC-RAS. The cross-sectional elevation data were derived from an existing DEM that include the channel and extending topography, while cross-sectional properties were defined from points of intersection between the created RAS layers. The required RAS layers created included the stream centreline and cross-sectional cut lines. The optional RAS layers created include the main channel banks, flow path centrelines, land use, ineffective flow areas and blocked obstructions. Data created were stored in a geodatabase based on the name of the map document and is stored in the same location as the .mxd file.

The river and reach network is represented by the stream centreline layer. The network was created on a reach by reach basis, starting from the upstream end and working downstream following the channel thalweg. Each reach is comprised of a river name and a reach name. The stream centreline layer was used for assigning river stations to cross sections and allow HEC-RAS geometric editor to display the distance chainage of each cross-section. It was also used to define the main channel flow path. The reach is defined as Vaal River with the reach section name being Riverton.

The bank lines layer distinguishes the main channel flow from flow in the overbanks. Bank stations were assigned to each cross section based on the intersection of the bank lines with the cut lines. Left and right bank lines were created. Only two bank lines may intersect each cut-line and the orientation is not important since the stations were computed from the intersection. The bank lines were constructed on the left and right embankments since no overbank flooding was modelled.

The flow path centrelines layer was used to identify the hydraulic flow path in the left overbank, main channel, and right overbank by identifying the centre of mass of flow in each section. Creating the flow path centreline layer assisted in properly laying out the cross-sectional cut lines. The stream centreline layer already exists and were copied for the flow path in the main channel. Flow paths were created in the direction of flow upstream to downstream. Downstream reach lengths were calculated for each cut line based on the distance between cut lines along the flow path centrelines for the left overbank, main

channel, and right over bank. Each flow path line was identified accordingly as being in the left overbank, main channel or right overbank.

The cross-sectional location, position, and extent are represented by the Cross-Sectional cut line layer. Cut lines should be constructed perpendicular to the direction of flow. It is therefore necessary to “dog-leg” the cut lines to conform to this one-dimensional flow requirement (Brunner 2016). These cut lines may not intersect each other and must cross the stream centreline only once. The cross-sectional cut lines should be oriented from the left overbank to the right overbank, when orientated downstream. The cut lines represent the horizontal location of the cross sections and the station-elevation data were extracted along the cut line from the DTM. Cross-sectional cut lines were created 30m apart, based on the stream centre line, and edited to conform to the specific rules. Additional cross sectional cut lines were added for features such as bridges, where contraction and expansion occur. Each cut line was attributed with a river and reach name based on the names defined in the stream centreline layer. A river station was calculated for each cut line based on the distance from the most downstream point on the river. Calculations were based on the from station and to station values in the stream centreline layer. The calculated station was used to order cross sections when computing water surface profiles in HEC-RAS. The main channel banks of each cut line were computed from the bank lines layer. The left bank and right bank fields were created from the distance along the cut line to the bank station position based on the intersection of the cut line and bank line. The downstream reach lengths were computed for the left overbank, main channel and right overbank based on the length of the flow path lines in the flow path centrelines layer (Brunner et al. 2015).

The Ineffective Flow Areas layer identifies portions of the channel or floodplain that do not actively convey flow. This layer was created in areas of zero velocity such as the dead-water zones upstream and downstream of the bridge. The position of ineffective areas was extracted based on the intersection of the Ineffective flow areas layer and the cross-sectional cut lines layer. Ineffective flow areas were also created for gullies where no active flow occur. The beginning and ending position of intersections between the ineffective flow area and the cut line was calculated as well as the corresponding elevation from the DTM. The elevation extracted from the DTM acted as a “trigger” elevation in HEC-RAS for turning off the ineffective areas.

The blocked obstructions layer identifies portions of the floodplain that permanently remove flow area from the cross section. The position of blocked obstructions was extracted based on the intersection of the blocked obstructions layer and the cross-sectional cut lines layer. Since no flood modelling will be done, flow will not exceed the bridge, and blocked obstructions were used for accounting for bridge supports within the river and were digitised from the aerial imagery. Blocked obstruction data were extracted based on the intersection of the cut lines and blocked area polygons and was written to the blocked positions table. The beginning and ending position of the intersection between the blocked area and the cut line was calculated as well as the corresponding elevation from the DTM. An elevation of 1095m is specified due to the blocked obstruction elevations not incorporated into the DEM. This elevation was based on the pillar elevations extracted from the DEM where the bridge starts at the bank.

A land use Layer was created from the previously created land cover layer. Manning's n values were extracted for each cross-sectional cut line. The output table is populated for each cut line and the Manning's n value with the corresponding location on the cut line were computed. The location of the beginning of each land use area polygon was reported as a fraction along the cut line.

HEC-GeoRAS keep track of the feature classes generated, data layers used for extracting attribute information and the tables that hold extracted data. The layer setup allows specified data to be written to the RAS GIS import file by choosing which RAS layers to use. The layers required by GeoRAS is the stream centreline (2D) layer, the cross-sectional cut Lines (2D) layer, and the cross sections (3D) layer (Brunner 2016). The optional layers incorporated within the study are bank lines, flow paths, ineffective flow areas, blocked obstructions and steam profiles. The manning, ineffective position and blocked position tables were added for export to HEC-RAS. The geometric data were then exported to an ASCII RASExport.sdf file to be imported into HEC-RAS. A sample of the geometric data created can be seen in Figure 3-10.

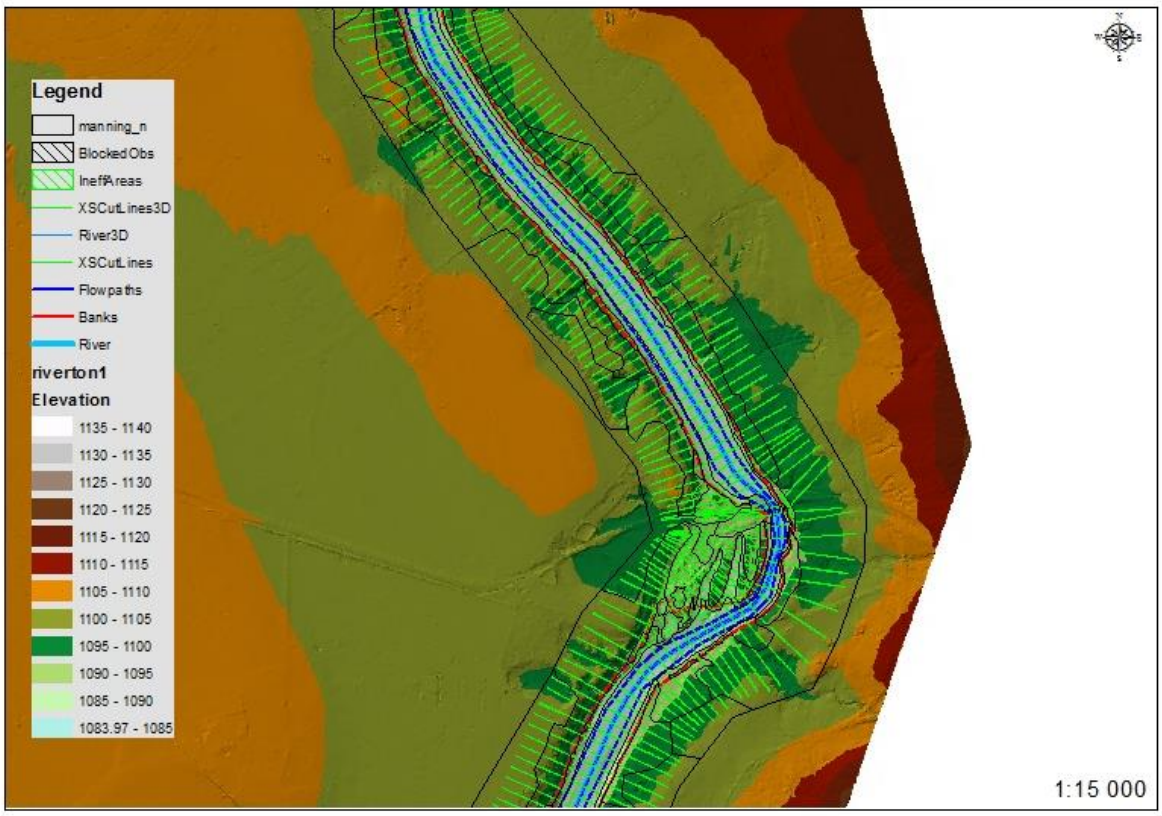

Figure 3-10. Sample of Geometric data created in HEC-GeoRAS.

3.8 1D model setup

The geometric data that has been processed in ArcGIS using HEC-GeoRAS was imported into HEC-RAS. The binary floating raster representing the DEM was also imported and the project spatial reference set to WG25. All bank stations, blocked obstructions, manning n values and orientations were defined with respect to cross-sectional cut lines from the calculations through HEC-GeoRAS. River stations are assigned a chainage according to the distance starting at the downstream cross sections. The imported data of the study area can be seen in Figure 3-11.

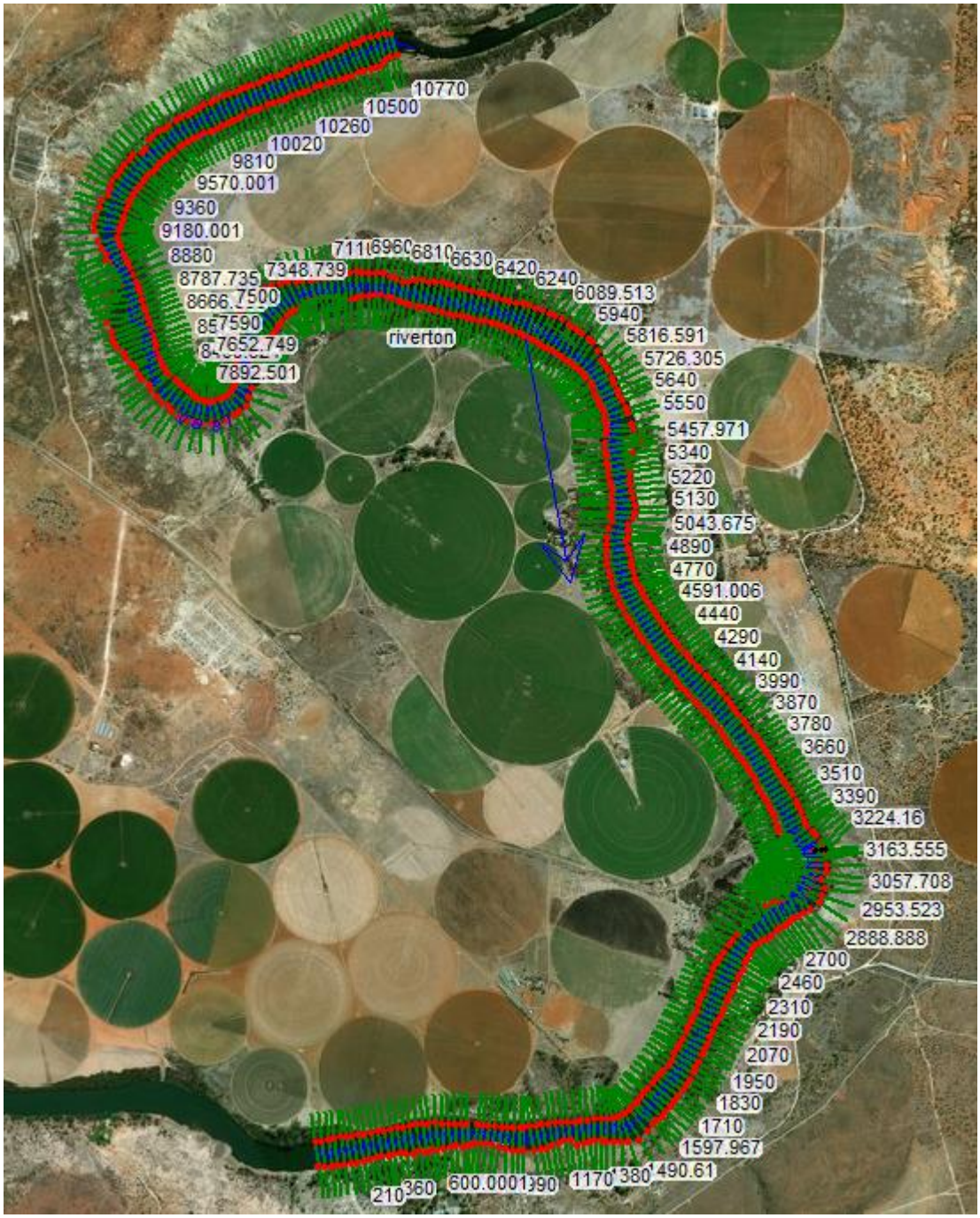

Figure 3-11 1D Geometry data HEC-RAS. Cross-sections- green; left and right stations on cross-sections- red; stream centre line- blue. In addition, the flow direction is indicated by a blue arrow as well as the cross-section directions. Cross-sections are labelled according to the chainage distance from downstream.

3.8.1 Boundary Conditions 1D

Once all the geometric data were defined and set up, flow data and boundary conditions were defined. Unsteady flow was used for this model due to the relative flat slope of the river section. Therefore, the 1D unsteady flow equations defined in section 2.6.2 were used.

It is required to enter boundary conditions at all of the external boundaries of the system, as well as any desired internal locations, and set the initial flow and storage area conditions at the beginning of the simulation. Boundary conditions were defined from the Boundary Conditions tab in the Unsteady Flow Data editor. River, Reach, and River Station locations of the external bounds of the system were automatically entered into the table. Boundary conditions were entered by first selecting a cell in the table for a particular location, then selecting the boundary condition type that is desired at that location. From the options menu, observed and measured data were defined. A rating curve was defined at river station 930. This station corresponds to the location of the Riverton station gauge. The calibrated values calculated in table 3-2 were used to define the rating curve and can be seen in figure 3-12.

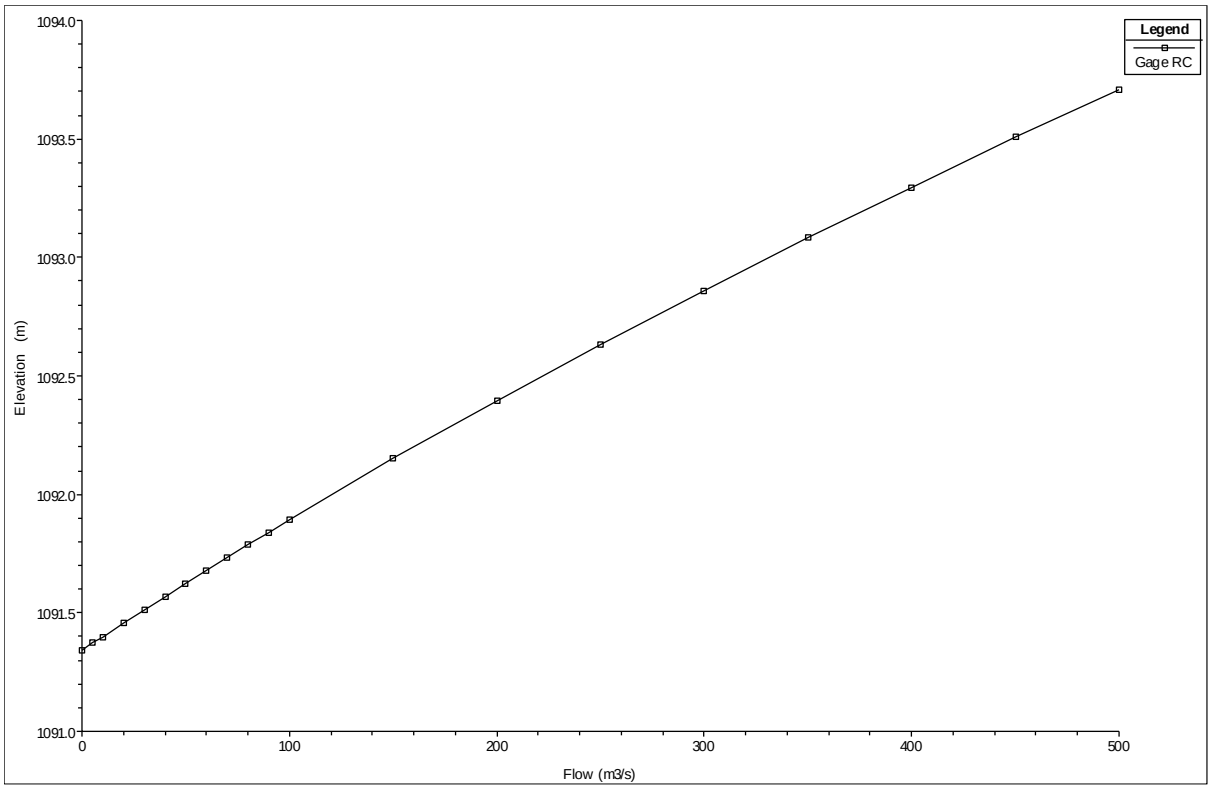

Figure 3-12 Rating curve at river station 930.

A flow hydrograph was used for defining the upper and lower boundary conditions at stations 30 and 10774, respectively. The predefined flow rate rage of 0 m^3/s-500 m^3/s was defined with a 1-day data time interval to allow for runoff and stabilisation between flow instances.

3.9 Accuracy and Calibration

Model accuracy can be defined as the degree of closeness of the numerical solution to the true solution (Brunner 2016). An unstable numerical model is one for which certain types of numerical errors grow to the extent at which the solution begins to oscillate, or the errors become so large that the computations cannot continue. This is a common problem when working with an unsteady flow model of any size or complexity (Brunner et al. 2015). A sensitivity analysis was carried out on the 1D model in order to determine the impact of geometric and computational parameters on the model results and stability. The parameters investigated for the sensitivity analysis were cross sectional spacing, time step interval, θ-weighting and manning friction coefficients.

3.9.1 Cross sectional spacing sensitivity analysis

Cross sections should be placed at appropriate locations in order to describe the changes in geometry. Additional cross sections should be added at locations where changes occur in discharge, slope, velocity, and roughness (Brunner 2016). The best way to estimate a computational time step for HEC-RAS is the Courant number (Brunner 2016). The Courant number is a numerical solution that measures how the water particles behave. The Courant number is defined as follows:

$$C = \frac{v * \Delta t}{\Delta x}$$

Where: C = Courant number

v = Flow velocity

Δt = Computation time step

Δx = Spatial step. Distance between cross-sections or size of mesh.

When cross sections are spaced far apart and the changes in hydraulic properties are great, the solution can become unstable (Brunner et al. 2015). Cross sections spaced too far apart will cause additional numerical diffusion due to the derivatives with respect to distance being averaged over to long of a distance (Brunner et al. 2015). If the distance between cross sections is too small, then the Courant number would be much smaller than 1.0 and the model may also become unstable(Brunner et al. 2015). Cross sections that are too close

together result in the derivatives with respect to distance to be overestimated (Brunner et al. 2015).

A cross sectional spacing of 30 m and 60m were used to determine the effect of cross sectional spacing on the model. For the 30m spacing the cross-sectional flow error was examined at the maximum water surface elevation. The flow error is within 0.07m^3/s for all the cross sections. For the 60m cross sectional spacing the flow error is within 0.08 m^3/s. These cross-section profiles were extracted from the DEM and not interpolated from other cross sections. These results show that the model output is affected by the cross sectional spacing. The extent of the effect is negligible for this study since it is very small. Therefore, the original cross sectional spacing of 30m will be used for further calculations for the study.

3.9.2 Time step sensitivity analysis

When the solution scheme solves the unsteady flow equations, the derivatives are calculated with respect to distance and time. If the changes in hydraulic properties at a given cross section are changing rapidly with respect to time, the program may go unstable (Brunner et al. 2015). If a time step is selected that is much larger than what the Courant condition would dictate for a given flood wave model, stability problems can occur (Brunner et al. 2015). Too small of a time step will cause the leading edge of the flood wave to steepen and possibly to the point of oscillating and going unstable (Brunner et al. 2015). The time steps assessed for the computational interval along with the minimum courant number and maximum courant number can be seen in table 3-3.

Table 3-3 Time step computational intervals results

Time step	Courant min	Courant max
6h	226.07	3886.691
1h	35.04	649.95
30min	17.49	325.01
10min	5.8364	108.319
2min	1.167	21.66
1min	0.583	10.83

It can be seen that the courant number lowered as the time decreased. The difference between the maximum and minimum courant number decreased drastically according to the computational interval. Lower courant numbers are obtained from broader cross sections with low flow velocities. The higher courant number occurred at section 3169 and corresponded to the cross section upstream of the bridge where major contraction occurred. The 2-minute interval have relatively close courant numbers (Table 3-3). By inspecting the stage error with a 2-minute computational interval a maximum error of 4.08 X 10^{-3} are obtained. The model ran smooth with the 2-minute time interval with no oscillating stage flow hydrographs and was therefore used for further computations.

3.9.3 Theta parameter sensitivity analysis

Theta is a weighting applied to the finite difference approximations when solving the unsteady flow equations. Theoretically Theta can vary from 0.5 to 1.0. However, a practical limit is from 0.6 to 1.0 Theta of 1.0 provides the most stability, but less numerical accuracy. Theta of 0.6 provides the most accuracy, but less numerical stability. The model was run with a theta factor of 1 and theta factor of 0.6. There is no change in the solution when a smaller theta weighting factor is used. It is concluded that the lower theta factor influence is insignificant in this model and therefore a theta weighting factor of 1 was used to ensure greater stability.

3.9.4 Manning's n sensitivity analysis

Roughness coefficients are one of the main variables used in calibrating a hydraulic model. For a free-flowing river, roughness decreases with increased stage and flow. If the banks of a river are rougher than the channel bottom due to trees and brush, then the composite n value will increase with increased stage. Sediment and debris can also play an important role in changing the roughness. The roughness coefficients can be changed from the manning tables within the model geometry. By inspecting the stage and flow hydrograph at station 930 where the observed data were obtained, a stage difference of 12 cm was observed for higher flow rates. This indicates that the base manning n values used were a good estimation but were altered within a realistic range. The manning coefficients for the main channel, channel sides and vegetation along the embankments were lowered by 0.01 to better match the observed stage and flow hydrograph. The calibration result from the manning n values can be seen in figure 3-13. The rating curve indicates a close match

between the modelled and observed data. A 3cm error occurred at the maximum flow rate of 500m^3/s.

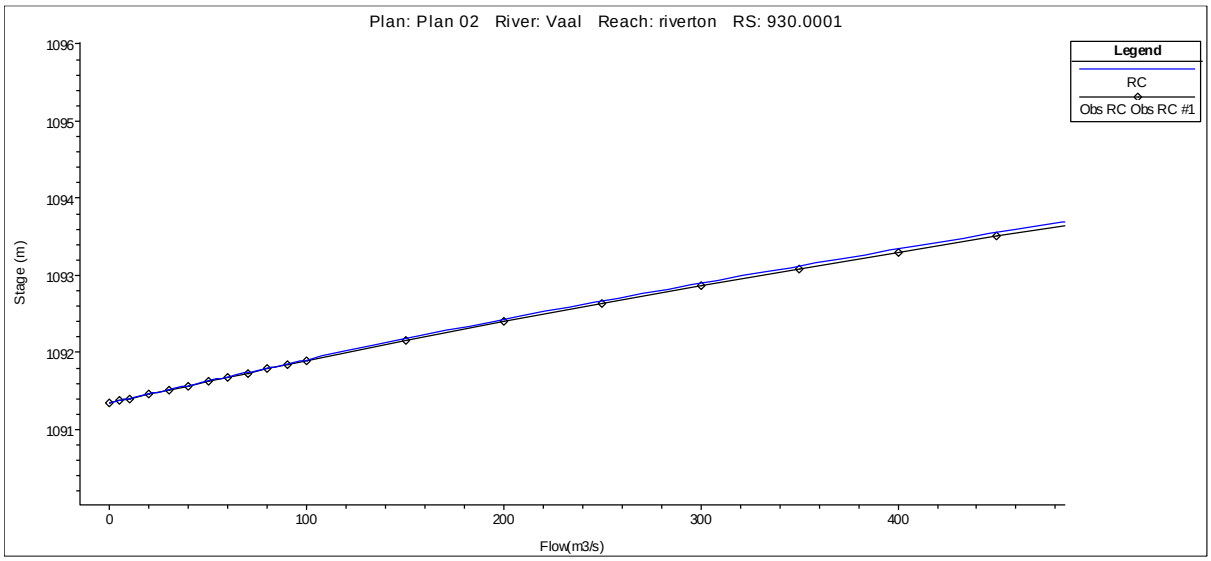

Figure 3-13 Rating curve at Riverton station 930.

The initial conditions of the manning n values closely represented the observed stage and flow hydrograph. This is due to the accurate assumptions made during base manning coefficients defined and low flow velocities. By comparing aerial imagery with the resulting surface elevations, no visual errors could be identified that may indicate contraction or manning coefficient errors.

3.10 2D model Setup

The 2D geometric setup was done through HEC-RAS. The DEM was imported as a terrain into HEC-RAS. The land cover layer representing the manning coefficients was directly imported into Ras mapper from the shapefile created and the attributes representing the cover and relative coefficient defined accordingly.

2D Flow Areas are regions of a model in which the flow through that region will be computed with the HEC-RAS two-dimensional flow computation algorithms. 2D flow areas are defined by laying out a polygon that represents the outer boundary of the 2D flow area. The HEC-RAS 2D model uses a finite mesh for solving computations. This algorithm was developed to allow for the use of a structured or unstructured computational mesh.

A 2D flow area polygon was drawn along the river covering the region of interest. From the 2D flow area editor a nominal grid size of 5m X 5m was defined. The computational points

were generated and amounted to 200563 points over the study area. These points were x and y coordinates that represented the cell centres. The mesh was then computed but with a default manning n value of 0.6. Since the cell size was relatively small with respect to the flow area, break lines were not defined for the embankments. Break lines were defined along the bridge featured in order to direct flow accordingly. Cells created next to the 2D flow area boundary and break lines were irregular in shape in order to follow the defined polygon or line. The mesh generation tools use the polygon boundary for creating the mesh and try to ensure that no cell is smaller in area than defined cell size. The cells around the boundary will be equal to or larger than the nominal cell size. From RAS mapper the Terrain and Land cover layer was associated with the 2D geometry. This enables elevation data and manning coefficients to be incorporated for calculation of the 2D area hydraulic tables. The default manning values are over written where covered by the land cover layer.

Additionally, three cross sections were imported from the 1D model geometry. These cross sections correspond to a downstream boundary, the 930 station for the observed data at the Riverton station and the upstream boundary. This was done to define the observed gauge plate reading and to compare the 2D model with the 1D model.

2D flow area boundary conditions were then assigned. By using the SA/2D Area BC Lines drawing tool on the Geometric Data editor Tools button bar, the inflow and outflow boundary conditions were defined and named accordingly. The boundary condition type was defined through the unsteady flow data editor. An example of the resulting 2D geometry can be seen in Figure 3-14.

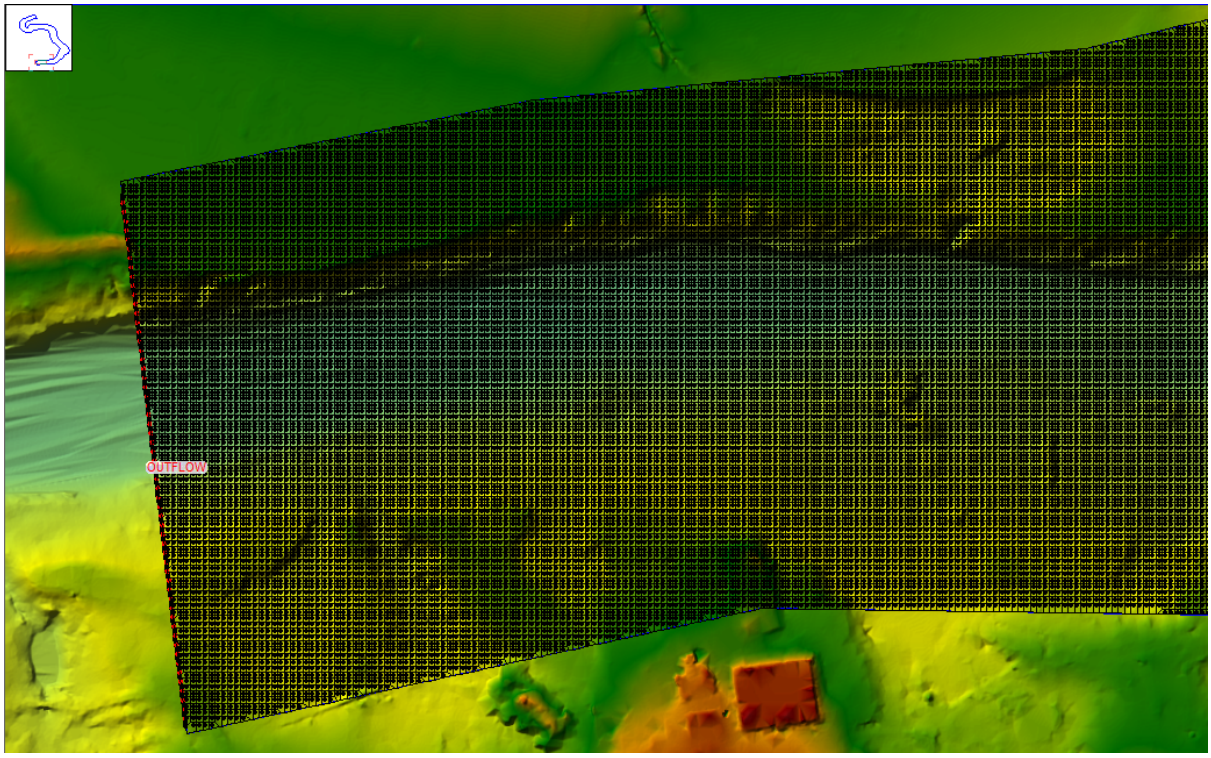

Figure 3-14 2D Geometry indicating the calculated mesh and downstream boundary condition.

The flow conditions for the 2D model were set up by defining a flow hydrograph for the inflow and outflow conditions. The flow hydrographs represent the predefined flow range of 0 m^3/s-500 m^3/s and were defined with a 1-day data time interval to allow for runoff and stabilisation between flow instances. An energy gradient slope of 0.05 was defined that correspond to the channel bed slope. The upstream and downstream boundary conditions for the cross sections were defined as flow hydrographs with a flow range of 0 m^3/s-500 m^3/s are defined with a 1-day data time interval from table 3-2. The cross section representing the Riverton station has a rating curve assigned as a boundary condition as calculated in table 3-2. The initial stage of the model was set to 1091.341m and correspond to the base water surface elevation at 0 m^3/s flow rate. The 2D model unsteady flow equations in section 2.6.3 was used for calculating the hydraulic properties.

A sensitivity analysis was carried out on the model and the computational time step interval was investigated. The model was run at various computational time step intervals ranging from 1 hour to 3 minutes. Longer computational time steps produced large elevation errors over cells and cross sections. The 3-minute time step interval produced elevation errors of over 3 meters, suggesting that the diffusive wave approximation became unstable. The

optimal time step interval observed was a 10-minute interval. With a 10-minute interval the maximum error was within 2cm of elevation with the majority of the errors below 1cm in elevation. The errors obtained were cell and cross section dependent. The inspection of the error locations referred to cells bordering 2D flow area. These relatively small errors occur outside of the flow area of the river maximum stage extent and were consequently ignored. The errors may be a result of the cell construction and affected by the edges.

The model proved to be sensitive to the computational time step interval. Due to the relatively small cell size used, computational times were greatly influenced by the time interval. Due to the interest of flow along the river embankments, cell sizes were not enlarged in order to improve computational time.

3.11 Hydraulic modelling interpretation

This section will discuss and interpret the calculated hydraulic properties and surfaces obtained from the 1D and 2D hydraulic models of the Riverton study area. This concerns the results produced by hydraulic computations as well as resulting maps of each model used for further analysis within the study. The hydraulic modelling results will be incorporated into the spatial analysis for identifying abstractions locations and concern velocity, water surface elevation and stream power surfaces.

3.11.1 1D model interpretation

After running the calibrated 1D model, a variety of output resulting maps and tables were generated (Figures 3-15,3-16,3-17). From the RAS Mapper environment, a velocity, depth and water surface elevation raster layers were created (Figures 3-15,3-16,3-17). The surfaces can be animated through the time series defined by the flow hydrographs from the boundary conditions. In the case of the study each day interval corresponded to the defined flow rate in the rage from 0 m^3/s-500 m^3/s. RAS Mapper allow for GIS functionality where the order, transparency, symbology and classification of layers can be changed. Velocity and flow directions can be viewed through static arrow and/or particle tracing for animated visualisation of the results.

Different stages of the surface results were inspected through RAS Mapper. This is to ensure that the model behaved as expected and no major errors occurred. The areas where ineffective flow areas occurred were inspected for sufficient coverage. Higher stages related to high flow rates were inspected along the river for identifying gullies and damming effects.

At these locations additional ineffective flow areas were defined to remove undesired flow that occur outside of the channel flow path. Contractions within the river were inspected to ensure that flow behave as expected. The placement of cross sections at significant contraction and expansion locations will greatly influence flow tendencies through these sections. This is due to the velocity head losses being calculated from the upstream cross section to the next downstream cross section. A sample of the resulting map inspected can be seen in figure 3-18. The map indicates the calculated river depth, flow velocities and flow direction.

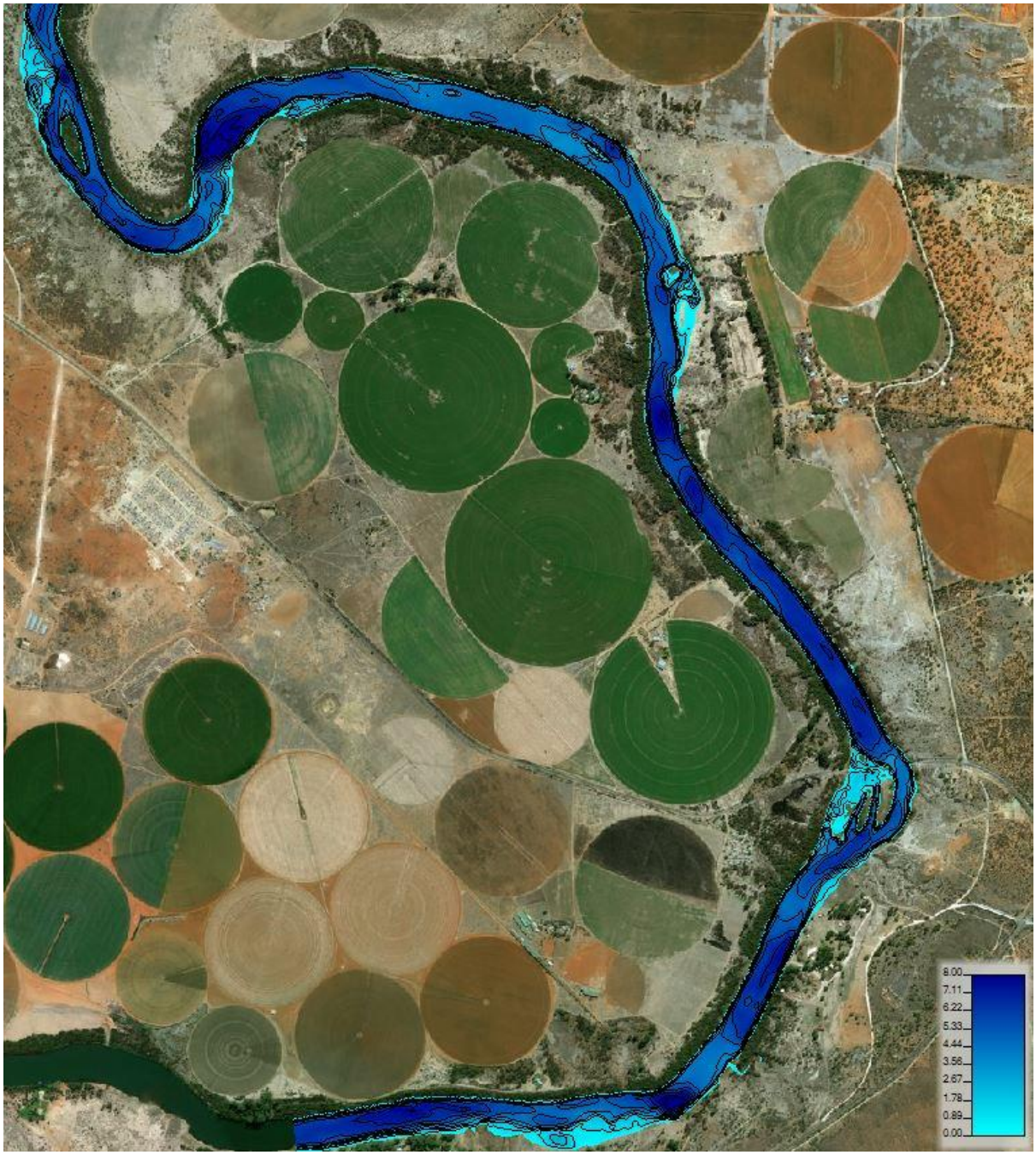

Figure 3-15 RAS mapper 1D model depth map. Black- Isobath; Shallow- Light Blue; Deep- Dark Blue.

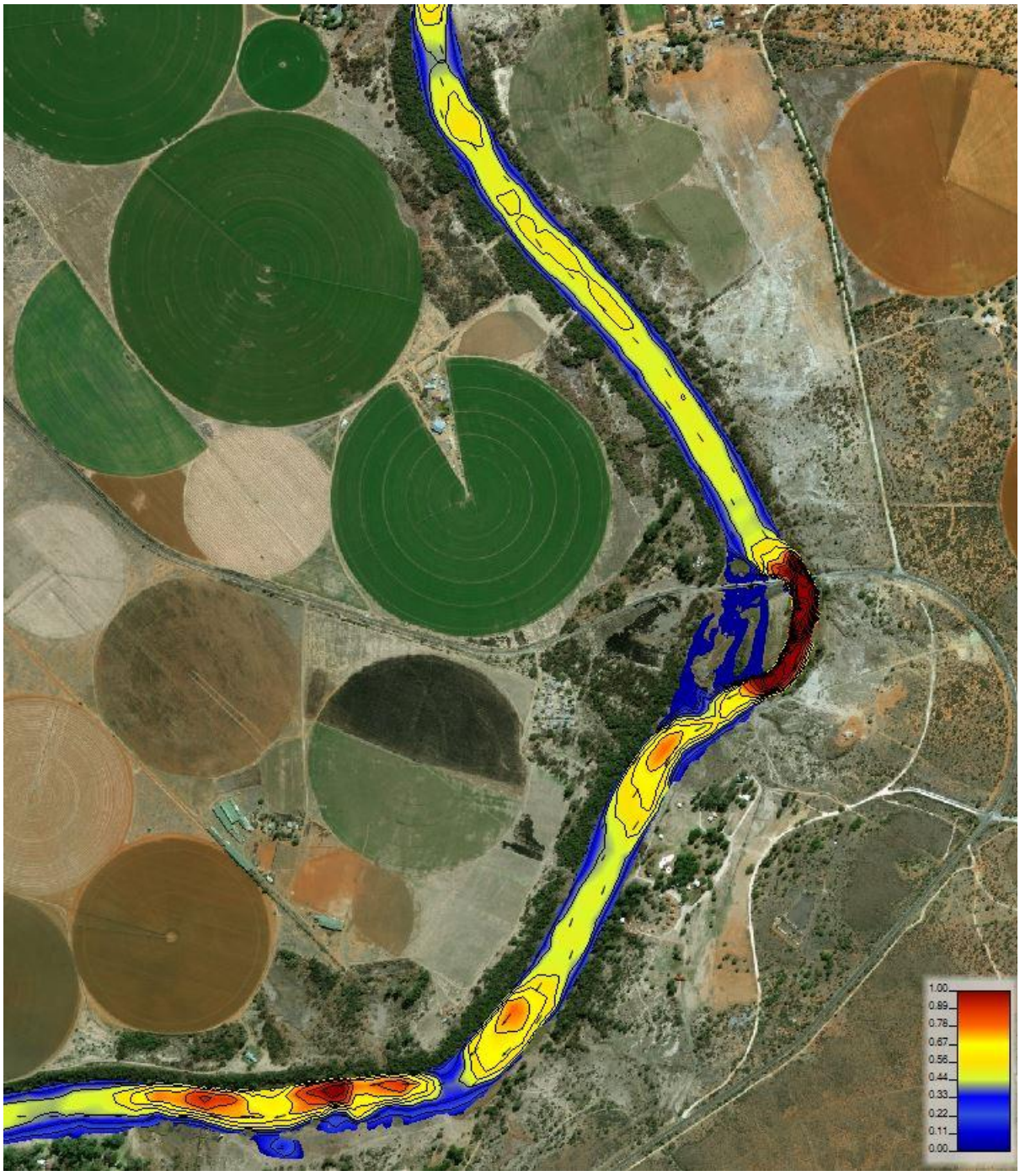

Figure 3-16 RAS mapper 1D model velocity map. Black- Isopleth indicating surface velocity; Red- high surface velocity; Blue- low surface velocity; Black arrows- surface velocity direction and magnitude.

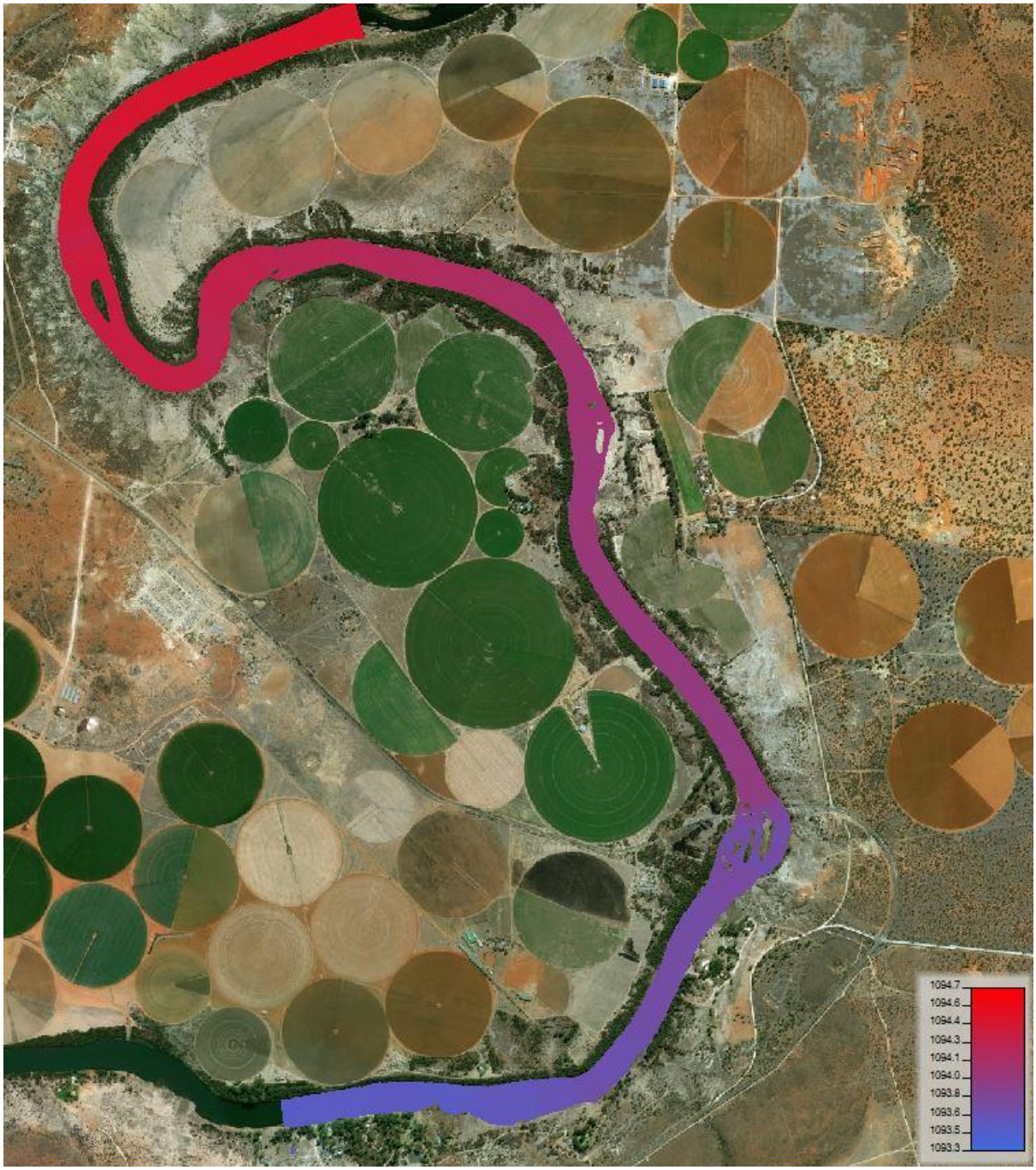

Figure 3-17 RAS mapper 1D model water surface elevation (WSE) map. Pink- High water surface elevation; Blue- Low water surface elevation.

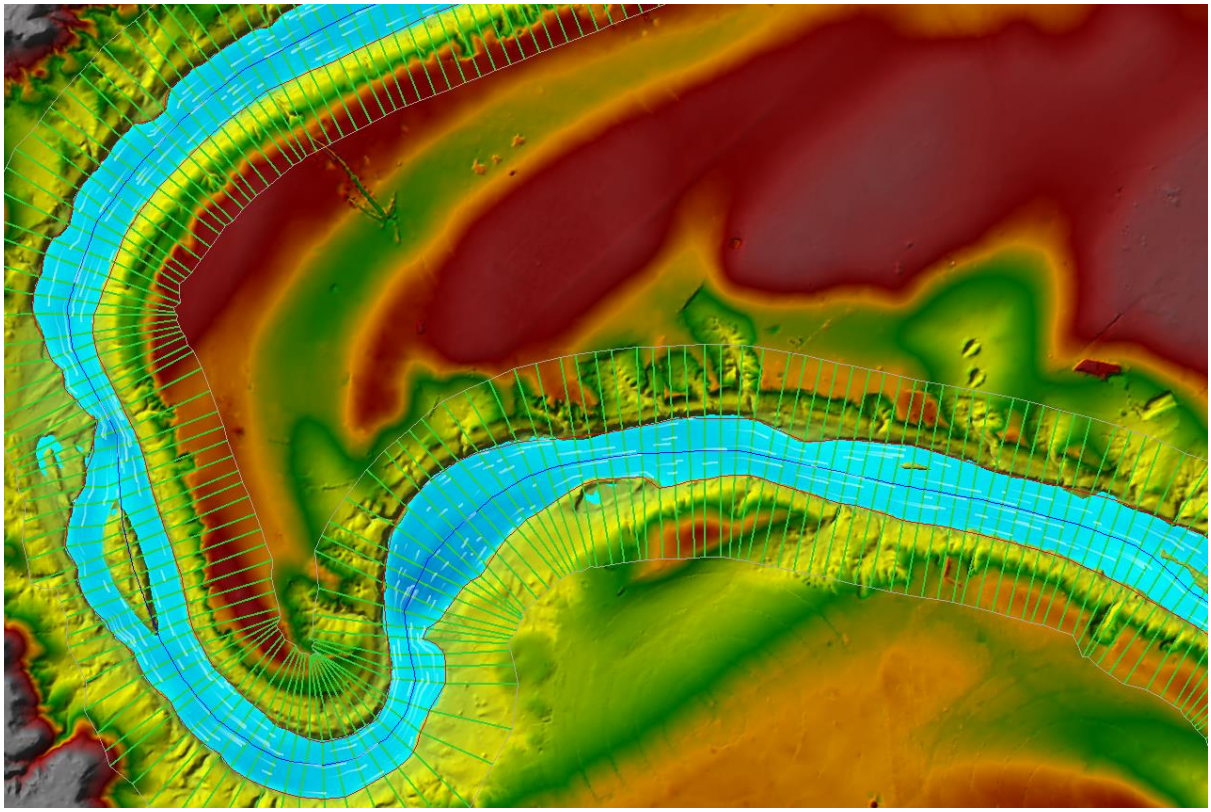

Figure 3-18 RAS mapper 1D model result. Green lines- cross-sections; Blue line- stream centre line; White- velocity particle tracing; Blue surface- depth range.

The profile plot allows for a quick overview of the entire study area. The plot was inspected for sudden changes to the energy grade line and the water surface. In general, these two variables should transition smoothly along the channel. Rapid changes in the energy or the water surface need to be inspected and ensured that the results are correct. The water surface at each flow rate can be seen on the profile plot in figure 3-19. It can be seen that at a flow rate of 0 m^3/s the water surface is flat. As the flow rate increases the slope of the water surface increases. Cross section locations where contractions within the river occurs produced less consistent water surface elevations. These deviations from a smooth line are expected due to the natural crump weir created. The water flowing over the weir produced a hydraulic jump. By inspecting the energy grade at these location, a smooth transition occurs.

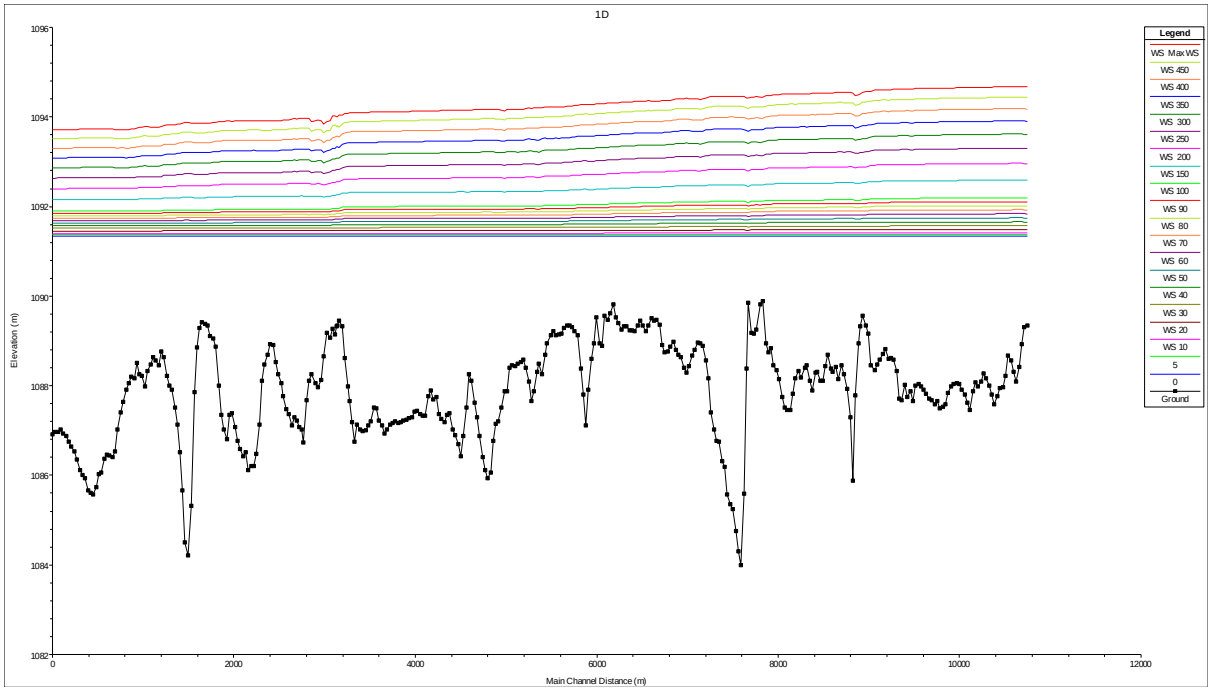

Figure 3-19 Profile plot of 1D model water surface. Black- river bed profile main channel; Coloured lines- predicted water surface at different flow rates.

The general profile plot allows for graphical and tabular displays of the model output for the entire river section. Any variable that is computed at a cross section can be displayed in the profile plot. An example of the channel velocity at the maximum modelled flow rate can be seen in figure 3-20. It is evident that the channel velocity changes as the channel dimension changes. From the graphs inspected for the range of flow rates, it can be seen that the flow rates of the left channel bank tend to be higher than the right channel bank for the majority of the time. The plotted Froude number is below 1 for the entire channel, indicating that the channel stays in a subcritical flow state, although a mixed flow regime was used for modelling.

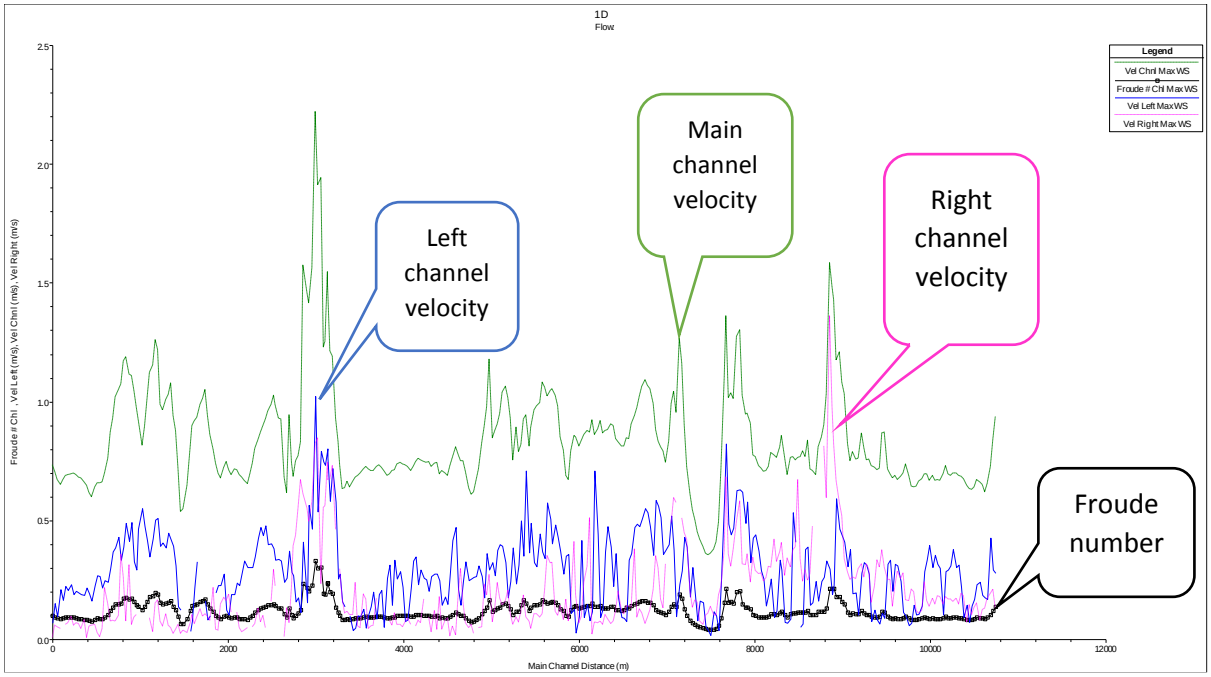

Figure 3-20 Velocity plot of channel main, Left channel and Right channel.

The results of the 1D model are satisfactory with no prominent computational errors observed from model result. Flow across the river bed behaved according to the river morphology. Hydraulic jumps occurred within the model and occurred at contractions within the river as expected. The depth map represents crump weir like morphological features that extend to the width of the river. Ineffective flow areas were applied sufficiently and correctly to contain flow within the active flow area. Cross sections were placed effectively and contractions within the river could be modelled with acceptable results.

3.11.2 2D model interpretation

The overall appearance of the 2D model is very smooth and represents natural flow in rivers. The inlet boundary condition flow stabilised quickly across the channel, confirming that the 0.05 energy gradient slope defined in the boundary conditions proved to be acceptable. Flow over the river reach represented flow as expected. External flow reaches represented flow accurately at higher stages. Areas where ineffective flow occurred were represented with no flow. Figure 3-21 represents the 2D model results. The map indicates the calculated river depth, flow velocities and flow direction.

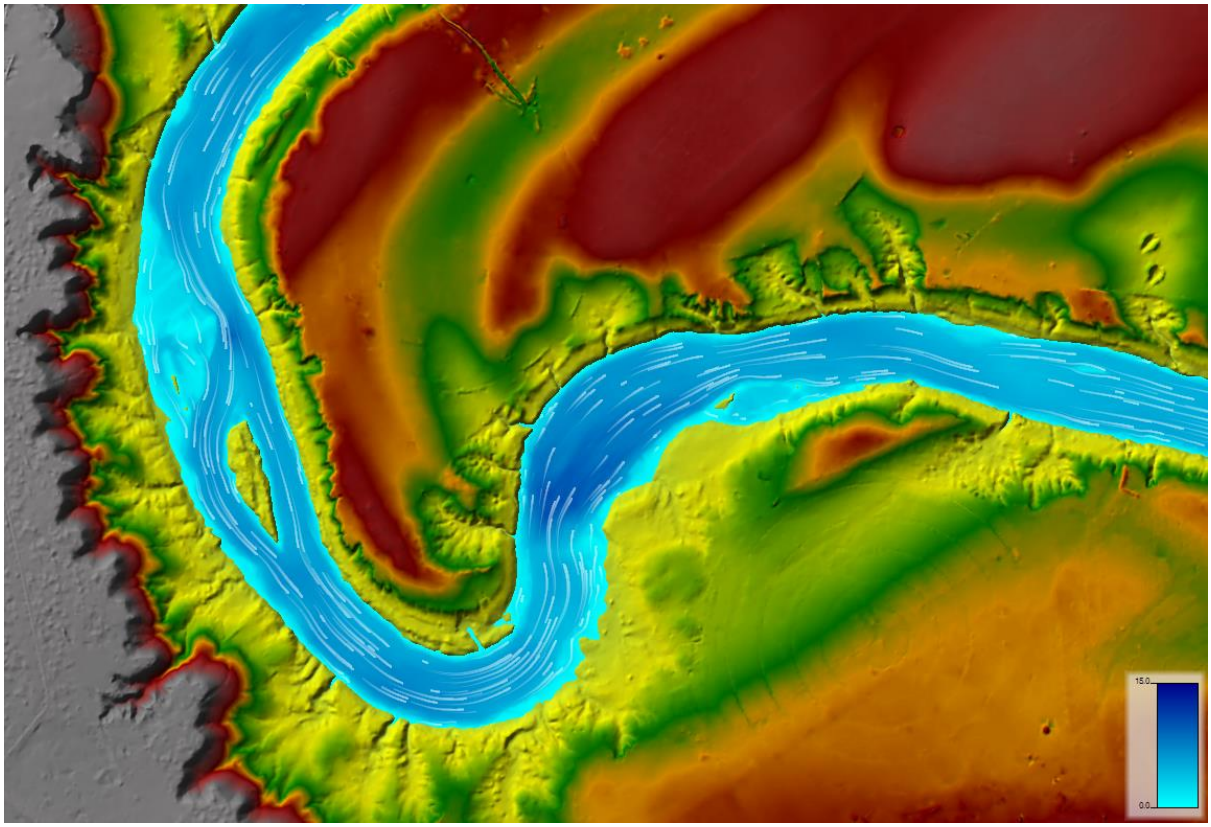

Figure 3-21 RAS mapper 2D model result. Blue surface- river depth; white- velocity particle tracing.

3.11.3 1D and 2D Model Comparison

Due to the finite mesh used for the 2D model, the resulting flow velocities and directions were much smoother. The average cross sectional spacing of the cross sections for the 1D model was 30m with exception to locations with rapidly changing river topography. The grid size of the 2D model is 5m X 5m and resulted in a better presentation of flow within the main channel. 2D models have the ability to represent lateral flow better and therefore visually represent flow along prominent features along embankments and islands better. The surface elevation between the two models was about the same with a 5cm difference at the upstream location of the river, when the maximum modelled flow of 500m^3/s was used to compare the stages. The setup of the 2D model was much faster than that of the 1D model due to the geometry requirements between models, while the computational time of the 2D model is much longer than the 1D model. The 2D model lacked effective velocity calculations near embankments due to the cell size of the finite mesh. To some extent the velocities can be corrected through break lines or denser mesh construction along these areas. This will be very time consuming and will not be feasible for a high surface area

change related to different stages. The comparison between the 1D and 2D model velocity calculations can be seen in Figure 3-22.

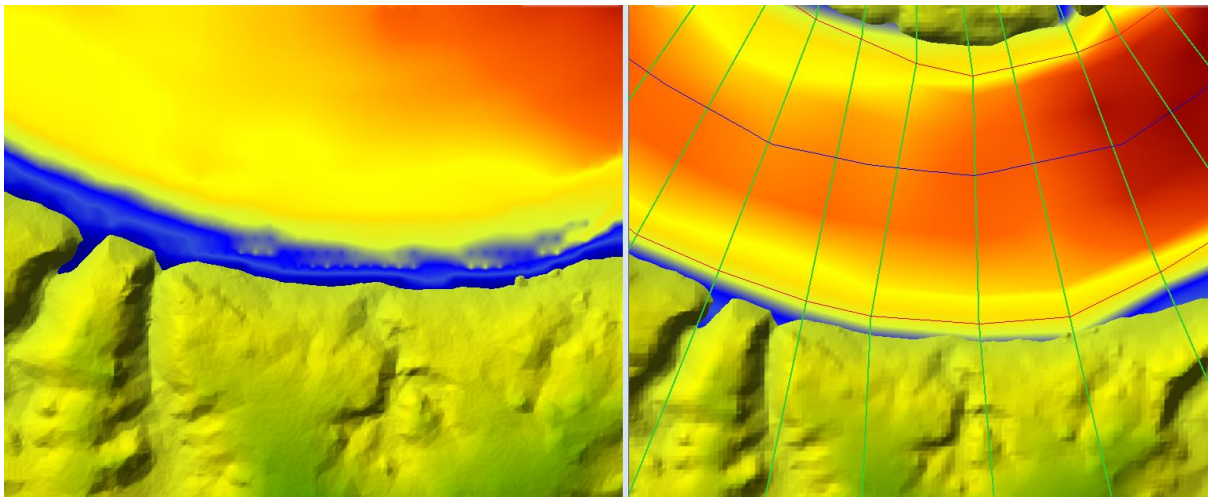

Figure 3-22 Model velocity comparison (2D Model left, 1D Model right). Red- high velocity; Blue- low velocity.

Both models produced satisfactory results, with the 1D model more accurate for velocities next to embankments. The choice of model will greatly be affected by the topography of the river studied. If complex geometric features occur and the extent of flow are contained within the embankments, 1D models will be used and 2D models for complex topography. The extent and detail required for modelling hydraulic flow for the purpose of identifying water abstraction locations will greatly affect the model choice. If a 2D is to be used for accurately modelling flow velocities against embankments, a small enough cell size need to be used. HEC-RAS allow for the simulation of models and is a great visualisation and interpretation tool. For the purpose of this study the 1D model will be used, due to the ability of better representing phenomena over the hydrograph flow range from cross sectional data. In addition, the velocity computations of the 1D model were more desirable for identifying water abstraction locations near embankments.

3.12 Abstraction location selection

A variety of factors may influence the preferred abstraction locations such as velocity, depth, distance from stages and sediment build-up. In order to account for all varying factors, ratios were used for obtaining relationships. From the results in this study (section 3.11.1), it can be seen that a homogeneous increase in velocity was evident at increasing flow rates (Figure 3-23). The steady increase in velocity indicates that no anomalies occurred

during the stages that redirect the flow as the flow rate increased. Figure 3-24 indicates the hydraulic property table of the channel at station 10774.37 (most upstream section). The relationship between the flow rate and conveyance can be seen in the formula below.

$$Q = KS_f^{1/2}$$

where: K = conveyance for subdivision

Q = Flow rate

S_f = slope of the energy grade line

From the flow rate and energy grade line, conveyance has a direct relationship to the flow area, hydraulic radius and manning coefficient. Therefore, any sudden changes along the conveyance will suggests rapid changes in the river morphology. By inspecting the hydraulic property table of each cross section, it was found that the conveyance increased homogeneously. Major changes occurred at the bridge area due to blocked ineffective flow areas with defined obstructions. From this observation and the assumption that water abstraction locations are highly influenced by minimum and maximum flow, not all stages were incorporated into the selection process.

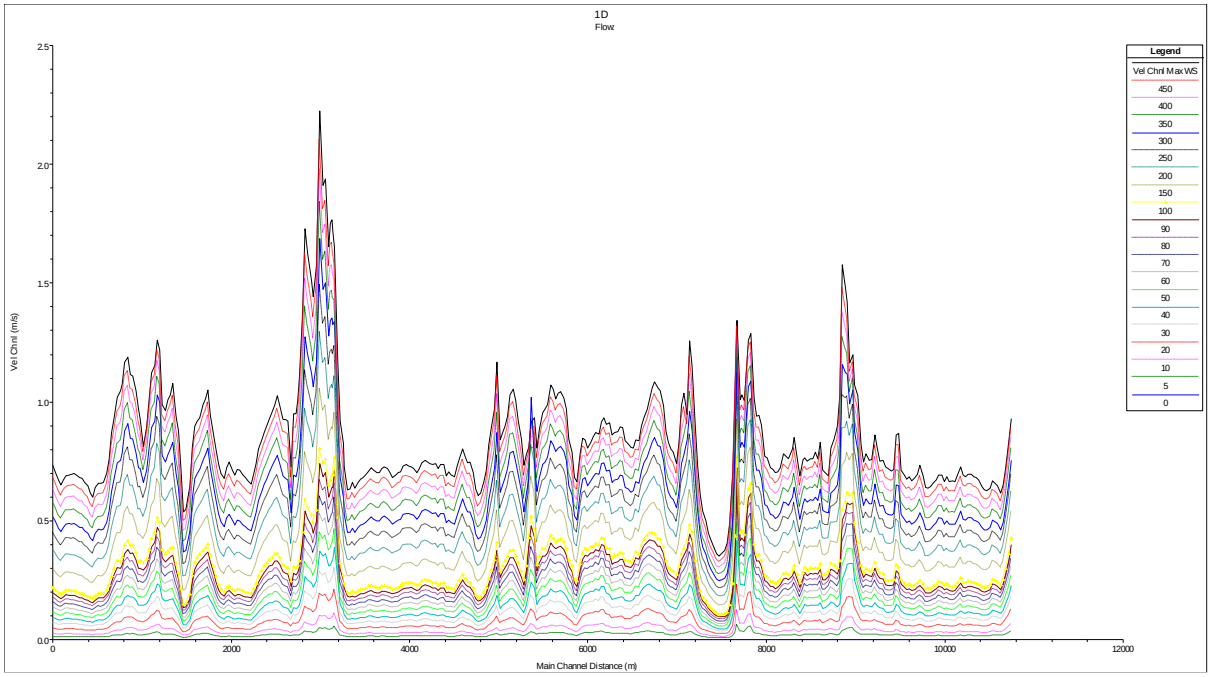

Figure 3-23 Main channel velocity over flow range for hydrograph instances modelled

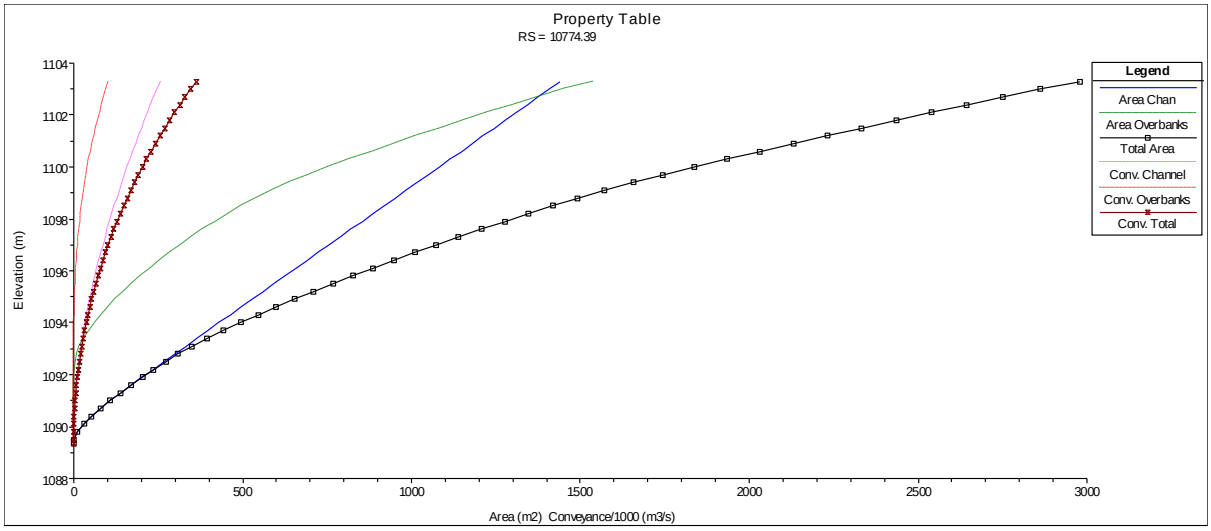

Figure 3-24 Hydraulic property table at the most upstream location.

3.12.1 Distance to high stage selection

The optimal location of a small-scale abstraction location is dependent on the distance from the minimum stage to a high stage, being the boundary of the water surface elevation. This is due to practical reasons such as construction for equipment mounting and distance of the suction head from the pump.

To investigate the optimal placement of abstraction locations in this study, the raster representing the stage at the maximum modelled flow (500m^3/s) was obtained from HEC-RAS. The raster is a floating point and converted to an integer raster needed for converting a raster to a polygon. Using the raster to polygon tool the raster was converted to a polygon around the boundary and island polygons were deleted since we are interested in embankments. The polygon in turn was converted to a line feature. The line was split at the upstream and downstream in order to delete sections not along the embankment. Only two lines now represent the location of the stage edge location on embankments.

From the spatial analysis distance tools, the Euclidean distance tool was used. This tool calculates the shortest distance from a raster cell to a feature. The stage edge lines were used as the input features, since the distance from the higher stage is of interest. The cell size was set to 2mX2m to match the HEC-RAS surface results. The distance limit was set to 400m to ensure the entire river is covered by the raster. The tool was run and the resulting raster clipped to the polygon of the high stage. The resulting distance layer can be seen in figure 3-25.

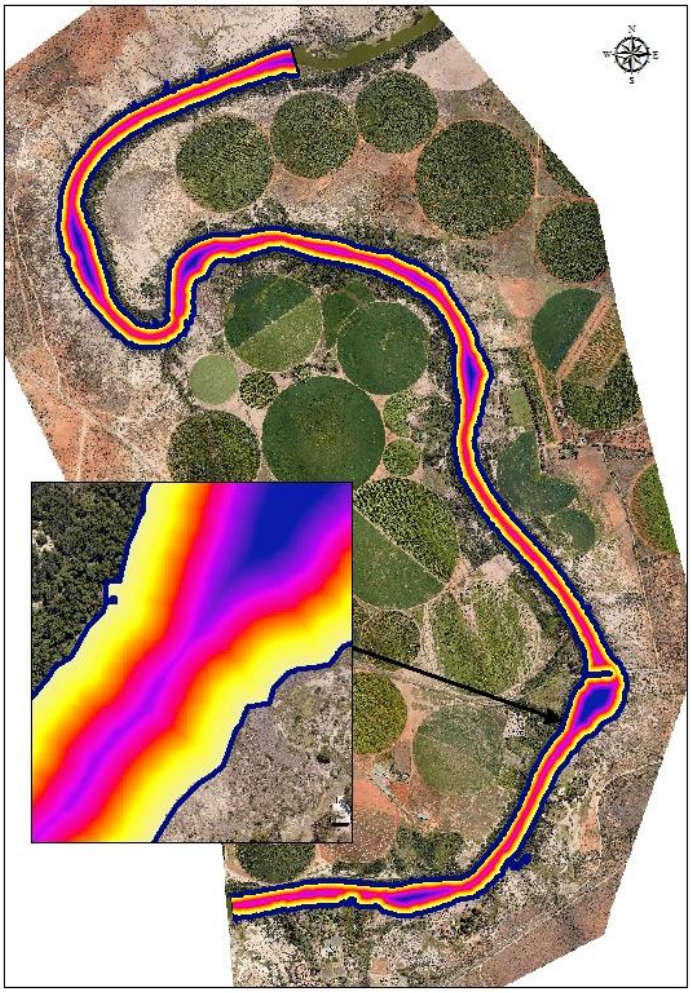

Figure 3-25 Euclidean distance results. Yellow is closer to the high stage boundary and blue further.

3.12.2 Distance Depth relationship

For an abstraction location the distance between the deeper sections of the river and embankments is crucial for sustainable water abstraction. The sustainability of the abstraction location will be of concern at minimum flow rates. Therefore, the initial stage occurring at a flow rate of $0m^3/s$ was obtained from HEC-RAS. The distance to depth relationship was obtained by calculating the ratio of distance to depth for each cell with respect to the highest flow stage. From the Spatial Analysis Map Algebra tool, the raster calculator was used. The values of the Euclidean distance raster calculated were divided by the depth raster values of the lowest stage. The result of the distance to depth ratio can be seen in figure 3-26. The lower distance to depth ratio values indicate deeper depths that occur close to the high stage boundary, which may indicate suitable locations for abstraction points.

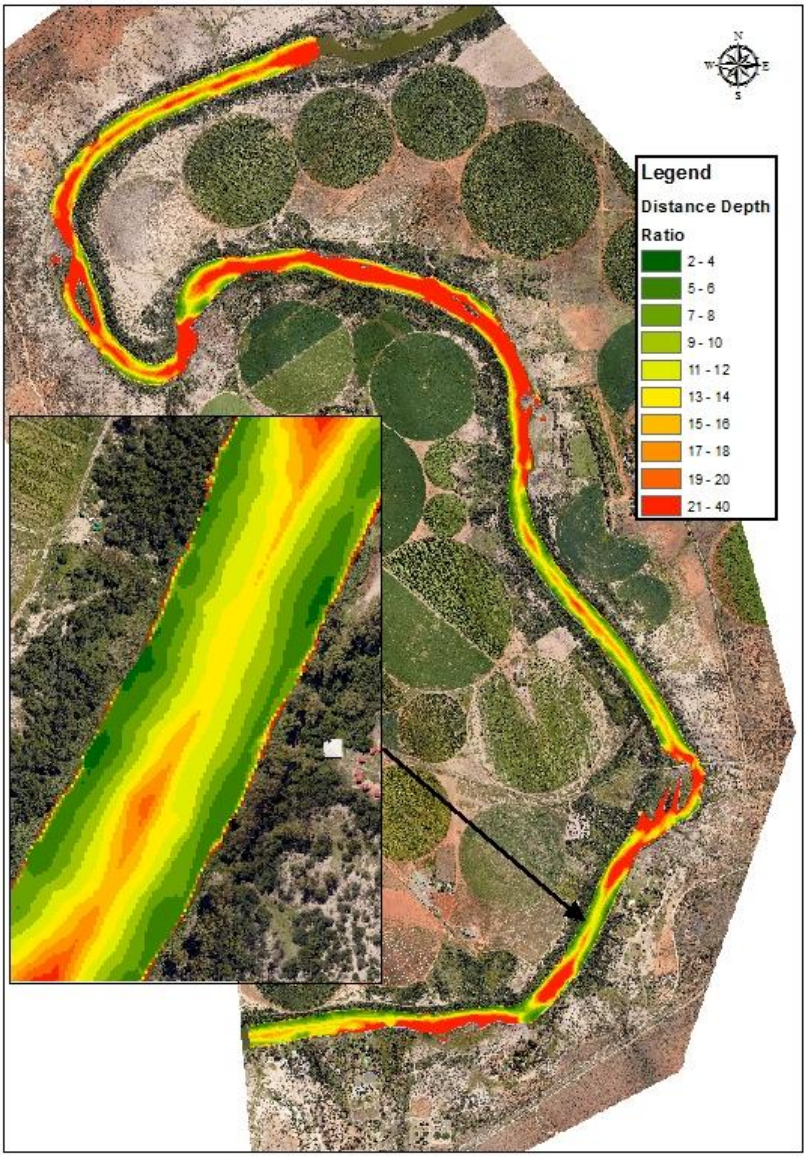

Figure 3-26 Distance to Depth ratio minimum stage

3.12.3 Depth Velocity Ratio

Abstraction locations are not only affected by distance but by velocity as well. Abstraction locations should not be within too high, velocity locations where the stream energy is very high. If the stream energy is too high the resulting forces will have a negative impact on suction head equipment. Therefore, the depth velocity ratio of the river was calculated. The low flow rate of $10m^3/s$ was considered. This is to obtain effects of lower flowrates but with sufficient velocity values for indicating the effects. Since higher velocities will greatly affect the stream power, the maximum considered flow rate of $500m^3/s$ will also be used for calculating a depth velocity ratio for the stream.

The depth and velocity layers were calculated and obtained from HEC-RAS for the flow rate of 10m^3/s. From the Raster calculator the depth was divided by the distance to obtain the relationship between the velocity and depth. The resulting layer of the depth velocity layer can be seen in figure 3-27. Green areas indicate more suitable locations for abstraction locations.

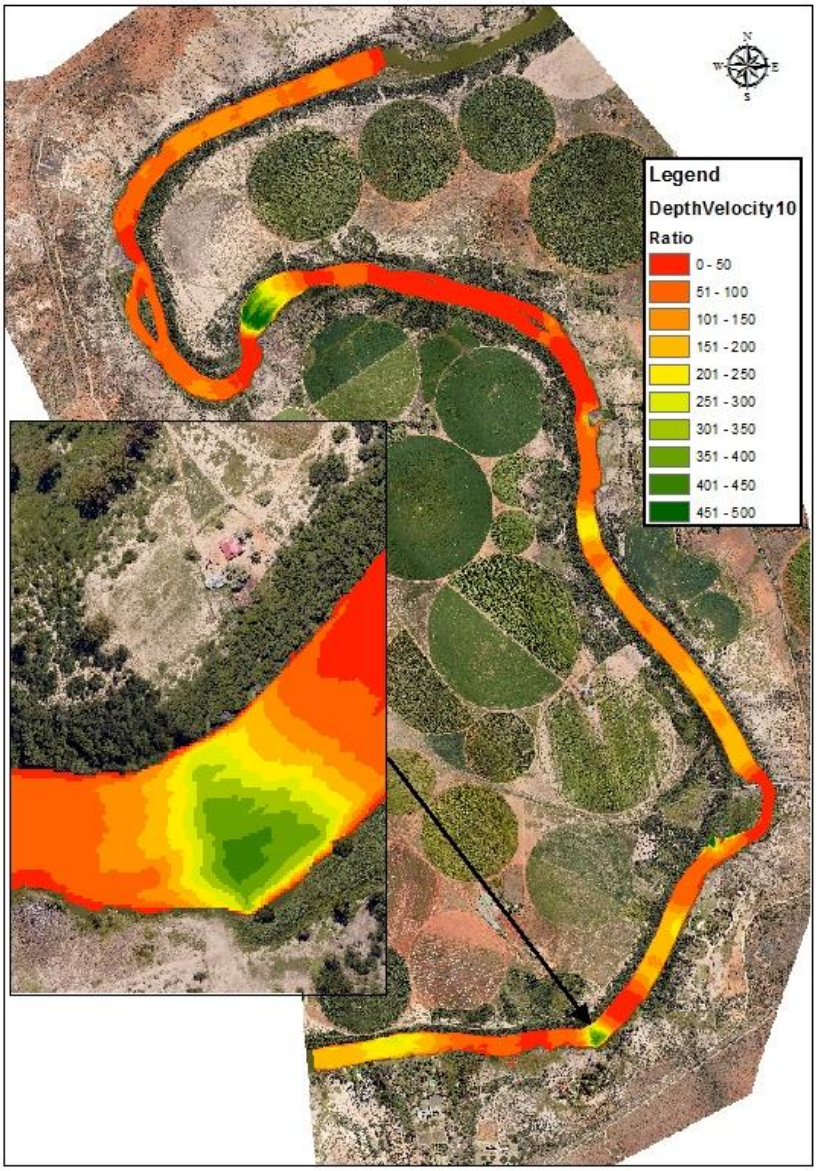

Figure 3-27 Depth Velocity ratio at flow rate 10m^3/s

Similarly, the velocity depth ratio for the maximum considered flow rate of 500m^3/s was calculated. Using the depth and velocity at 500m^3/s the layer in Figure 3-28 was obtained.

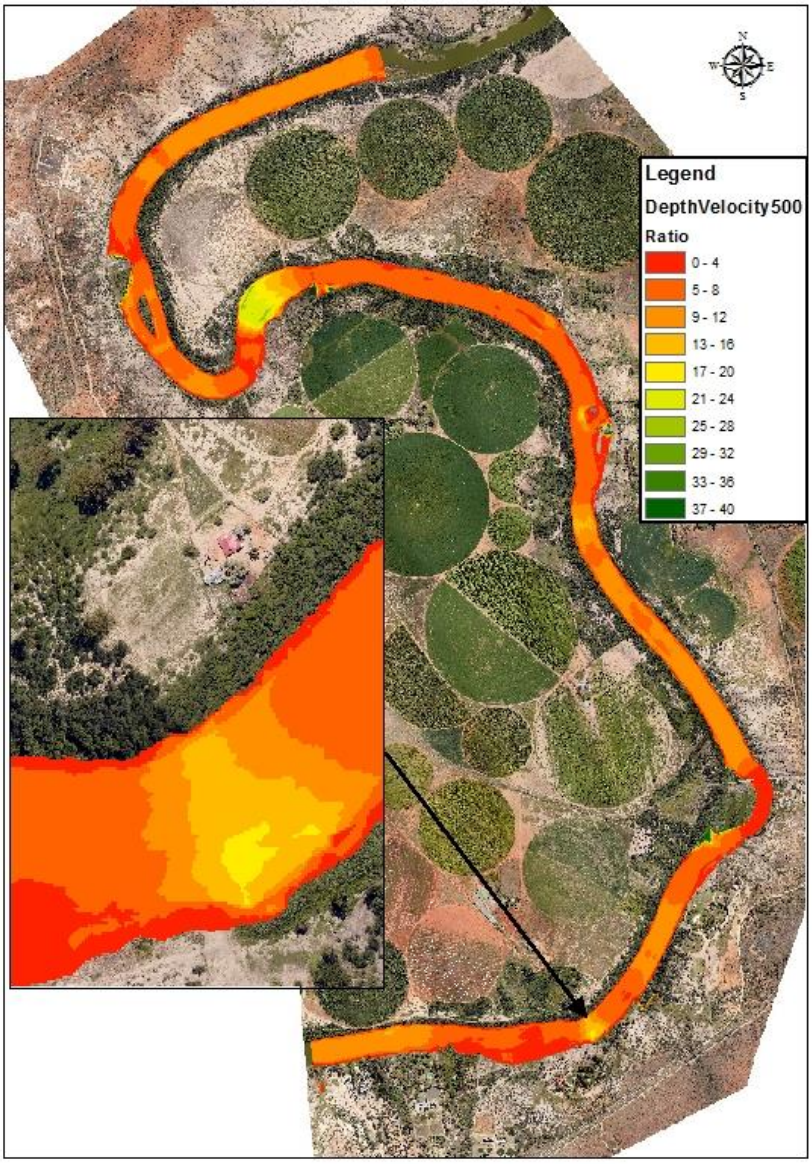

Figure 3-28 Depth Velocity ratio at flow rate 500m^3/s

Optimal abstraction locations related to depth and velocity can be identified from the higher values of the maps (Figures 3-27,3-28). These are locations where a high depth with low flow velocities occur. By inspecting the relationship between depth and velocity from the two maps at different flow rates, it can be seen that the values change with relation to each other for this particular case study. Therefore, it is not necessary to account for the effect of different stages, when considering depth to velocity ratios, for identifying abstraction locations in this study.

3.12.4 Stream Power

Stream power is essentially the product of stream discharge, stream slope and the weight of water and has a direct relationship with sediment transport. This relationship has been used to characterize sediment transport and investigate geomorphic questions (Gartner n.d.). The equation for stream power is as follows:

$$\Omega = \rho g Q S$$

Where: Ω = stream power

ρ = density of water

g = gravity

Q = river discharge

S = energy gradient equivalent to channel slope in uniform flow.

The stream power was calculated from HEC-RAS for the maximum considered flowrate. This was done due to the direct relationship to velocity and cross-sectional vector area that will result in a stable reduction of stream power until negligible, as the flow rate decreases. The resulting stream power map can be seen in figure 3-29.

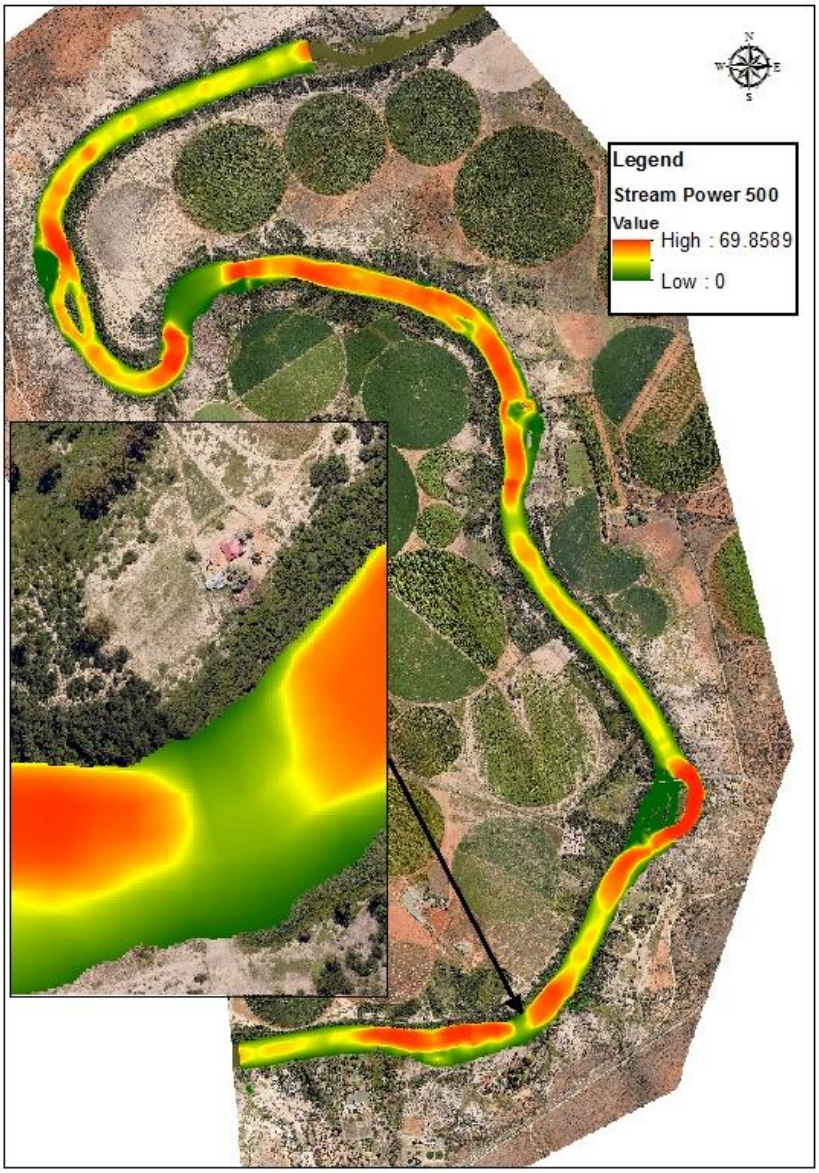

Figure 3-29 Stream power at 500m^3/s.

From the stream power map (Figure 3-29) high and low stream power locations could be identified and the relationship between velocity and the cross-sectional vector area could be visualised. Higher stream power areas indicated in red are less desirable abstraction locations.

3.12.5 Final selection

For the final selection of the abstraction locations, depth velocity and distance were taken into account. The stream power was directly related to the velocity and no additional variations of interest will be obtained by incorporating the stream power into the results. Due to the high correlation between high and low flow rate results, the considered low flowrate of $10m^3/s$ will be used for identifying the optimal abstraction locations since low flow rates have a great influence on the effectiveness of an abstraction location.

To combine all participating variables, the distance to depth ratio and velocity depth ratio raster layers were combined. Since the distance to depth values have the lowest values being optimal with the minimum being 1.94, an invert variable range needed to be calculated. This allowed the optimal range of variables to be in the same range as the depth to velocity ratio. The invert variable range will also invert the values so that higher values represent more optimal location. The invert variable range was calculated by dividing 1000 by the values of the distance to depth raster through the raster calculator.

The two ratio layers have their values within the same range and were added together. The resulting raster in figure 3-30 were calculated as follows: (invert distance depth ratio+ velocity depth ratio)/2. The added values are arbitrary values and divided by 2 to obtain a smaller range of values for interpretation purposes.

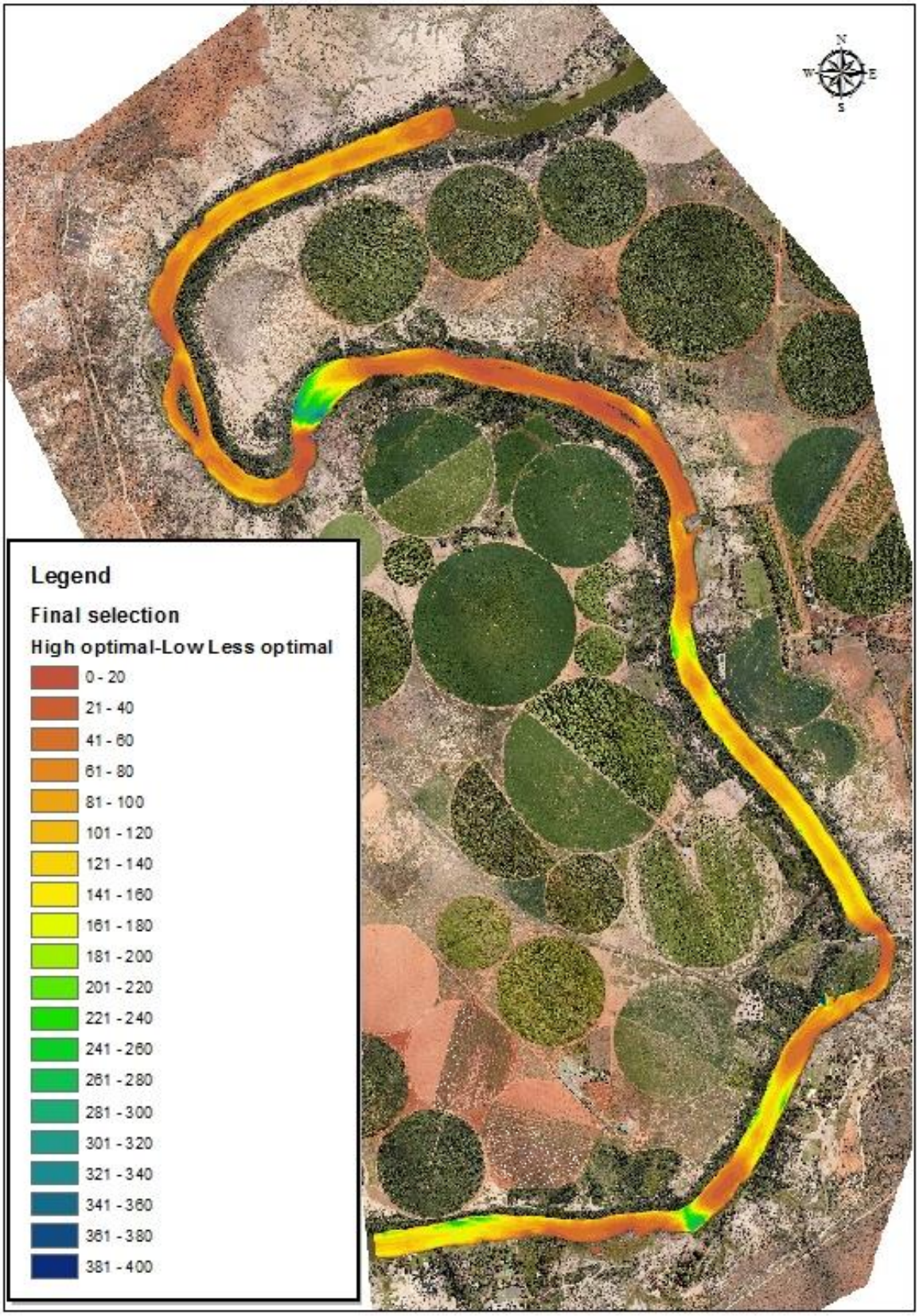

Figure 3-30 Final selection surface.

Chapter 4 Results and discussion

This chapter reports observed tendencies from the hydraulic computational results and the modelled surface for identifying optimal abstraction locations. In addition, identified abstraction locations are compared with current locations.

The created surfaces inspected consisted of the velocity, stream power, depth, water surface elevation at the minimum and maximum considered flow rates of the hydrograph and the final abstraction location surface (Figure 4-3). This was done to interpret individual hydraulic properties under high and low flow rate conditions that effect abstraction locations. Additionally, of trends and patterns could be identified from the hydraulic properties and the effects thereof on the final abstraction location surface identified.

4.1 Weir effects

Because the hydraulic modelling of the river section only calculated surface velocities, the effect of hydraulic obstructions within the three-dimensional environment need to be considered. By inspecting the velocity, depth and stream power maps, a hydraulic flow pattern could be identified along the reach (Figure 4-1). This flow pattern is directly related to the river bathymetry due to velocity that increases as depth decreases. The effect of the alternating high-low velocities along with the relative alternating depth can be interpreted as crump weirs. These locations may be affected by geological or river morphological factors. The extent of deviation varies greatly, with less prominent deviations occurring in long relatively straight sections of the river.

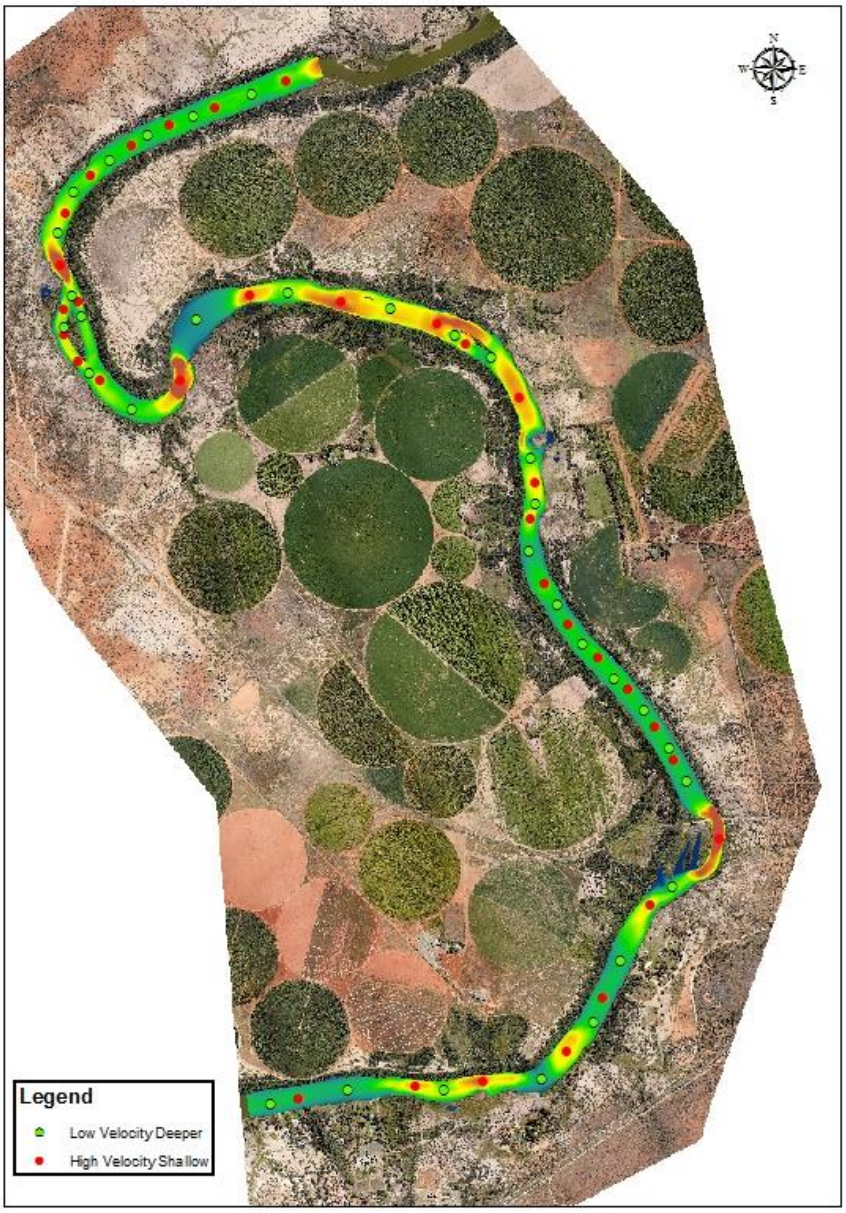

Figure 4-1 Velocity to depth ratio surface with high and low value pattern. Red- high, Green- low.

From figure 4-2 the basic construction of a weir can be seen. The diagram relates to effects seen within the modelled river section where natural weirs occur. The water is elevated behind the weir with sediment often dropped behind the weir where lower energy levels occur. High velocities occur over the weir and increase as it flows down. The momentum of the water is directed at an angle to the bottom of the weir. As the water connects with the bottom of the weir, a hydraulic jump occurs. The changed direction and momentum of the water continue to connect with the stilling basin and erode the stilling basin. The effect of bedload sediment removal in the study area can be seen from the deeper sections in figure

4-1. As the water level settles and the slope of the channel returns to normal, the river has less stream power and sediment is deposited downstream. This effect can be seen from the results (Figure 4-1) where elevated areas occur after bed load sediment removal at the bottom of the weir.

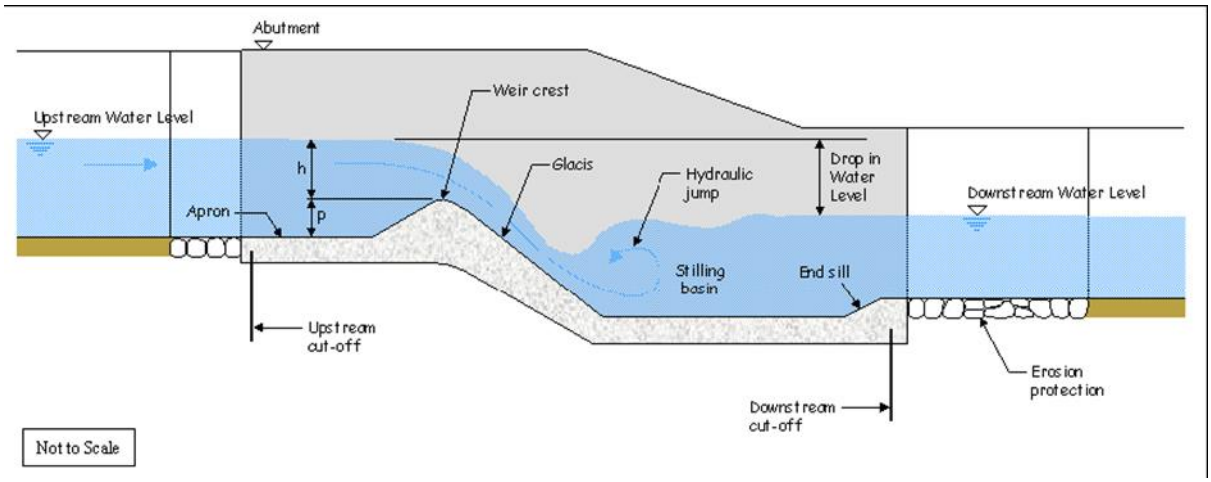

Figure 4-2 Basic components of weir structure (Tapp n.d.).

The weir effect occurring in the river creates a highly desirable environment for abstraction locations. The placement of an abstraction location at the lower ends of the stilling basin is advantageous due to the depth, velocity, sediment transport and stream power. The deeper section created in the stilling basin ensure that water will be available for abstraction during low stage conditions. The surface velocity and stream power are low at the stilling basin end and will prevent damage or loss of equipment related to perpendicular forces applied by the water. The removal of sediment from the river bed occur in the stilling basin due to downward momentum of the water. This sediment removal is advantageous for abstraction locations since sediment promote wear and damage to pumps and pipelines. Additionally, future build-up of sediment is prevented.

4.2 Abstraction location selection results

From the final selection surface generated, desirable abstraction locations were identified Figure 4-3; green and blue symbolised values. Although the pipeline for the project connects to the abstraction locations from the East (Figure 4-3), the results also supply valuable information for water abstraction to the West due to the agricultural irrigation practices. The left and right banks of the river were modelled and will enable farmers along the river section to make informed decisions on the abstraction location used.

For the purpose of the study, four of the most desirable locations will be discussed along with the location of the Riverton station abstraction location and the abstraction location selected by the engineers for the project (Figure 4-3). The consulting engineers for the municipal project was Aurecon. The first location of interest to the engineers was below the bridge on the concave bank of the bend. Complications occurred at the area of interest due to private ownership and the location north of the bridge (Figure 4-3) was recommended based on the depth.

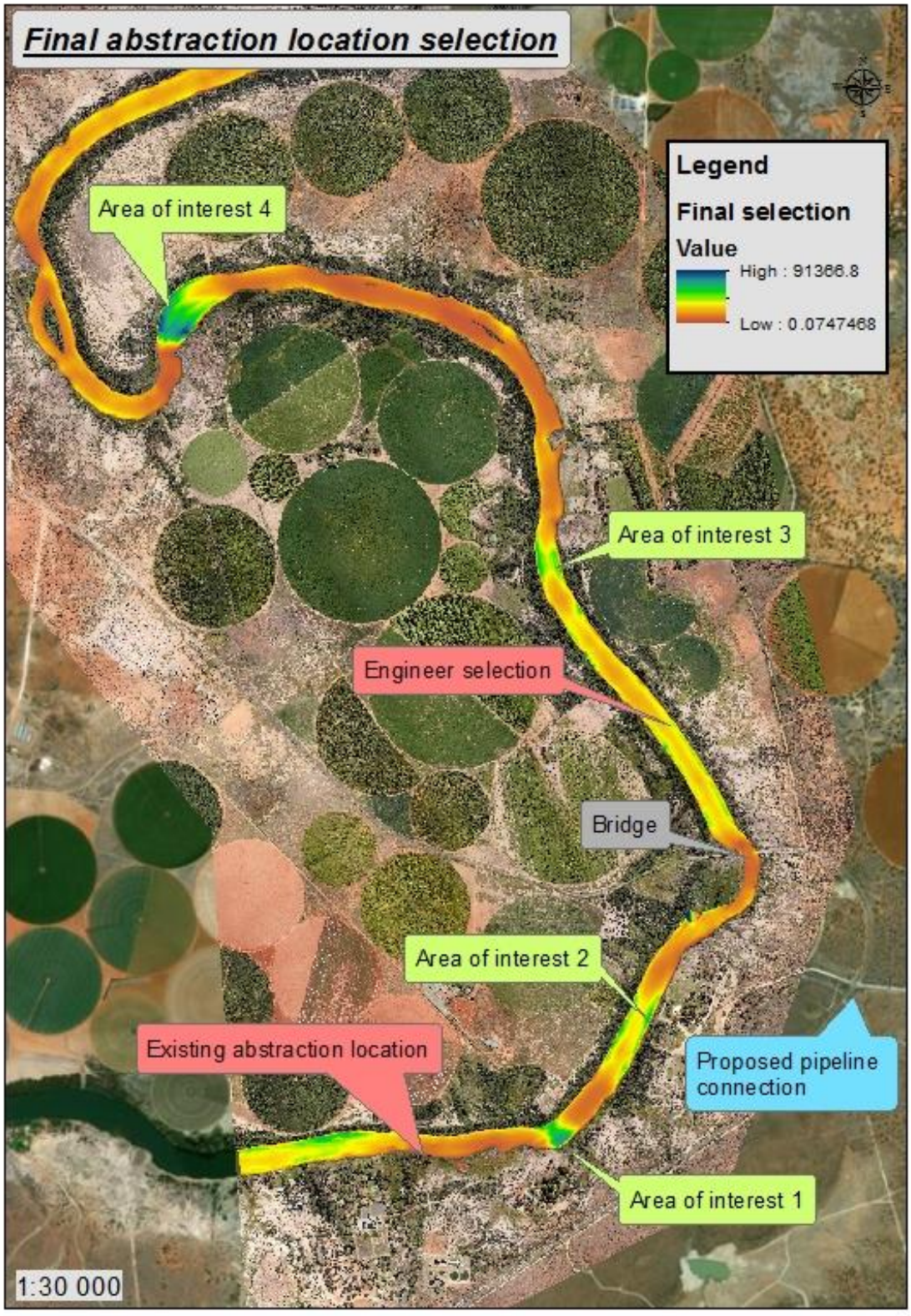

Figure 4-3 Map depicting final abstraction location selection. Four areas of interest were identified through this study for optimal abstraction point placement. The existing abstraction point location is also shown along with the abstraction point proposed by engineers for the municipality's project.

The first location is one of the most desirable locations (Figure 4-4). A deep section of river is created on a slight turn in the river. The deeper section is located close to the high stage boundary and minimal construction is necessary. The deeper section is located after the natural raise in the river that creates a weir effect and will allow for sediment transport. The bend in the river directs the momentum of the water to the embankment and assists in preventing sediment build-up. Low velocities and stream power occur next to the embankment and limits the possibility of unwanted erosion of the embankment. In addition, this location is close to the pipeline route and located on government property.

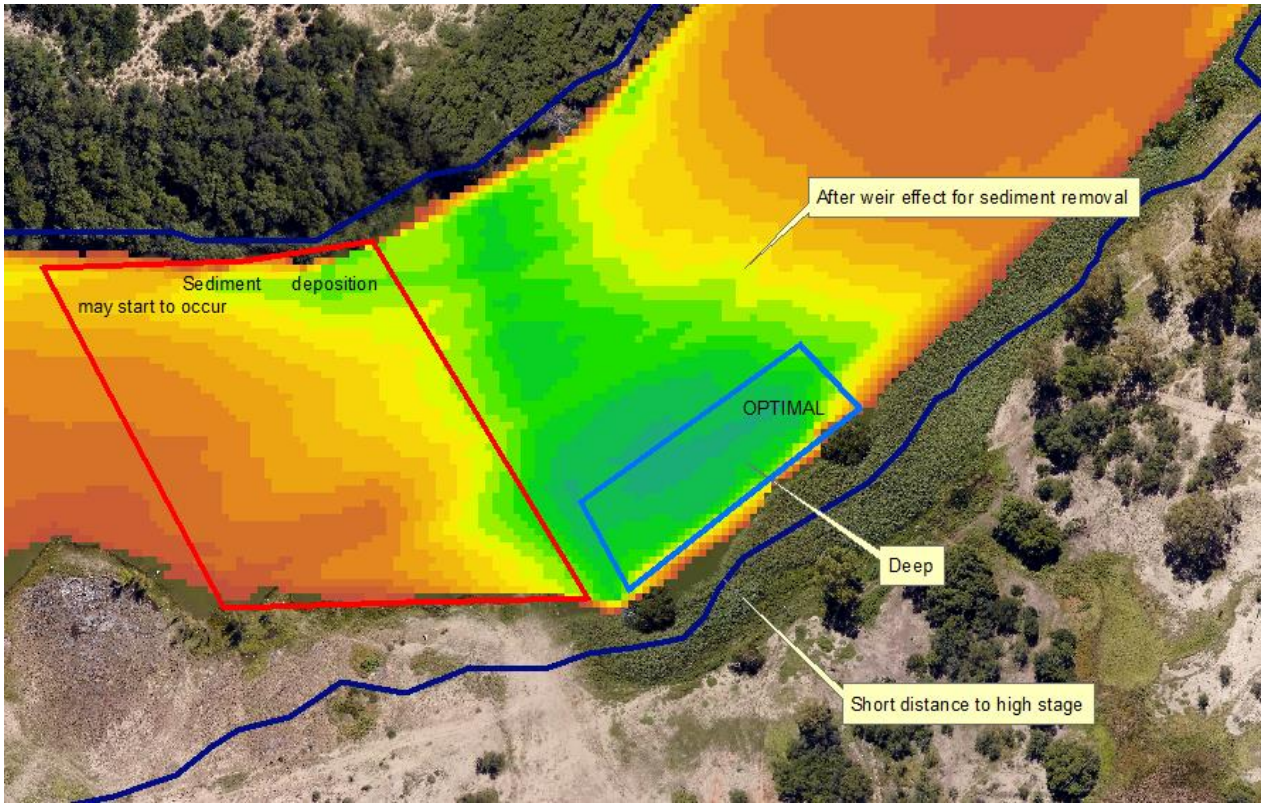

Figure 4-4 First desirable abstract location.

The second optimal location (Figure 4-5) is located 700m upstream of the first location. This location represents the same characteristics of the first location but without the bend within the river. Although no bend is present, the weir effect allows for sufficient sediment removal from the riverbed. The seemingly undesirable effect obtained closer to the centre of the river is due to the distance to the high stage boundary. However, this location is characterised by low stream power and surface velocity, which indicate less stress and risk of loss to equipment. Additionally, the strait river section where this location occur will be less likely to have excessive bank erosion due to negligible lateral directional change in

momentum. The location is close to the proposed pipeline connection and located on government property.

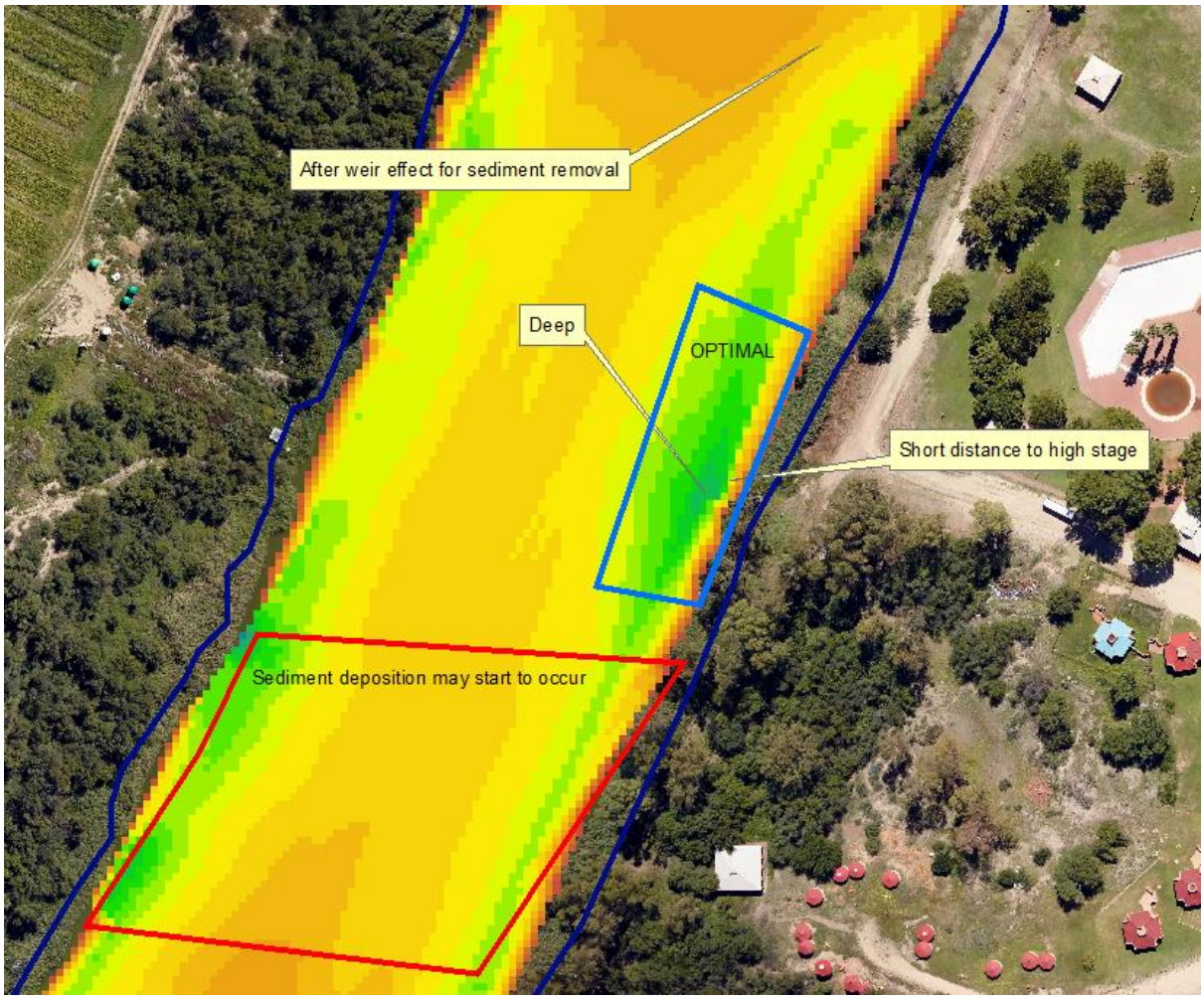

Figure 4-5 Second desirable abstract location.

The third possible desirable location (Figure 4-6) is located at cross section 4800 and located 900m upstream from the location selected by the engineers for abstraction. This location represents the same characteristics as the second location, but much further away from where the pipeline route connects to the river. Further distances from proposed pipeline routes may result in additional planning or construction cost and time This location is also on private property and may involve additional permissions and related costs.

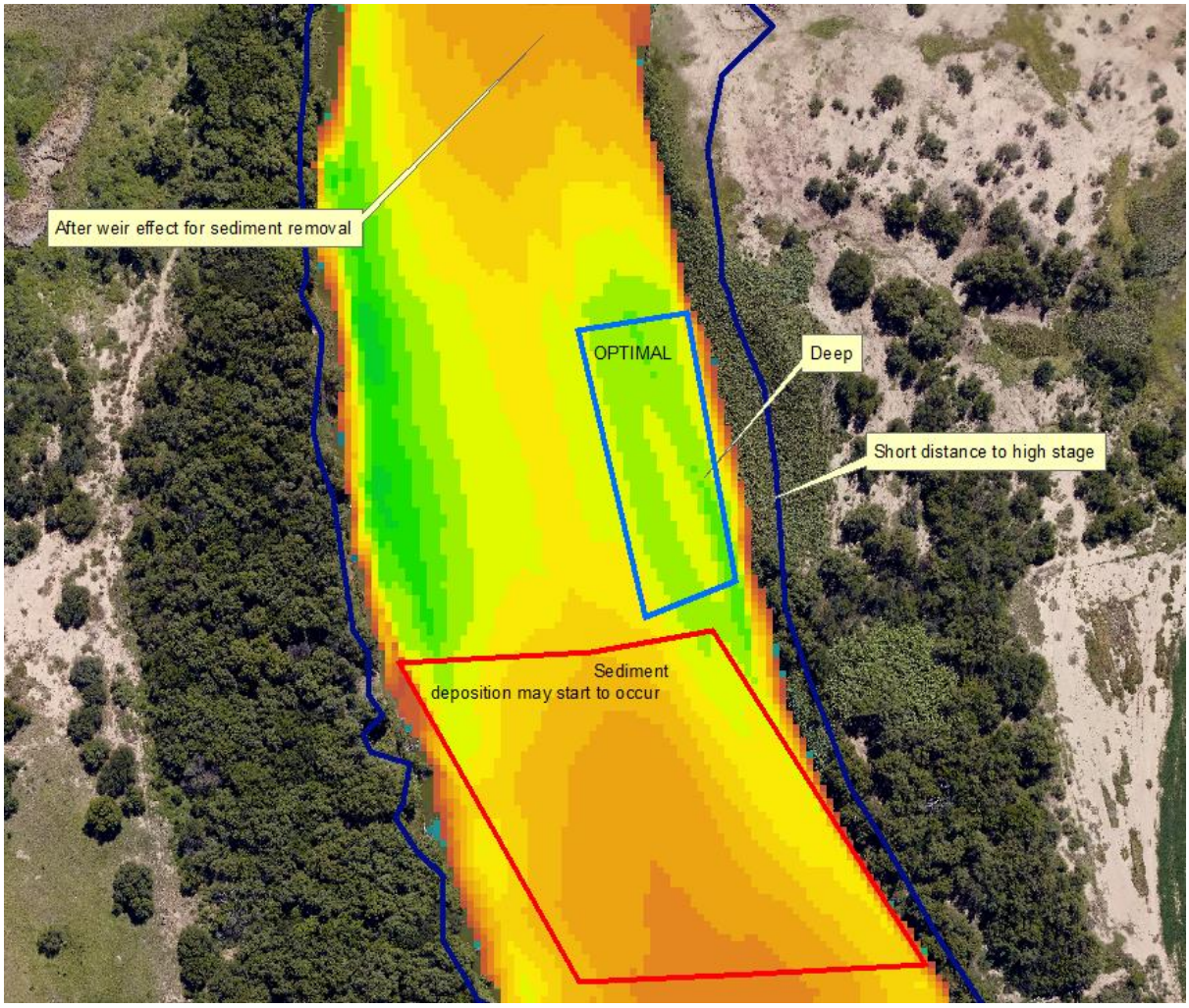

Figure 4-6 Third desirable abstract location.

The fourth location (Figure 4-7) is located at cross section 7563 and behind a weir effect caused by a rock formation across the river. It shows the same characteristics as the previous locations but with a highly prominent sharp bend within the river. This location is a good indication of the effect that river morphology has on hydraulic properties and tendencies. For example, the rock bank crossing the river create the weir effect directing the momentum of the water towards the riverbed, creating a deep cut-hole. The bend in the river direct the flow direction towards the concave bank creating deep sections next to the embankment. The sediment build-up after the deep section, due to energy loss, is prominent at this location and should be avoided as a possible abstraction location. This is a good abstraction location, because of the deep section created next to the embankment and low surface velocity. Low stream power and surface velocity for the maximum considered flow rate occur at this location. Most of the kinetic energy has been depleted

when arriving at this location indicating that excessive erosion of the embankment should not be problematic at this location. However, this location is on private property and far from the pipeline connection route.

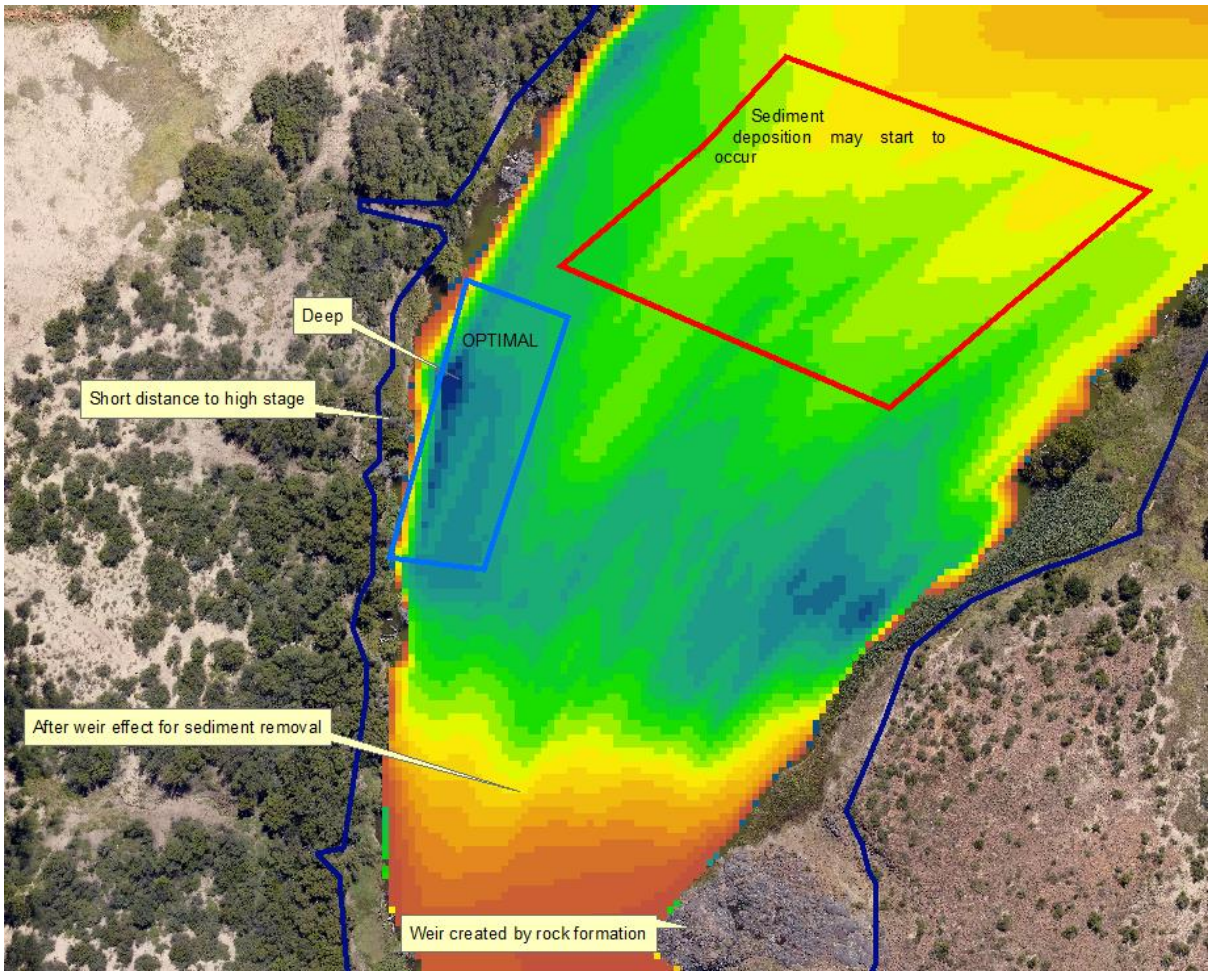

Figure 4-7 Fourth desirable abstract location.

The locality of the Riverton Station was also assessed in this study (Figure 4-8). Since the Riverton Station is a much larger scale abstraction location that the study is intended for, and the structure and operation of such an abstraction location varies greatly. Nevertheless, the abstraction location is located in a shallow area, while the main flow path of the river is located on the opposite bank from the abstraction location. High and long catwalks were constructed for access to the abstraction location, due to the effect of higher stages on the wetted/flooded area. From the survey, high sediment build-up was observed and this build-up was to such an extent that observations could not be obtained in that area. This suggests that the Riverton Station is not ideally situated for the continuous removal of sediment by the hydraulic action of the water, which increases maintenance costs to the equipment. The

study confirms the unfavourable conditions at the Riverton station compared to the site observations made.

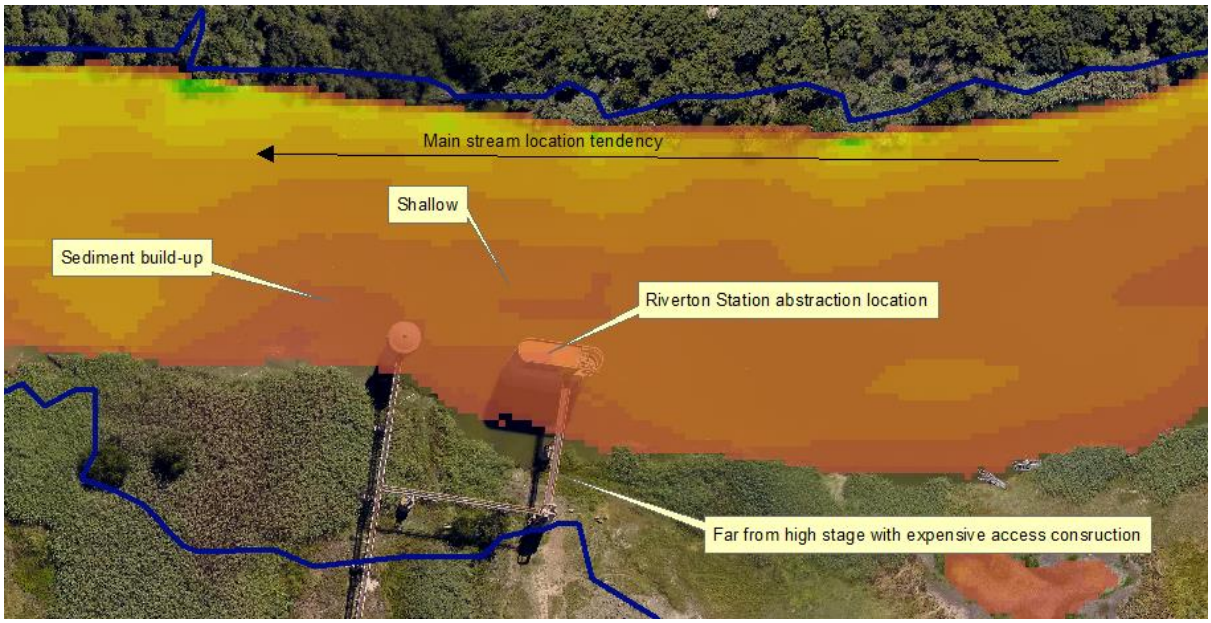

Figure 4-8 Riverton station abstraction location

The abstraction location selected by Aurecon, the consulting engineers, for the municipal project is located at cross-section 3870 about 700m upstream from the bridge (Figure 4-9,4-3). This location is to some extent desirable. It has a deeper section to extract water from that is desirable but to a lesser extent than the optimal abstraction locations identified in this study. This location also has high stream power and velocity that might cause damage and equipment loss. This location may be less prone to high embankment erosion, due to the relatively straight section of river where it is located related to lateral change in the water momentum direction. However, the flushing away of sediment is less prominent compared to the optimal abstraction locations identified. Furthermore, this location is situated on private property and special permissions need to be obtained for operation and construction. It is also relatively far away from the pipeline route connections. The first and second location identified would have been more reliable and cheaper if used as abstraction locations.

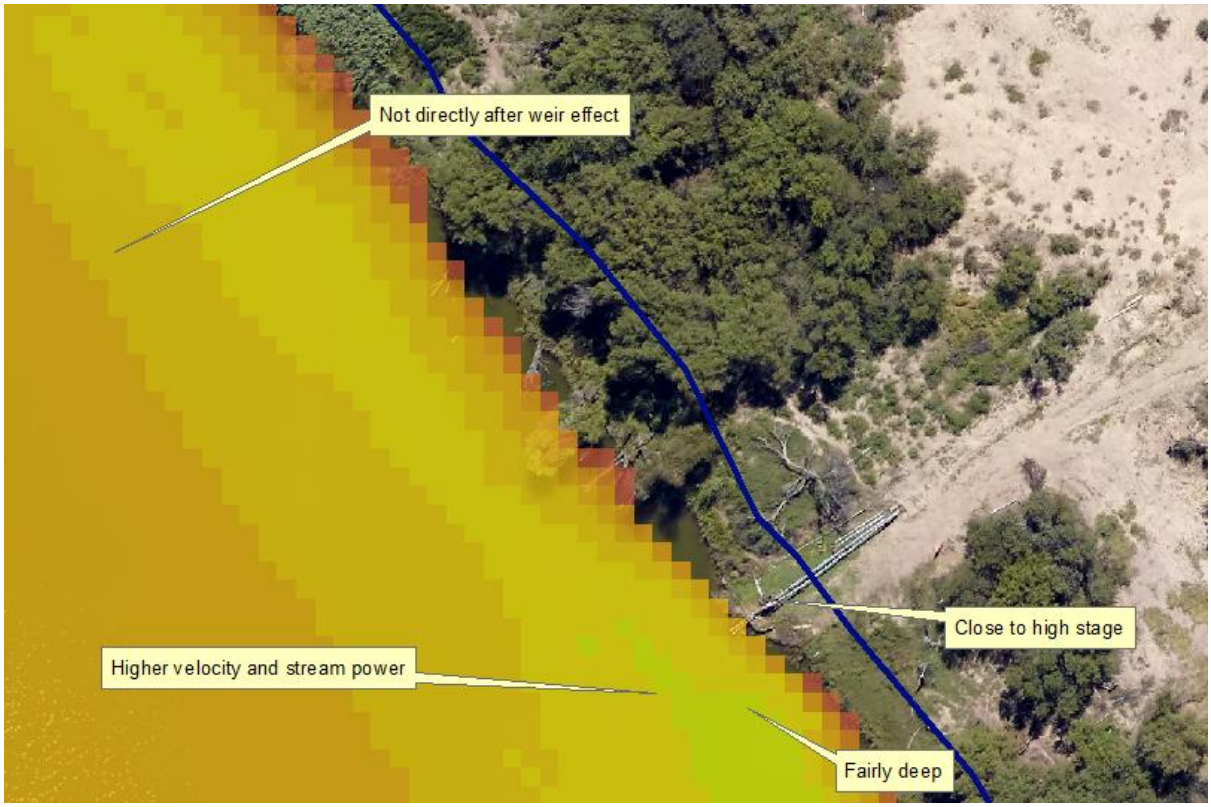

Figure 4-9 Selected abstraction location for project by engineers.

Chapter 5 Conclusions

The study has highlighted some of the requirements needed to obtain an accurate flow model for use in identifying water abstraction locations. These include an accurate DEM, hydraulic flow models, spatial analysis and interpretation of intermediate results.

In order to create accurate hydraulic models an accurate DEM is needed. Due to cross-sectional surveying methods most often used for bathymetric surveys, conventional interpolation algorithms will not supply an accurate DEM. Embankments are of high interest when identifying abstraction locations and therefore need to be modelled accurately. By using TIN modelling, the model triangles can be edited to obtain the best representing surface along the embankments. A TIN model allows for accurate interpolation between topographic and bathymetric survey results based on knowledge of river topography. However, the interpolation method used may be influenced by the survey data acquisition method and resulting distribution of survey points.

Many factors need to be taken into consideration when developing a flow model for a study area. This study shows that the river morphology, hydrology and scale greatly influence the decision of flow model selection. For the modelling of flow within a river where overbank side reaches are minimal, 1D flow modelling supplies an accurate model. In this study the 1D model supplied better results with respect to velocity estimation next to embankments. The 2D model is not a feasible model to use if the sell sizes in the finite mesh is not small enough. The lack in ability of the 2D model to incorporate geometric features also need to be considered when choosing model types. For larger study areas 1D flow modelling should be used. The 1D model may be combined with 2D flow areas where complex flow paths occur. For small detailed models, 2D models can be used if the finite grid cell size can be reduced to supply expectable results along embankments or areas of interest. Hydraulic models need to be calibrated to ensure accurate results and representations are obtained. The calibration process will validate manning coefficients, sufficient cross-sectional spacing or cell size and correct time step computational intervals used.

Boundary conditions established for the hydraulic model need to be on the same reference of the DEM and survey results. The interpretation of flow conditions when creating a flow

hydrograph need to be based on accurate historic flow measurements or hydrological computations.

Although only surface velocities were calculated through HEC-RAS, it was sufficient for identifying certain hydraulic tendencies within the river. In the study high stream power and velocities directed to embankments could be identified from the resulting HEC-RAS surfaces created for the hydrograph range (Figures 3-16,3-29). The weir effect caused could be better modelled and interpreted through the use of the hydraulic modelling results. The effect of the river topography for the flow rate range could be established. This effect was assessed and no need for additional flow instance results was necessary for the study area. The resulting data need to be interpreted with sufficient knowledge of fluid mechanics and specifically open channel flow hydraulics. This is necessary when creating the geometry for models, manning coefficients and setting up of model parameters. Care should be taken when deciding between steady or unsteady flow modelling and the use of full momentum equations or diffusive wave approximation. Knowledge regarding open channel flow fluid mechanics will assist in interpreting the hydraulic results and to identify logical model errors or deviations.

The four abstraction locations identified in the study prove to be optimal locations based on the hydraulic modelling performed. The locations are located in deep cut-holes created by flow over bathymetric features. The deep holes will minimise the possibility of abstraction locations from becoming ineffective during dry conditions. Additionally, the cut- holes are located between two shallow sections described as weirs in the study. This will act as a storage area during extreme droughts and extend time of extracting water from the location (Figure 5-1). The amount of water available in the storage areas can be quantified at different stages, for the abstraction location using GIS.

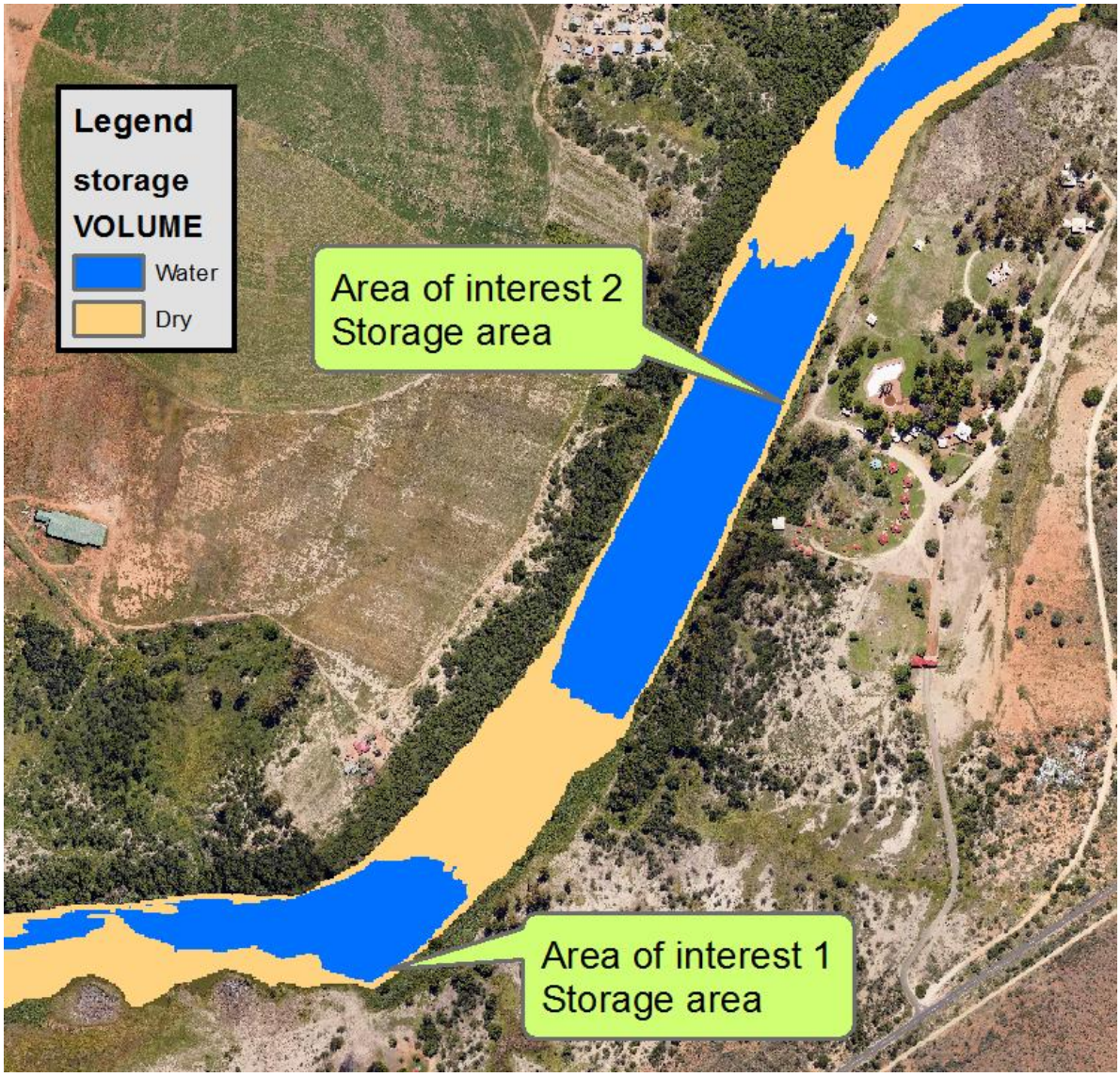

Figure 5-1 Water availability between elevated bathymetric segments at abstraction locations.

The surface velocities at these locations prove to be very low. Related to the low stream velocity and depth at these locations is low stream power. Low velocity and stream power indicate that minimal force will be applied on extraction equipment by the water. This in turn will minimise the possibility of equipment loss or damage. The low stream power and velocity at these locations is related to low sediment transport at the surface, minimising the possibility of unwanted embankment erosion. Excessive erosion at extraction locations can lead to equipment loss or damage to pumps and their fixtures. Although the surface velocities are low, it was established that sediment is removed from the river bed, due to directional momentum change caused by the weir effect. This change in direction allows the

deep cut-holes to form and prevent sediment build-up. It is evident that after these cut-holes a high sediment build-up occurs. This is due to the water losing energy after the weir effect as the channel slope returns to normal. These settling locations produce a lot of sediment build-up and resulting increases in velocity and stream power start to occur. Abstraction locations should not be place too far downstream of these weir effects since the abstraction points will be in the area where the sediment drop occurs (Figures 4-4, 4-5, 4-6, 4-7).

The hydraulic models produced valuable information regarding water surface elevations at different flow rates. In the study the maximum considered flow rate was 500m^3/s based on the daily average flow rate for 2014-2017 (Appendix A). The water surface elevation obtained from the 500m^3/s flow rate was used for establishing optimal distances to low flow rate stages. Smaller distances were considered since access to abstraction locations will be possible during high flow rates and the resulting construction cost may be less. The four identified locations have close distances between the low and high stage boundaries. This distance effect is related to high slopes of the embankments (Figure 5-1). However, a high slope is not necessarily related to optimal abstraction locations due to river morphology from long term erosion and historic flow paths (Figure 5-2).

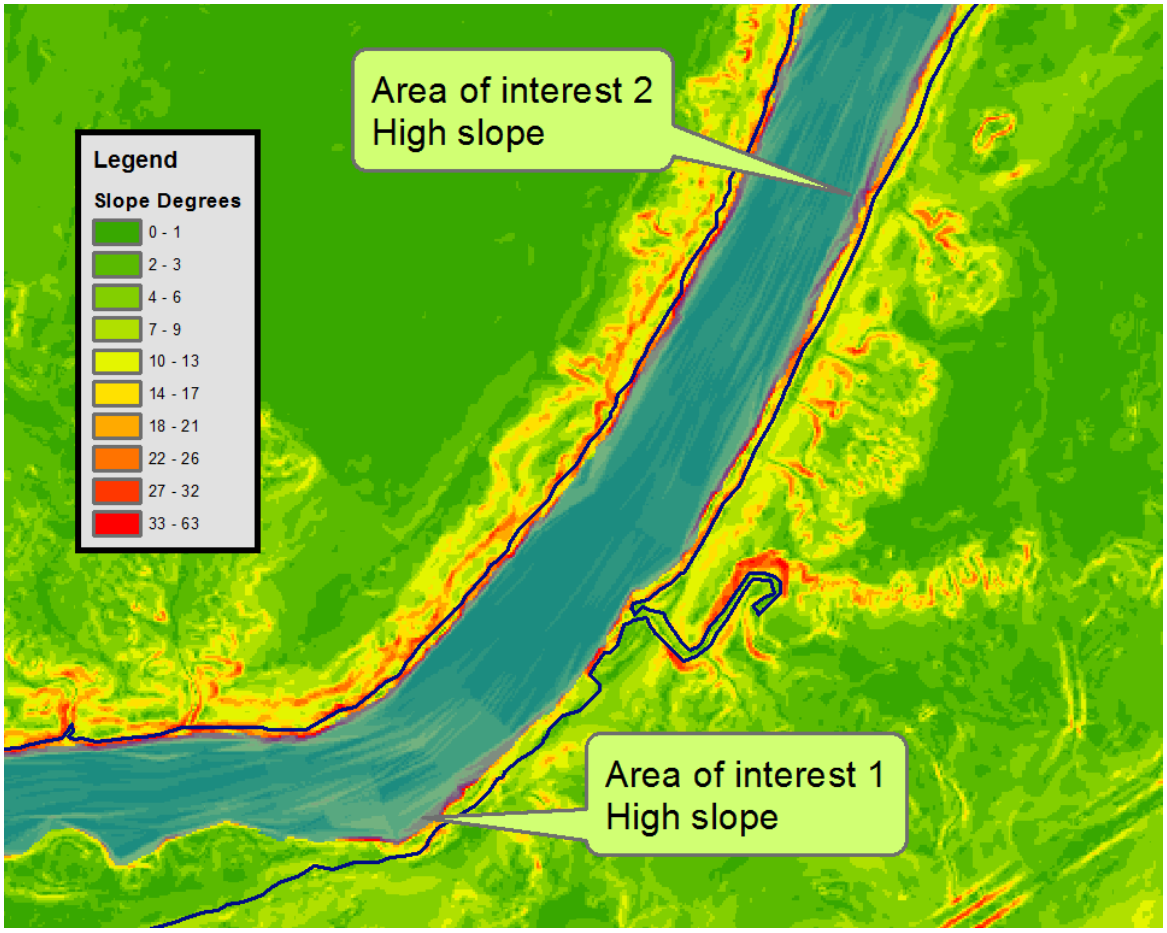

Figure 5-2 Slope at identified abstraction locations.

The study showed that geometry created within the GIS environment could easily be imported into HEC-RAS. The study also showed that hydraulic results obtained in HEC-RAS is highly interoperable with the GIS environment. This allows the use of GIS for further analysis and make use of the extensive GIS capabilities for interpretation and visualisation, as shown in the study.

The study indicates the importance of using GIS for analysis, when identifying abstraction locations. By using GIS, the spatial relationship between distance between stages, surface velocity and depth could be established. The raster calculator was used for demining relationships between distance, depth and velocity (Figure 3-26,3-27). By using relationships hydraulic factors influencing abstraction locations could be combined into a single surface. Care should be taken when using multiple relationships so that unwanted weight is not inherited to variables. Calculations should be planned in such a way that sufficient weight is added to highly influencing variables. In the study the distance to depth and depth to

velocity ratio were calculated. Therefore, more weight was inherited regarding depth. This was accurate for the study since depth is a highly influential factor for identifying the abstraction location. When combining relationship surfaces, values need to be in an appropriate range to ensure accurate weighting of participating variables. For example, in the study it was necessary to invert the distance to depth ratio surface and stretch the values to a range, matching that of the depth to velocity ratio (Figure 3-30).

Influencing variables within such a study can be incorporated within the GIS analysis selection process. This will allow for flexibility for determining abstraction locations influenced by varying options applies to variables such as ownership, existing or planed infrastructure or abstraction methods. Rapidly changing hydraulic flow tendencies need to be accounted for when considering different stages. These locations may vary in characteristics and influence areas that might be of interest for abstraction locations. Such locations need to modelled and interpreted at sufficient stage intervals.

This study focussed on identifying abstraction locations based on hydraulic properties identified. The use of GIS enabled analysis of the data and supplied a single surface indicating desirable abstraction locations. Further analysis may be conducted on a surface as created in the study. For example, variables such as pipeline connections, land ownership and geology can easily be applied to the resulting hydraulic surface created within the GIS environment, for better representation and selection of abstraction locations.

This study shows that the conventional theory of placing water abstraction locations along the concave bank of a river bend may not necessarily be the optimal location for abstraction locations (Figure 5-3). For example, the first major upstream bend in the river section of the study area has a prominent concave bank and will be of high interest as an abstraction location based on the conventional empirical rules (Figure 5-3, 5-4 left). High velocities are obtained at these locations and transport a lot of sediment (Figure 5-3). In addition, the concave bank of a river bend is prone to erosion due to the high velocities. Furthermore, the high stream power against embankments at these locations may affect the feasibility of many water extraction designs, due to the erosion and force on abstraction equipment. From the study it is evident that geological and morphological features influence optimal abstraction locations greatly. These optimal locations allow for sediment removal from the river bottom along with low surface velocities and deep sections. Figure 5-4 indicates an

example from the study area where the concave bank on a river bend (Left) is not an ideal abstraction location. The concave bank is not very deep and has high surface velocities and stream power that may be problematic for abstraction equipment. This location is also associated with high sediment transport that will support embankment erosion and unwanted bigger sediment particles that can promote equipment wear. In contrast, the straight section (Right) indicates a desirable abstraction location. These optimal locations are created from the bathymetric and morphological features within the river. This comparison indicates that detailed analysis of hydrological, topographic and bathymetric information, if available, allow informative decisions to be made regarding abstraction locations.

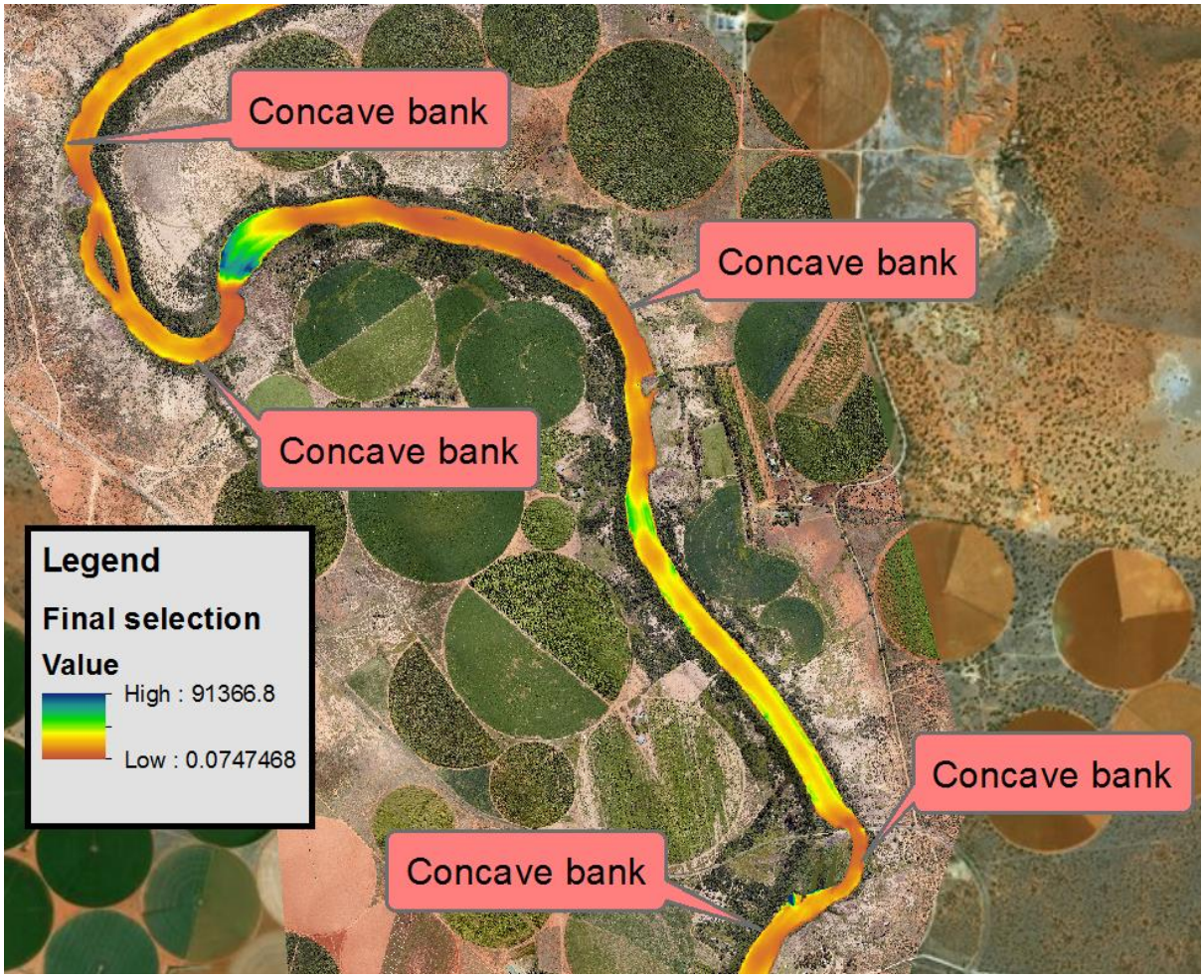

Figure 5-3 Concave banks that prove not to be optimal abstraction locations.

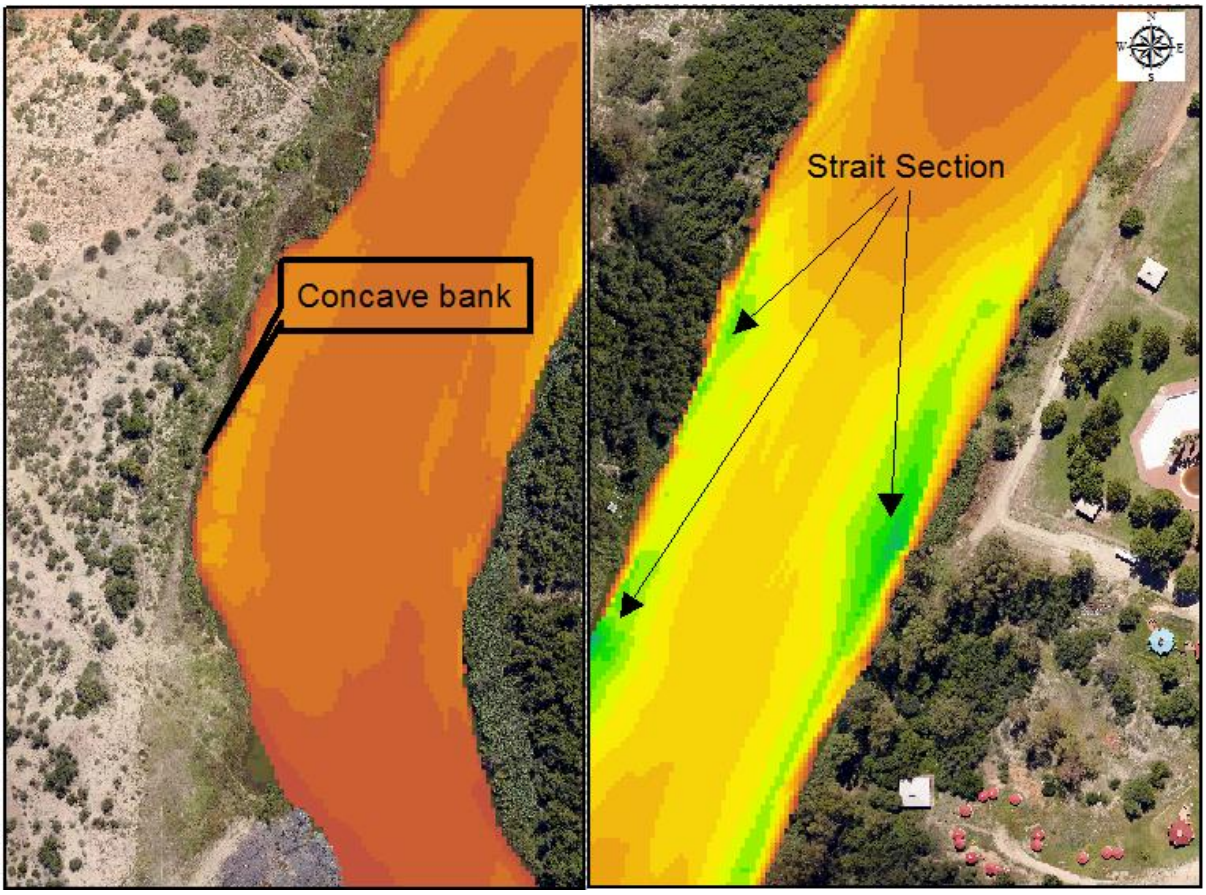

Figure 5-4 Conventional abstraction location left. Study abstraction location right.

A recommendation for future studies is that the conditions of such a study need to be clearly defined. The conditions, referring to influencing hydraulic properties that affect the conditions to be modelled for identifying optimal abstraction locations. For example, only high or low flow rates and the resulting stages may be considered to minimise risk to abstraction location. A combination of high and low flow rates may be considered, as used in this study. The purpose will greatly influence the required hydrograph for modelling as well as model selection. A 1D model should be used with additional 2D flow areas incorporated if necessary. Attention should be given to topographic and bathymetric survey results when interpolating a DEM. An accurate DEM needs to be used for hydraulic modelling, especially if the embankments are of interest. TIN models prove to be accurate with the necessary editing on triangles at embankments. Influences of hydraulic variables need to be weighted appropriately. The GIS environment should be used for analysis, interpretation and visualisation due to extensive capabilities available.

References

Ahmad, Sajjad, and Slobodan P. Simonovic
1999 Comparison of One-Dimensional and Two-Dimensional Hydrodynamic Modeling Approaches for Red River Basin.

Aksoy, Hafzullah, Veysel Sadan Ozgur Kirca, Halil Ibrahim Burgan, and Dorukhan Kellecioglu
2016 Hydrological and Hydraulic Models for Determination of Flood-Prone and Flood Inundation Areas. Proceedings of the International Association of Hydrological Sciences 373: 137–141.

Alvarado, Anthony
N.d. Hydro Survey: Multi-Beam vs. Single Beam (Part 1) » Hydraulically Inclined. http://ayresriverblog.com/2011/08/02/hydro-survey-multi-beam-vs-single-beam-part-1/, accessed January 10, 2018.

Amante, Christopher J., and Barry W. Eakins
2016 Accuracy of Interpolated Bathymetry in Digital Elevation Models. Journal of Coastal Research 76(sp1): 123–133.

ARR: A Guide to Flood Estimation
N.d. http://book.arr.org.au.s3-website-ap-southeast-2.amazonaws.com/, accessed January 15, 2018.

Ball, J, M Babister, R Nathan, et al.
N.d. Australian Rainfall and Runoff: A Guide to Flood Estimation, Commonwealth of Australia.

Basson, G. R.
2006 Consideration for Design of River Abstraction Works in South Africa.

Bernoulli Equation
N.d. https://www.engineeringtoolbox.com/bernouilli-equation-d_183.html, accessed January 26, 2018.

Betsholtz, Alexander, Nordlöf, Beatrice
2017 BetsholtzNordlof.Pdf.

Betsholtz, Alexander, and Beatrice Nordlöf

2017 Potentials and Limitations of 1D, 2D and Coupled 1D-2D Flood Modelling in HEC-RAS. Master Thesis, Lund University. http://lup.lub.lu.se/student-papers/record/8904721, accessed May 20, 2017.

Bosman, D.E, G.K Prestedge, A Rooseboom, and P.T Slatter
2002 An Investigation Int the Removeal of Sediments from Water Intakes on Rivers by Means of Jet-Type Dredge Pumps.

Brunner, Gary W.
2016 HEC-RAS River Analysis System Hydraulic Reference Manual. US ARMY CORPS OF ENGINEERS HYDROLOGIC ENGINEERING CENTER (HEC).

Brunner, Gary W., Steven S. Piper, Mark R. Jensen, and Ben Chacon
2015 Combined 1D and 2D Hydraulic Modeling within HEC-RAS. *In* World Environmental and Water Resources Congress 2015 Pp. 1432–1443.

Cameron, T, and P.E Ackerman
2012 HEC-GeoRAS User's Manual, vol.10.

Camporeale, C., P. Perona, A. Porporato, and L. Ridolfi
2005 On the Long-Term Behavior of Meandering Rivers. Water Resources Research 41(12): W12403.

Chen, Wei-Bo, and Wen-Cheng Liu
2017 Modeling the Influence of River Cross-Section Data on a River Stage Using a Two-Dimensional/Three-Dimensional Hydrodynamic Model. Water 9(3): 203.

Coordinates : River Cross-Section Surveying Using RTK Technology
2006. http://mycoordinates.org/river-cross-section-surveying-using-rtk-technology/, accessed July 23, 2018.

Department of Water Affairs
N.d. http://www.dwa.gov.za/hydrology/Verified/HyDataSets.aspx?Station=C9H003, accessed February 13, 2018.

Deterministic Methods for Spatial Interpolation
2018. http://desktop.arcgis.com/en/arcmap/latest/extensions/geostatistical-analyst/deterministic-methods-for-spatial-interpolation.htm, accessed July 23, 2018.

Dorn, Helen, Michael Vetter, and Bernhard Höfle
2014 GIS-Based Roughness Derivation for Flood Simulations: A Comparison of Orthophotos, LiDAR and Crowdsourced Geodata. Remote Sensing 6(2): 1739–1759.

Gámez, Pablo Sánchez
2014 Comparison of Laser Bathymetry with Single Beam and Multibeam Data in the Southwestern Baltic Sea. HafenCity University Hamburg.

Gartner, John
N.d. Stream Power: Origins, Geomorphic Applications, and GIS Procedures: 36.

Gharbi, M., A. Soualmia, D. Dartus, and L. Masbernat
N.d. Comparison of 1D and 2D Hydraulic Models for Floods Simulation on the Medjerda Riverin Tunisia. http://www.jmaterenvironsci.com/Document/vol7/vol7_N8/315-JMES-1772-Gharbi.pdf, accessed June 26, 2017.

Haile, Alemseged Tamiru
2005 Integrating Hydrodynamic Models and High Resolution DEM (LIDAR) For Flood Modelling. Enschede.

Harrison, L. R., C. J. Legleiter, M. A. Wydzga, and T. Dunne
2011 Channel Dynamics and Habitat Development in a Meandering, Gravel Bed River. Water Resources Research 47(4): W04513.

Huang, Guoxian, Binliang Lin, Jianjun Zhou, Roger Falconer, and Qiuwen Chen
2014 A New Spatial Interpolation Method Based On Cross-Sections Sampling.

Jansen, Ada Isobel
2008 Ph. D. Thesis–A. Jansen JANSEN, ADA.(2012). Aspects of the Economics of Water Management in Urban Settings in South Africa, with a Focus on Cape Town. Policy 2007: 2006.

Kristen, E, I Christopher, and SR Thornton
2005 ACCURACY OF HEC-RAS TO CALCULATE FLOW DEPTHS AND TOTAL ENERGY LOSS WITH AND WITHOUT BENDWAY WEIRS IN A MEANDER BEND. Colorado State University.

KSB Pumps

2013 Pumps for Water Extraction. https://www.ksb.com/ksb-ca-en/News/technical-articles/archives-2013-ca-en, accessed July 4, 2018.

Legleiter, Carl J.
2014 A Geostatistical Framework for Quantifying the Reach-Scale Spatial Structure of River Morphology: 2. Application to Restored and Natural Channels. Geomorphology 205: 85–101.

Legleiter, Carl J., and Phaedon C. Kyriakidis
2008a Spatial Prediction of River Channel Topography by Kriging. Earth Surface Processes and Landforms 33(6): 841–867.

2008b Spatial Prediction of River Channel Topography by Kriging. Earth Surface Processes and Landforms 33(6): 841–867.

Merwade, Venkatesh
2009 Effect of Spatial Trends on Interpolation of River Bathymetry. Journal of Hydrology 371(1–4): 169–181.

Mosaddad, S. M., A. A. Bidokhti, and M. Ezam
2009 Current Modeling of Water in a River Meander Considering Civil Engineering Problems in Building the Coastal Walls. *In* Advances in Water Resources and Hydraulic Engineering Pp. 945–950. Springer, Berlin, Heidelberg. https://link.springer.com/chapter/10.1007/978-3-540-89465-0_166, accessed January 18, 2018.

National Water Resource Strategy
2004 Overview of the South African Water Sector. Department of Water and Sanitation.

Nicandrou, Aphrodite
2010 HYDROLOGICAL ASSESSMENT AND MODELLING OF THE RIVER FANI CATCHMENT, ALBANIA. UNIVERSITY OF GLAMORGAN.

Open Channel Flow
2018. http://www.fsl.orst.edu/geowater/FX3/help/8_Hydraulic_Reference/Open_Channel_Flow.htm, accessed July 23, 2018.

Ponce, Victor M
2014 FUNDAMENTALS OF OPEN-CHANNEL HYDRAULICS. San Diego State University, California.

Rivers | World Machine Development Diary
N.d. https://www.world-machine.com/blog/?p=470, accessed January 18, 2018.

Rodriguez, Rachel
2015 Integration of Topographic and Bathymetric Digital Elevation Model Using ArcGIS Interpolation Methods: UNIVERSITY OF SOUTHERN CALIFORNIA.

SA Water board, South Africa
2005 Overview of the South African Water Sector.

Tan, Y
1996 Design of Silt Related Hydraulic Structures, Int. Conf. on Reservoir Sedimentation.

Tapp, Nicky
N.d. River Weirs – Good Practice Guide: 157.

US Department of Commerce, National Oceanic and Atmospheric Administration
2017 What Is LIDAR. https://oceanservice.noaa.gov/facts/lidar.html, accessed December 13, 2017.

World Health Organisation
2017 2.1 Billion People Lack Safe Drinking Water at Home, More than Twice as Many Lack Safe Sanitation. World Health Organization. http://www.who.int/news-room/detail/12-07-2017-2-1-billion-people-lack-safe-drinking-water-at-home-more-than-twice-as-many-lack-safe-sanitation, accessed July 4, 2018.

Zhang, Yanjun, Cuiling Xian, Huajin Chen, et al.
2016 Spatial Interpolation of River Channel Topography Using the Shortest Temporal Distance. Journal of Hydrology 542: 450–462.

Appendix A

This section contains historic average daily flow rate data observed from the Riverton station from the year 2014-2017.

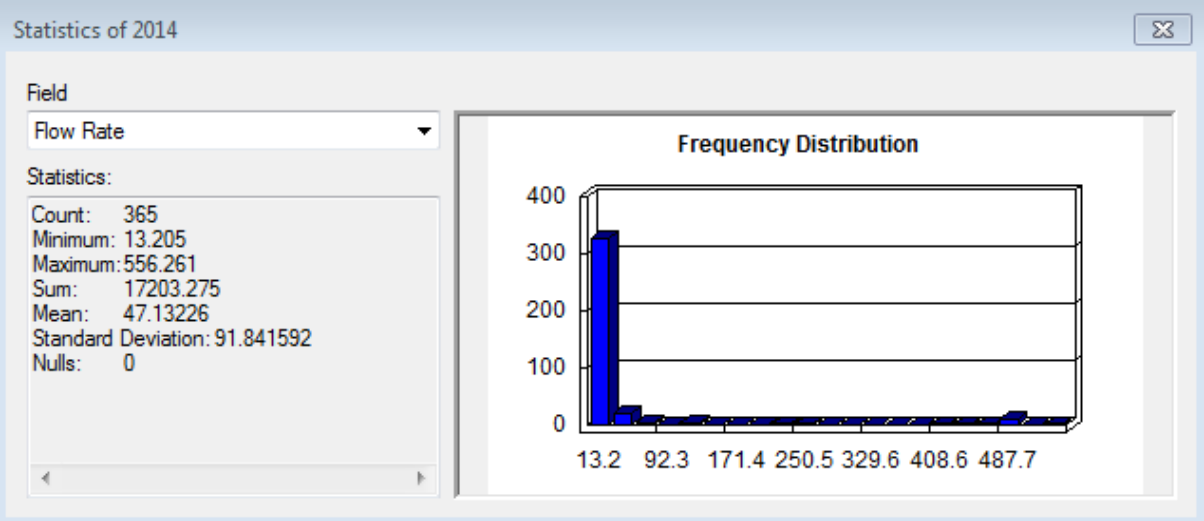

Figure A-1 Flow rate frequency distribution 2014

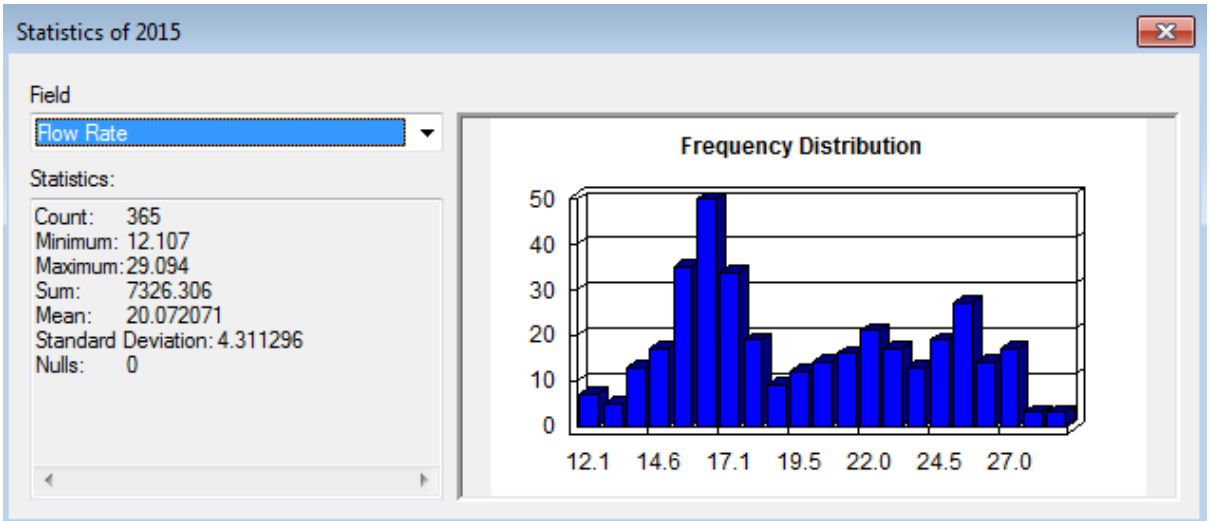

Figure A-2 Flow rate frequency distribution 2015

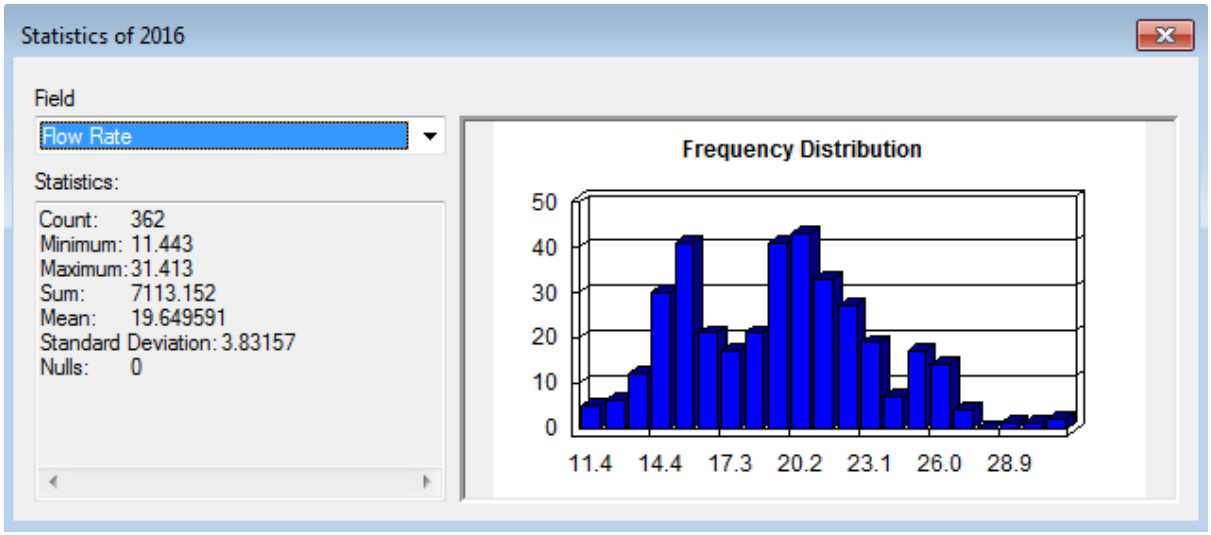

Figure A-3 Flow rate frequency distribution 2016

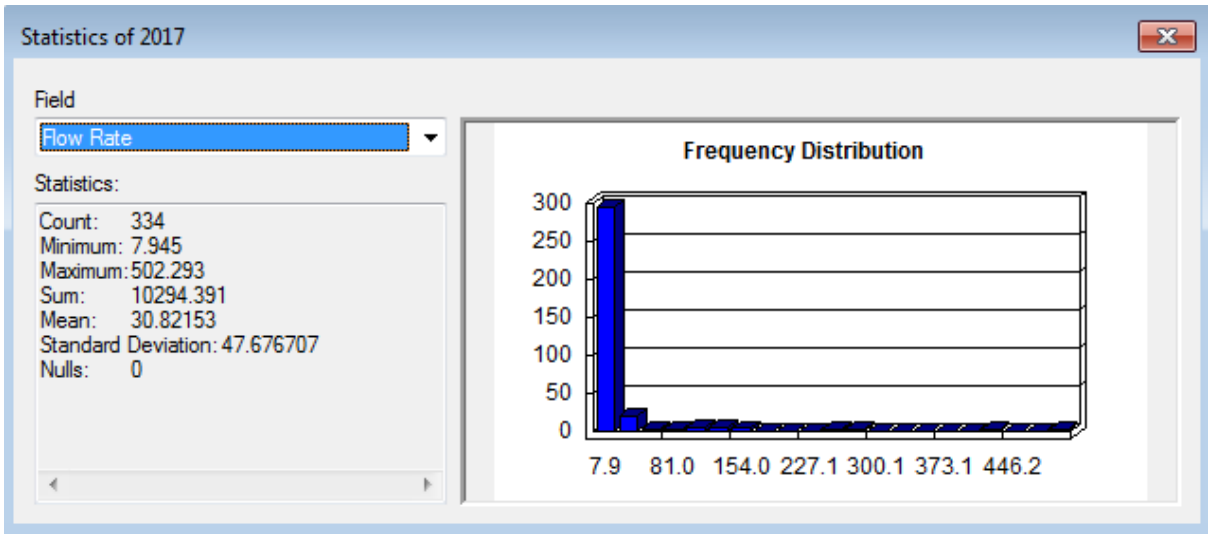

Figure A-4 Flow rate frequency distribution 2017